Design of Ultrawideband Digitizing Receivers for the VHF Low Band

D. Wyatt A. Taylor III

Thesis submitted to the faculty of the Virginia Polytechnic Institute and State University
in partial fulfillment of the requirements for the degree of

Master of Science
In
Electrical Engineering

Dr. Steve Ellingson, Chair
Dr. William Davis
Dr. Sanjay Raman

May 9th, 2006
Blacksburg, VA

Keywords: wideband, receiver, VHF, design methodology

Copyright 2006, D. Wyatt A. Taylor III

Design of Ultrawideband Digitizing Receivers for the VHF Low Band

D. Wyatt A. Taylor III

ABSTRACT

The next generation of receivers for applications such as radio astronomy, spectrum surveillance, and frequency-adaptive cognitive radio will require the capability to digitize very large bandwidths in the VHF low band (30 to 100 MHz). However, methodology for designing such a receiver is not well established. The difficulties of this design are numerous. There are various man-made interferers occupying this spectrum which can block desired signals or spectrum, either directly or through intermodulation. The receivers will typically use simple (i.e., narrowband) antennas, so the efficiency of power transfer to the preamplifier needs to be carefully considered. This thesis takes these design challenges into account and produces a seven step design methodology for direct sampling wideband digitizing receivers. The methodology is then demonstrated by example for three representative receivers. Finally, improvements to the analysis are suggested.

Contents

List of Figures

List of Tables

Chapter 1 Introduction

Receivers for certain current and future applications in the VHF low band (30-100 MHz), including radio astronomy, spectrum surveillance, and frequency-agile cognitive radio, need to digitize bandwidths in excess of 20%. Whereas methods for the design of receivers with narrow fractional bandwidths are well known, methods for the design of the analog sections for VHF low band receivers with bandwidths in excess of 20% are not well established.

Wideband receiver design in the VHF low band is difficult for a several reasons. First, there are many strong man-made signals that occupy this spectrum which can block the signal or spectrum of interest. Further, receiver-generated intermodulation products can easily fall into the wide bandwidth of the receiver, further blocking the desired signal or spectrum. This thesis considers the case where a simple (dipole or monopole) antenna is used for a wideband receiver. This is advantageous for both design simplicity and cost, and difficult to avoid when frequencies of interest correspond to long wavelengths. Such antennas are inherently narrowband, resulting in inefficient power transfer from the antenna to the preamplifier, except at frequencies near resonance.

This thesis describes the challenges of designing a wideband receiver in the VHF band below 100 MHz, presents a design methodology, and applies it to three example receiver cases. Chapter 2 ("Principles of Receiver Design") describes the architecture of a receiver and identifies important parameters and design considerations. The focus is on "direct sampling" receivers, which digitize the spectrum directly with no frequency conversion. The design of such receivers depends to a large degree on the spectrum environment that the radio must operate in. To this end, Chapter 3 ("VHF Radio Environment") describes the noise (both natural and man-made) as well as other sources of signals below 100 MHz. One finding is that either natural noise (originating primarily from astrophysical emission) or anthropogenic (man-made) noise can be very strong, and in fact may be the limiting factor in receiver sensitivity. Chapter 4 ("Antenna Matching") addresses the problem of impedance matching between a simple antenna and a preamplifier. It is shown that matching with high efficiency is typically not practical over large bandwidths. However, the limiting effect of external noise results in a situation where even receivers with poorly matched antennas can achieve the best possible sensitivity. The remaining concern is dynamic range. Once sensitivity is determined, the dynamic range must be large enough to accommodate external signal sources without resulting in excessive blocking due to intermodulation. Chapter 5 ("Linearity Analysis") describes a model for the receiver's nonlinear response and presents a method of analysis that quantifies the effect of intermoduation blocking in terms of fraction usable spectrum. Chapter 6 ("Receiver Design and Examples") presents a design methodology that accounts for the issues described above. The methodology is illustrated using three example receiver designs. Chapter 7 ("Conclusions") summarizes the results of this thesis and proposes future work that could improve the results presented here.

Chapter 2 Principles of Receiver Design

2.1 Introduction

The goal of traditional receiver design is to acquire a signal which is narrowband; i.e., with small fractional bandwidth. Fractional bandwidth is the ratio of the signal's bandwidth to the carrier frequency, and a narrowband signal is typically defined as one with a fractional bandwidth of 10% or less. The most common narrowband receiver architecture is the heterodyne receiver, shown in Figure 2.1. The heterodyne receiver downconverts the received signal to a lower frequency prior to the digitization stage. Variations of this architecture are frequently used as well. The multiple-IF receiver is similar, with the difference being that there are several stages of frequency conversion, resulting in several intermediate frequencies. The zero-IF ("direct-conversion") receiver is also similar, with the difference being that the frequency conversion stage downconverts the carrier frequency directly to zero Hz, instead of to an intermediate frequency. The design challenges that must be overcome when using the heterodyne receiver, or its mentioned variants, are well understood [1].

The heterodyne receiver can also be used to acquire wideband signals; i.e. signals with fractional bandwidth greater than 10%. However, another approach to acquiring a wideband signal is to use a direct sampling receiver, shown in Figure 2.2. The direct sampling receiver is similar to the heterodyne receiver, but the frequency conversion stage is eliminated. The removal of the frequency conversion stage in a wideband receiver is possible if the highest frequency in the passband can be digitized directly. This is advantageous because mixers tend to decrease the linearity of the receiver, and since power consumption is not considered here, do not provide any significant benefits in this case (see Section 2.2.3). Unfortunately, the design methodology for the wideband direct sampling receiver is different than the design methodology for the narrowband heterodyne receiver, and the issues associated with the wideband direct sampling design case are as not well understood.

This chapter will individually consider each stage of the wideband direct sampling receiver, examining the stage's purpose in the receiver, and the design challenges that must be overcome.

In describing these stages, it will be useful to refer to the performance metrics of sensitivity and linearity. Sensitivity is the minimum signal power that the receiver can detect with an acceptable signal-to-noise ratio (SNR), and is often characterized in terms of minimum detectable signal power (Ψ). If the minimum acceptable SNR is chosen to be 1, the resulting Ψ given by

$$\Psi = kT_O BF \quad [\text{W}] \tag{1}$$

where k is Boltzmann's constant (1.38×10^{-23} J/K), T_O is the noise reference temperature (290 K), B is the detection bandwidth, and F is the receiver's noise figure.

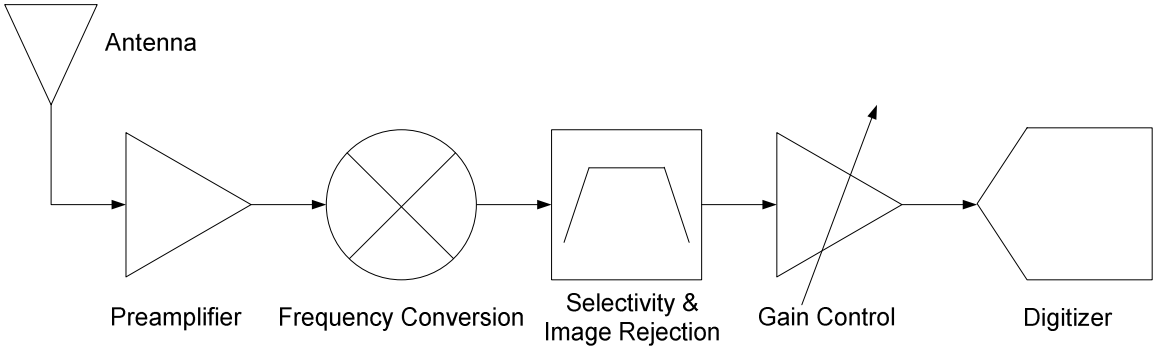

Figure 2.1. Heterodyne Receiver.

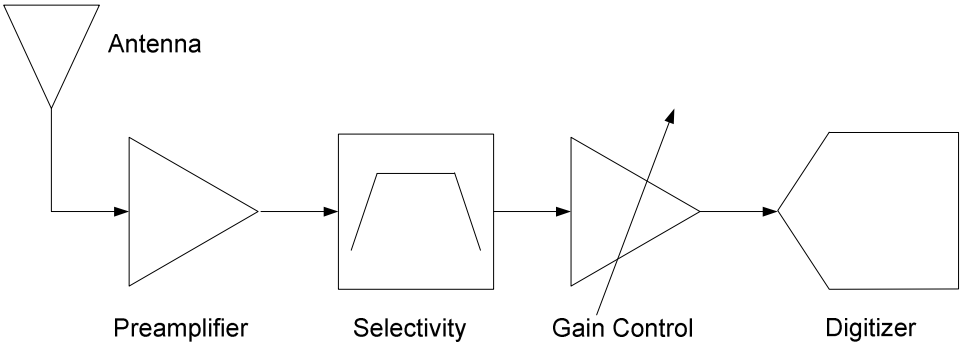

Figure 2.2. Direct Sampling Receiver. Selectivity, amplification, and gain control stages may occur in various combinations different from shown here.

Ideally the components in the receiver chain would each have linear power transfer functions of the form

$$y = Ax \qquad [\sqrt{\text{mW}}] \tag{2}$$

where x and y are the input and output signals, respectively, and A is the gain. However, real world components have nonlinear power transfer functions of the form

$$y = Ax + Bx^2 + Cx^3 ... \qquad [\sqrt{\text{mW}}] \tag{3}$$

This transfer function leads to the generation of intermodulation products at the output of the receiver. These intermodulation products can fall into the spectrum of interest and interfere with receiving the desired signals. To quantify the impact that the intermodulation products have on the receiver, there are three useful parameters: the 1 dB compression point (P_{1dB}), the second order intercept point (IP_2), and the third order intercept point (IP_3). A graphical illustration of these parameters is shown in Figure 2.3.

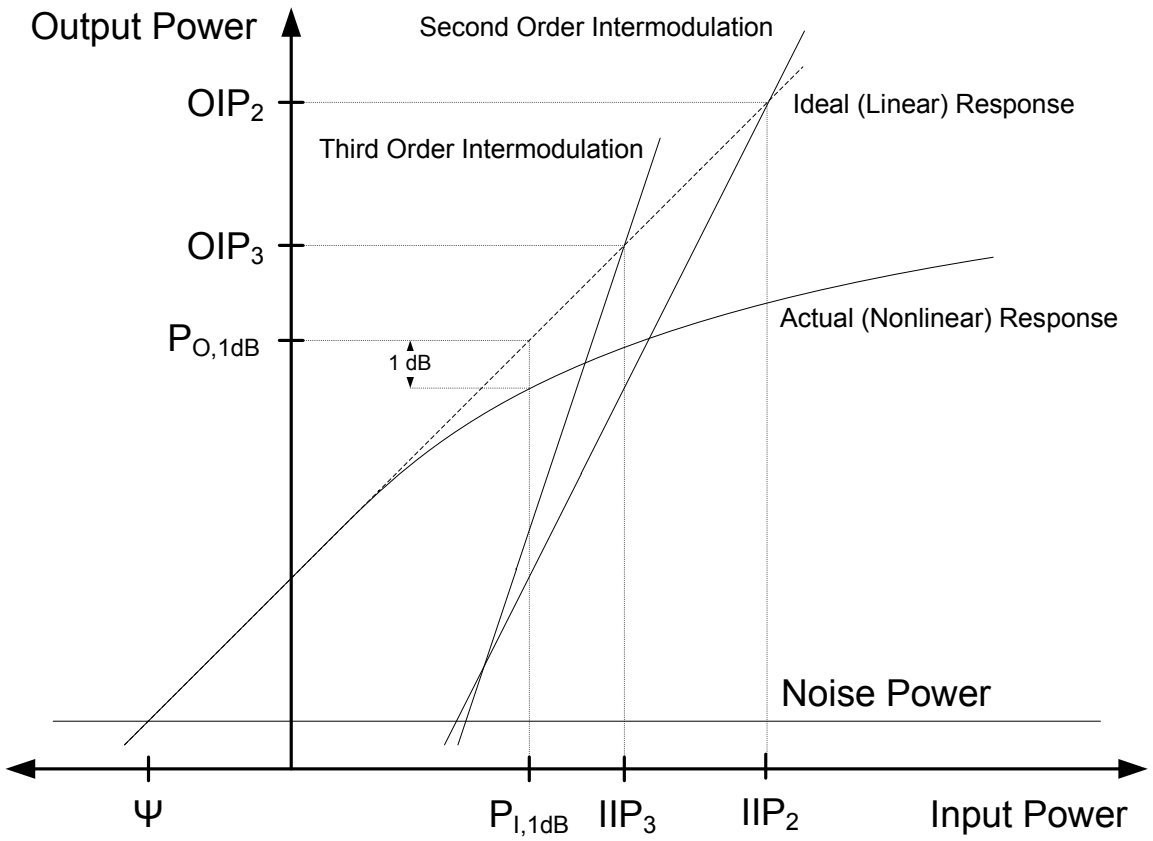

Figure 2.3. Graphical explanation of Ψ, P_{1dB}, IP_2, and IP_3.

When referred to the input, the 1 dB compression point is defined as the input power that causes the output power to be 1 dB lower than the ideal linear response. The variable $P_{I,1dB}$ is used to indicate input-referred P_{1dB}. Alternatively, the 1 dB compression point can be referred to the output, and is then defined as the ideal output power that is 1 dB greater than the actual output power. The variable $P_{O,1dB}$ is used to indicate output-referred P_{1dB}. These two parameters are related linearly by the gain, as shown below (assuming source and load impedance are the same).

$$P_{O,1dB} = A^2 P_{I,1dB} \tag{4}$$

When referred to the input, the second order intercept point is defined as the input power that causes a second order intermodulation product to have the same power as the ideal fundamental tone. The variable IIP_2 is used to designate input-referred IP_2. Alternatively, the second order intercept point can be output-referred, and is then defined as the output power where a second order intermodulation product has the same power as the ideal fundamental tone. The variable OIP_2 is used to specify output-referred IP_2. The two parameters are related linearly by the gain (assuming source and load impedance are the same).

$$\mathrm{OIP}_2 = A^2 \mathrm{IIP}_2 \tag{5}$$

The third order intercept point can be referred to the input, and is then defined as the input power that causes a third order intermodulation product to have the same power as the ideal fundamental tone. The variable IIP_3 is used to signify input-referred IP_3. Alternatively, the third order incept point can be output-referred, and is then defined as the output power where a third order intermodulation product has the same power as the ideal fundamental tone. The variable OIP_3 is used to indicate output-referred IP_3. The two parameters are related linearly by the gain (assuming source and load impedance are the same).

$$\mathrm{OIP}_3 = A^2 \mathrm{IIP}_3 \tag{6}$$

One thing to note is that the IP_2 and IP_3 are not power levels where the receiver will normally operate; they are simply specifications that provide insight to the nonlinear behavior of the receiver. In this thesis IP_3 is used as the primary metric of linearity, and IP_2 is not considered.

2.2 Architecture

This section will individually consider each stage of the receiver chain. Specifically, Section 2.2.1 will examine the antenna; Section 2.2.2, the preamplifier; Section 2.2.3, frequency conversion; Section 2.2.2, gain control; Section 2.2.5, digitization; and Section 2.2.6, post-digitization processing.

2.2.1 Antenna

The purpose of the antenna is to capture the propagating signal of interest. The ideal antenna for the wideband receiver would itself be wideband. That is, the antenna would nominally provide constant impedance over the bandwidth. This would facilitate efficient power transfer between the antenna and the preamplifier. However, due to cost and size limitations, wideband antennas are often not practical. Thus, most receivers are limited to simple antennas, such as the dipole, monopole, or variants. These antennas are inherently narrowband, exhibiting a wide range of impedances over the bandwidth.

For the purpose of antenna-receiver integration, it is useful to model the antenna using the Thévenin equivalent shown in Figure 2.4. v_A is the open circuit voltage at the antenna terminals, and Z_A is the antenna impedance, comprised of the antenna resistance (R_A) and antenna reactance (X_A). This impedance is nominal around its resonant frequency, which is defined as the frequency at which X_A equals zero. For some simple antennas, formulas exist to analyze the antenna impedance away from resonance [2]. However, these formulas rely on assumptions that may not always be true, and are not applicable for all antennas of interest. For these reasons, it is usually necessary to use other methods of analysis.

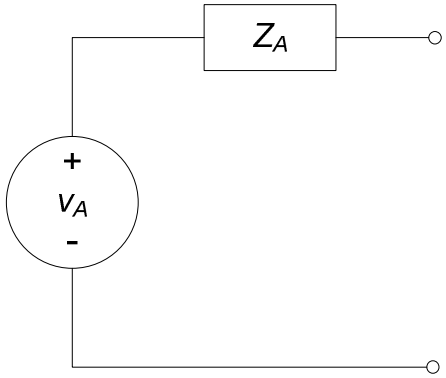

Figure 2.4. Thévenin model of the antenna.

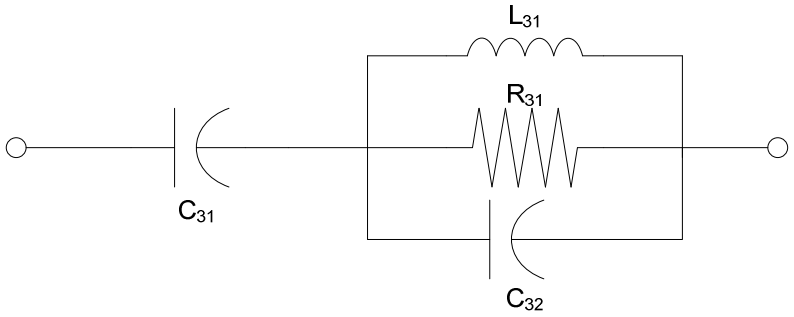

Figure 2.5. Equivalent circuit model for Z_A resulting from the TTG model.

One method is computational electromagnetics, such as the moment method (MM) [2]. This popular method is implemented in various commercially available software packages. However, this method yields only numerical results; e.g. a list of impedance versus frequency. In many cases, an equivalent circuit is preferred.

For the purposes of receiver design, the preferred characterization of the antenna's impedance is in the terms of a circuit consisting of passive elements that accurately models the antenna's frequency response. Many methodologies that produce circuit models for canonical antenna types (such as the dipole) exist, notable among these being the method of Tang, Tieng, and Gunn [3], which will be denoted here as TTG. Given h, the half-length of a dipole, and a, the radius of the dipole, the TTG approach provides a circuit model of the form shown in Figure 2.5. Equations (7) through (10) show the calculations for the antenna model circuit elements.

$$C_{31} = \frac{12.674\,h}{\log(2h/a) - 0.7245} \quad \text{[pF]} \tag{7}$$

$$C_{32} = 2h\left\{ \frac{0.89075}{[\log(2h/a)]^{0.8006} - 0.861} - 0.02541 \right\} \quad \text{[pF]} \tag{8}$$

$$L_{31} = 0.2h\{[1.4813\log(2h/a)]^{1.012} - 0.6188\} \qquad [\mu H] \tag{9}$$

$$R_{31} = 0.41288[\log(2h/a)]^2 + 7.40754(2h/a)^{-0.02389} - 7.27408 \qquad [k\Omega] \tag{10}$$

where h and a are in meters. This procedure only applies for the straight dipole, so the TTG model will be less accurate when modeling the Z_A of other antennas. The procedure is, however, easily adapted to monopole antennas. From image theory it is known that

$$Z_{A,Monopole} = \frac{1}{2} Z_{A,Dipole} \tag{11}$$

It is shown in Appendix A that to attain a circuit with one-half the impedance, the resistor and inductor values should be divided by two, and the capacitor values multiplied by two. This procedure is used to attain an equivalent circuit for a monopole antenna from Equations (7) through (10).

To demonstrate the validity and limitations of the TTG model, consider the following example. Here the example antenna will be a 38 MHz resonant dipole antenna, with h = 1.974 meters and a = 0.005 meters. The TTG model results in the circuit shown in Figure 2.6 with impedance shown in Figure 2.7 and Figure 2.8. The results of a MM computation, as implemented in EZNEC[1] software, are also shown. It is seen here that both methods of analysis are in reasonable agreement between 10 and 70 MHz. The TTG method resulted in a model that is resonant at 36 MHz, slightly lower than the anticipated resonance of 38 MHz, which was correctly predicted by the MM. Both analysis methods produce a radiation resistance of about 63.5 Ω at resonance. This gives confidence that the circuit model attained from the TTG method is a reasonable characterization of the impedance of a dipole or monopole antenna up to a frequency approximately twice the resonant frequency.

2.2.2 Preamplifier

The preamplifier has two primary purposes. The first is to interface the antenna impedance over the band of interest to a standard input impedance, such as 50 or 75 Ω. The second purpose of the preamplifier is to provide adequate gain at sufficiently low noise figure to meet system sensitivity requirements. In the VHF low band, a preamplifier may not necessarily need to be a *low noise* amplifier. It will be shown in Section 4.4 that an amplifier noise temperature of several hundred Kelvin will usually be acceptable.

Without a matching circuit, the input impedance of a wideband preamplifier is usually designed to be approximately constant over a wide range of frequencies. As shown in the previous section, the antenna impedance can vary significantly over a wide bandwidth. The resulting impedance mismatch may result in an unacceptable loss of power efficiency between the antenna and the preamplifier. The use of matching networks to overcome this impedance mismatch is discussed in Chapter 4.

---

[1] Software available at http://www.eznec.com/.

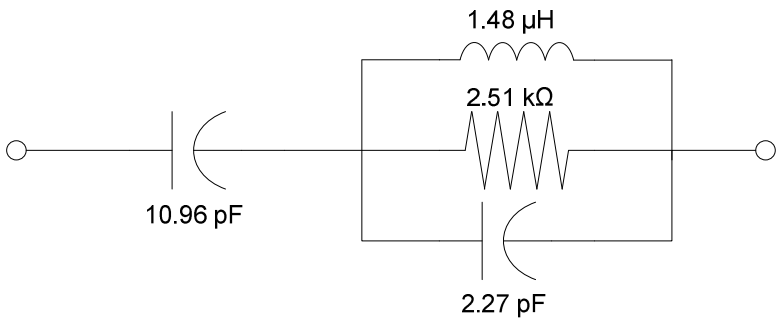

Figure 2.6. TTG model for the impedance of a dipole antenna with h=1.974 m and a=0.005 m.

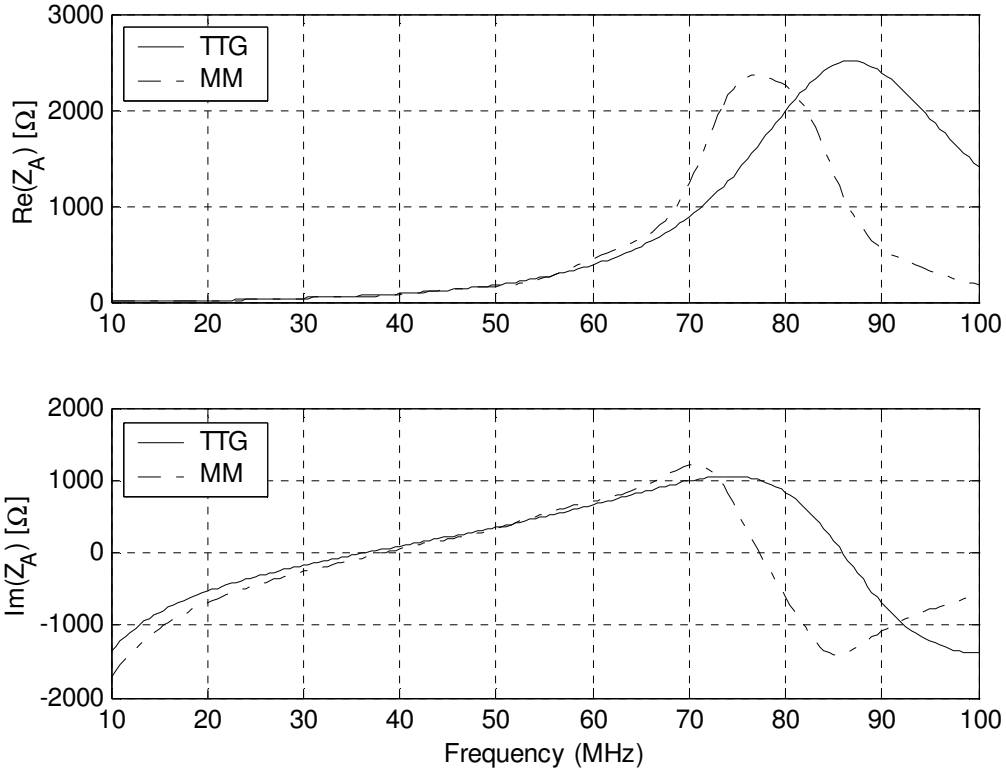

Figure 2.7. Comparison of Z_A as determined using the TTG model and the MM for a 38 MHz dipole.

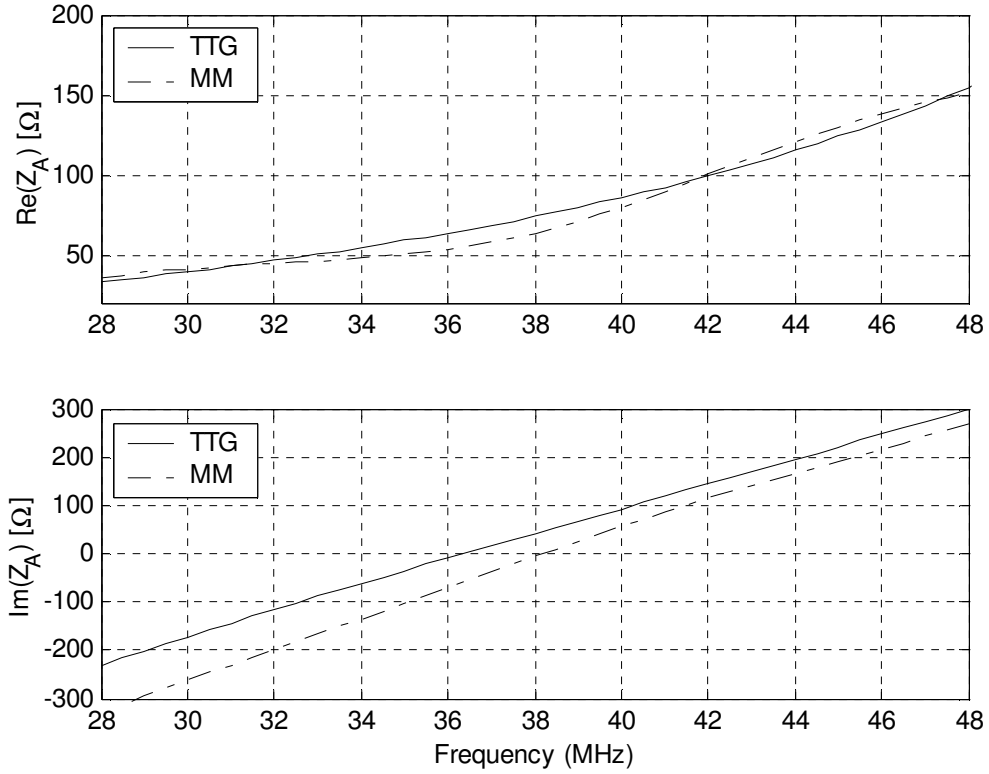

Figure 2.8. Comparison near resonance of Z_A as determined using the TTG model and the MM for a 38 MHz dipole.

Ideally the sensitivity of a receiver will be limited only by unavoidable external noise. This can often be achieved at VHF frequencies and below, because external noise is relatively strong [7]. At higher frequencies, however, the external noise is lower, so the preamplifier tends to dominate the total noise acquired by the receiver, hence the sensitivity. In wideband designs, loss of efficiency through the inability to attain a wideband match to the antenna can exacerbate this problem.

2.2.3 Frequency Conversion

The heterodyne receiver in Figure 2.1 includes a frequency conversion stage. This stage converts the signal to a lower intermediate frequency. For a narrowband receiver, this conversion allows for the sampling rate used in the digitization stage to be dramatically reduced. This approach could be used for a wideband receiver; however, there are limitations. Because the fractional bandwidth of the wideband signal is large, downconverting to an intermediate frequency may not significantly reduce the sampling rate. Also the frequency conversion process is inherently nonlinear, and mixers often have low IP_2 and IP_3 values. Thus, including the frequency conversion stage could also decrease the linearity of the receiver. For these two reasons the frequency conversion stage is not considered further, and only direct sampling receivers are considered.

2.2.4 Gain Control

Analog-to-digital converters (ADCs) can encode an input signal only for a limited range of magnitudes. Because the power at the input to a receiver can vary over several orders of magnitude, it is usually beneficial to vary the gain in the receiver chain to ensure that the ADC's dynamic range is optimally used.

Narrowband receivers are often designed to receive only one signal at a time, and can vary their gain in direct response to this signal's level. However, wideband receivers must be capable of receiving multiple signals simultaneously, which renders the narrowband gain control approach impractical. Instead, gain control for wideband receivers should respond slowly to the power level in the acquisition bandwidth, with the goal being to optimally use the ADC's dynamic range. Thus, a time constant on the order of seconds or minutes is often appropriate for wideband receivers. This is true even for *mobile* receivers, since the passband may contain many signals which fade independently.

Unfortunately, there is a tradeoff between sensitivity and linearity which complicates the design of the gain control. This is easily demonstrated using a simplified receiver consisting of three components: a preamplifier, a gain control stage, and a second amplifier, each of which has a specified gain, OIP_3, and noise figure. This configuration is shown in Figure 2.9. The Ψ and IIP_3 of the complete system can be determined from the stage values of G, OIP_3, and F using a stage-cascade gain, noise figure, and third order intercept (GNI) analysis, as described in Appendix B. Figure 2.10 shows the effect on Ψ and IIP_3 as attenuation is varied. Note that improvements in Ψ as attenuation is varied are accompanied by degradation in IIP_3, and vice versa. Thus, it is difficult to achieve jointly optimum Ψ and IIP_3.

2.2.5 Digitization

Digitization is the process of converting an analog signal into digital form. One purpose of the selectivity stage (i.e. a bandpass filter) in Figure 2.2 is to avoid aliasing.

Let P_{clip} be the input power corresponding to the maximum level the ADC can properly encode. The quantization noise of an ideal ADC is known to be [4]

$$P_Q = -1.76 - 6.02N_b \quad [\text{dB relative to } P_{clip}] \tag{12}$$

where N_b is the number of bits of the ADC. However, due to additional analog noise generated by the digitizer the quantization noise is typically about 2 dB worse, so a simpler and more realistic model is

$$P_Q = -6N_b \qquad [\text{dB relative to } P_{clip}] \tag{13}$$

The problem of determining the nominal gain and N_b for a particular receiver is now considered. A suitable method is described in [5] and is generalized here. Let P_t be the total power input to the receiver. This power is the sum of P_{ext} (total external noise power captured by

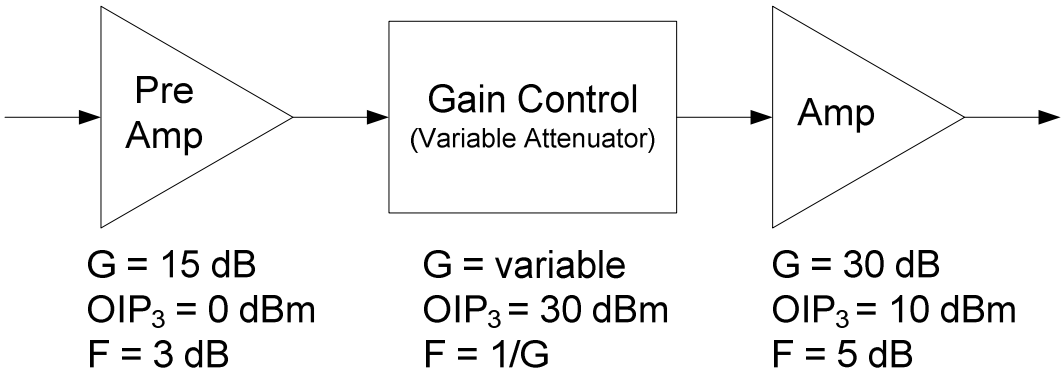

Figure 2.9. Simple system for Ψ-IIP_3 trade-off analysis. Variable attenuator OIP_3 is fixed at 30 dBm.

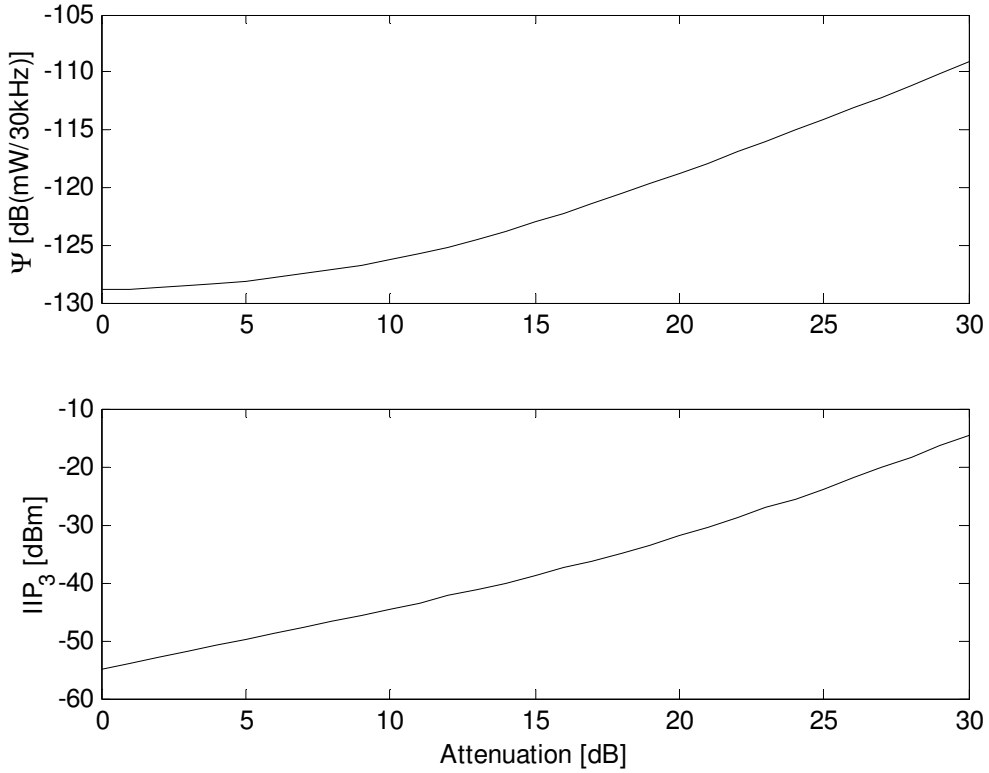

Figure 2.10. Sensitivity (Ψ) and IIP_3 vs. attenuator setting for the receiver shown in Figure 2.9.

the receiver), P_S (total external power due to external signal sources), and $N_O = kT_OBF$. The nominal receiver gain G_r is then given by

$$G_r = \frac{P_{clip}\delta_r}{P_t} \tag{14}$$

where δ_r is chosen to accommodate temporary increases in power due to intermittent signals and the spurious co-phasing of individual signals. In modern ADCs the full scale output power is typically on the order 1 V_{RMS} into 50 Ω, resulting in a P_{clip} of about +10 dBm. Thus, using a representative value of δ_r = -10 dB, the resulting G_r is (1 mW)/P_t. This expression serves as a useful rough estimate of the gain required in a wideband direct sampling receiver.

With the receiver gain set to G_r, the external power referred to the input of the ADC is given by

$$P_i = P_{ext}G_r \tag{15}$$

and the quantization noise power is given by

$$P_Q = P_{clip}10^{-6N_b/10} \tag{16}$$

The ratio of external noise to quantization noise (γ_q) at the input of the ADC is then given by

$$\gamma_q = \frac{P_i}{P_Q} = \frac{P_{ext}}{P_t}\delta_r 10^{6N_b/10} \tag{17}$$

Since it is usually desired for external noise to dominate over quantization noise, γ_q is typically chosen to be around 10. Solving for N_b yields

$$N_b \geq 1.67\log_{10}\left(\frac{P_t}{P_{ext}}\frac{\gamma_q}{\delta_r}\right) \tag{18}$$

This is the number of bits required for quantization noise to be dominated by external noise by a factor of γ_q at the output of the ADC. From Equation (18) it can be seen that to determine N_b both P_{ext} and P_S must be known, and that γ_q and δ_r are design parameters.

The result is illustrated in Figure 2.11. Note that when P_t is roughly equal to P_{ext} (i.e., noise-dominated receiver input) only 3 or 4 bits are required, even accounting for large headroom (δ_r = -10 dB) and a large margin over quantization noise (γ_q = 10 dB). However, as the input becomes dominated by external signals (i.e., increasing P_S), the required number of bits increases significantly. As will be shown in Chapter 3, a P_t to P_{ext} ratio of 10^6 is not uncommon.

2.2.6 Post-Digitization

Processing following the digitization includes channelization, detection, demodulation, etc, and is application-specific. However, for the most part these processes do not impact the

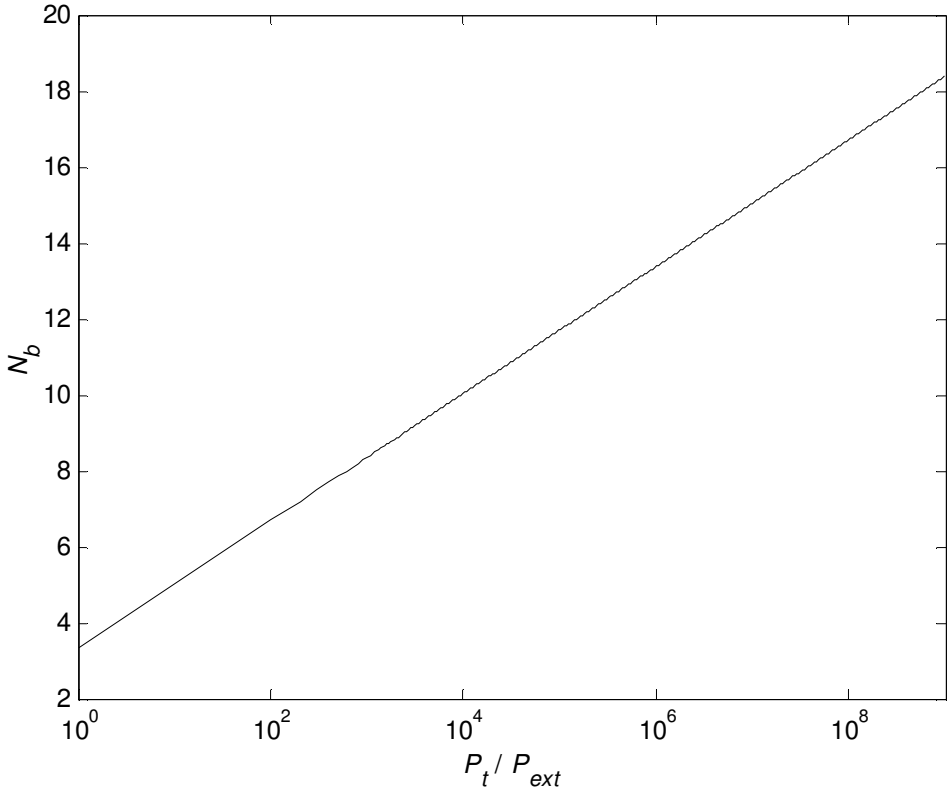

Figure 2.11. Minimum N_b as a function of P_t / P_{ext} when γ_q = 10 dB and δ_r = -10 dB.

design of the preceding stages. Thus, post-digitization processing falls outside of the scope of this thesis, and is not considered from this point forward.

2.3 Summary

This chapter introduced the architecture of the wideband direct sampling receiver. Differences between the wideband direct sampling receiver and traditional narrowband receivers were identified. There are two key issues for wideband receiver design that must be further considered. First, there is an increased potential for large interfering signals to fall into the band of interest; thus, these signals should be analyzed so the effect on the receiver can be better understood. Second, the antennas used are likely to be inherently narrowband, resulting in a loss of power transfer efficiency due to impedance mismatch with the preamplifier. These two issues will be addressed in the following chapters.

Chapter 3 VHF Radio Environment

3.1 Introduction

It is important to understand the VHF radio environment for two reasons. First, receivers operating in this band can easily be external noise-limited. Secondly, there are various large anthropogenic signals that occupy this band. These large signals result in two problems: 1) the signals can block signals of interest; 2) nonlinearities may result in intermodulation products that can block signals of interest. The second problem is further discussed in Chapter 5.

At VHF frequencies the two sources that dominate the external noise are Galactic noise and anthropogenic noise, covered in Sections 3.2 and 3.3, respectively. The five types of man-made signals that tend to dominate the VHF spectrum are FM broadcast, TV broadcast, shortwave HF broadcast, ham/utility communication, and 2-way radio communication. These signals are individually described and mathematically modeled in Section 3.4. Finally, in Section 3.5 a measurement example is considered to verify the VHF models.

3.2 Galactic Noise

Galactic noise is naturally-occurring background noise generated by astrophysical processes, and is often quite strong in the VHF band. The intensity of the galactic noise background is given by [6].

$$I_v = I_g v_{MHz}^{-0.52} \frac{1-e^{-\tau(v_{MHz})}}{\tau(v_{MHz})} + I_{eg} v_{MHz}^{-0.80} e^{-\tau(v_{MHz})} \qquad [\text{W m}^{-2}\ \text{Hz}^{-1}\ \text{sr}^{-1}] \tag{19}$$

$$I_g = 2.48\times10^{-20} \tag{20}$$

$$I_{eg} = 1.06\times10^{-20} \tag{21}$$

$$\tau(v_{MHz}) = 5.0 v_{MHz}^{-2.1} \tag{22}$$

where v_{MHz} is frequency in MHz. The precise value for I_v can vary as different parts of the Galaxy pass overhead, but is typically within a few dB of the calculated value. As shown in Figure 3.1, the spectrum becomes log-linear above 10 MHz, and can be approximated by Equation (23).

$$I_v \approx I_g v_{MHz}^{-0.52} + I_{eg} v_{MHz}^{-0.80} \quad [\text{W m}^{-2}\ \text{Hz}^{-1}\ \text{sr}^{-1}] \tag{23}$$

It is useful to express the intensity of the Galactic noise spectrum in terms of an antenna temperature. This can be done using Rayleigh-Jeans approximation, giving

$$I_v = \frac{2v^2}{c^2} kT_{SKY} \tag{24}$$

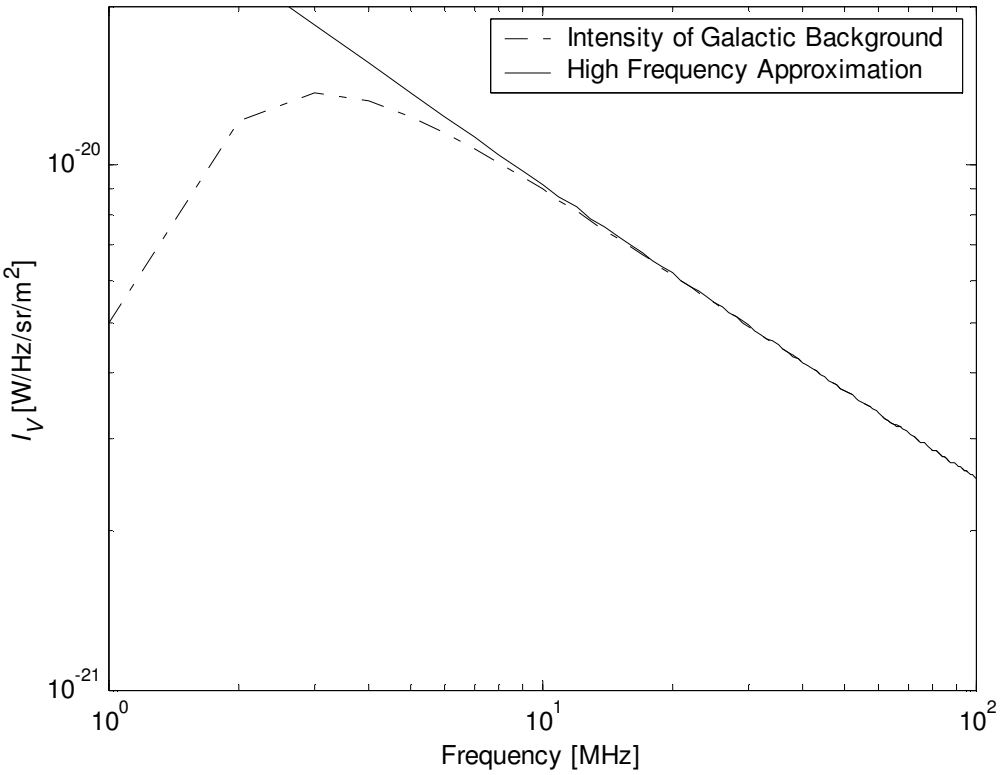

Figure 3.1. Intensity of the Galactic background, and the approximation of this intensity.

where v is frequency, c is the speed of light, and T_{SKY} is the antenna temperature associated with the Galactic noise. S_{SKY}, the power spectral density delivered to the antenna terminals, is given by

$$S_{SKY} = kT_{SKY} \tag{25}$$

Which combined with Equation (24) gives

$$S_{SKY} = \frac{1}{2} I_v \frac{c^2}{v^2} \tag{26}$$

Figure 3.2 shows the Galactic background against frequency.

3.3 Anthropogenic Noise

In [7], four categories of anthropogenic noise are defined. These categories, in order of descending noise power, are "business", "residential", "rural", and "quiet rural". The noise categories can be all be modeled using a log-linear approximation. Equation (27) models the

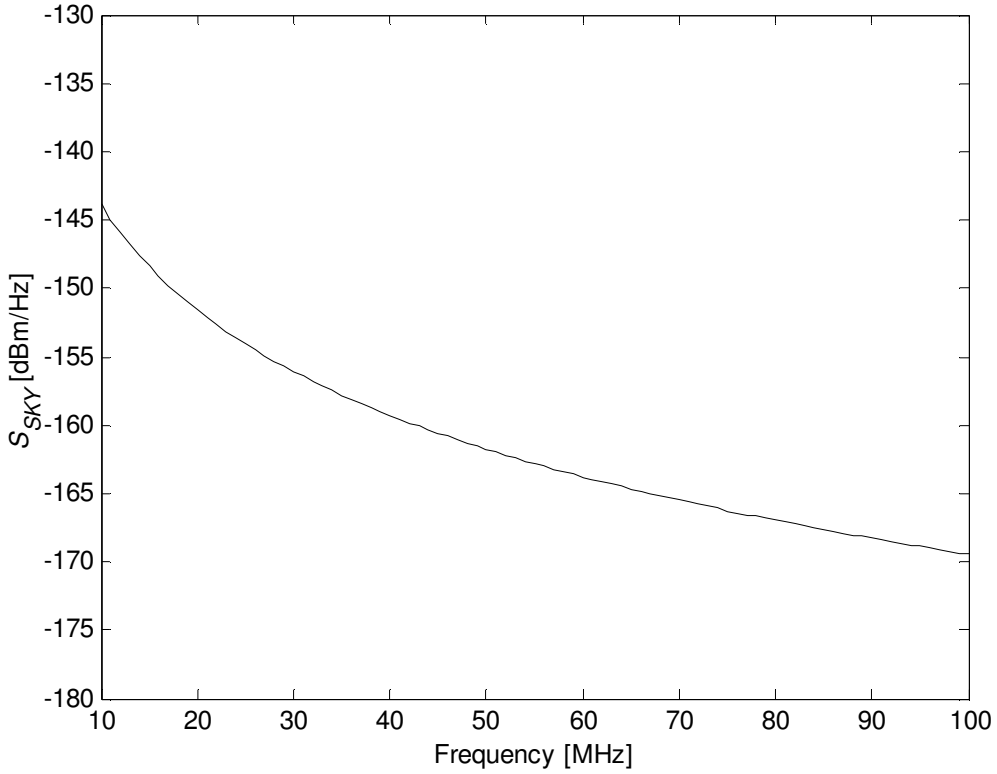

Figure 3.2. PSD of S_{SKY} due to the Galactic noise background at the terminals of an antenna.

Table 3.1. Median values for noise model parameters [7].

Environment Category	c	d
Business	76.8	27.7
Residential	72.5	27.7
Rural	67.2	27.7
Quiet Rural	53.6	28.6
Galactic Background	52.0	23.0

equivalent noise figure relative to the reference temperature (290 K) for the four noise categories.

$$F = c - d \log_{10} \nu_{MHz} \quad \text{[dB]} \tag{27}$$

where c and d are given in Table 3.1. Note that the Galactic background is also well described by this model. It is more useful to have the power spectral density for each noise category, and this can be obtained using Equation (28).

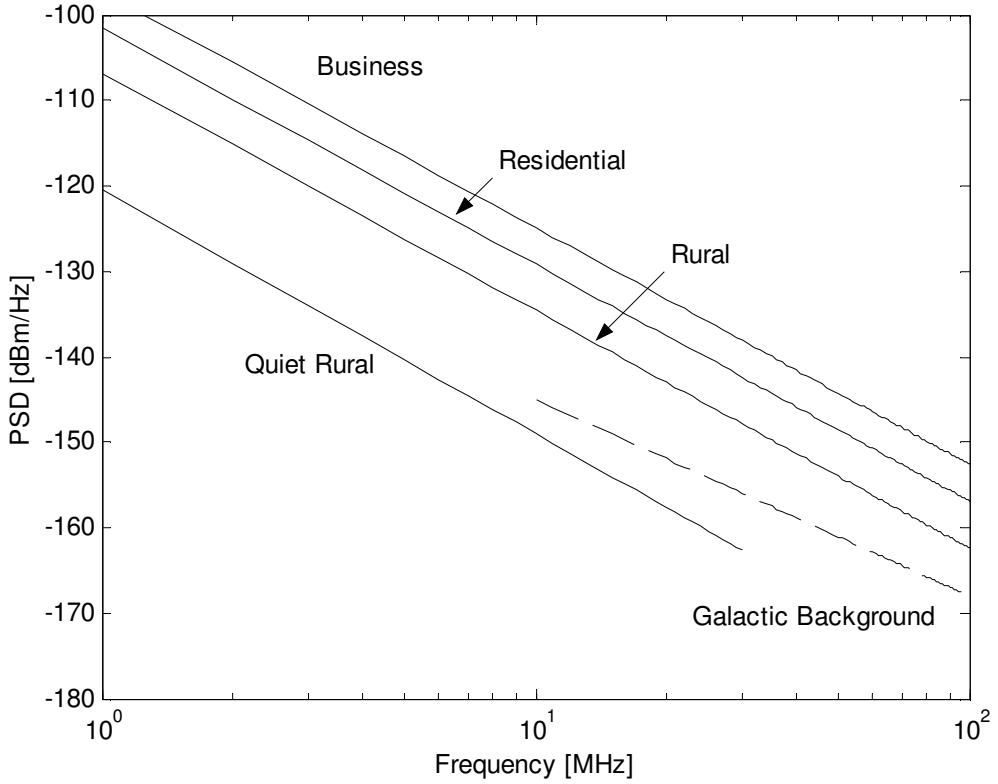

Figure 3.3. Anthropogenic noise models for a short vertical lossless grounded monopole antenna.

$$S = 10\log_{10}[(kT_O)(\text{RBW})] + c - d\log_{10} v_{MHz} \quad [\text{dBW/RBW}] \tag{28}$$

where RBW is the resolution bandwidth of the spectrum. Figure 3.3 shows the noise power spectral density vs. frequency. It should be noted that Equation (28) is only valid for the frequency range of 0.3 to 250 MHz, with two exceptions: the quiet rural model is valid from 0.3 to 30 MHz, and the Galactic background model is valid from 10 to 250 MHz.

The Galactic background model presented in [7] is a different model than the one derived in Section 3.2. However, upon inspection, the two models produce a similar result, as shown in Figure 3.4. Furthermore, this result has recently been verified by measurement [16]. Because these two models provide similar results, and agree with measurements, either option is viable. From this point forward the model shown in [7] will be used.

3.4 Intentional Transmissions

In this section, man-made interfering signals are modeled. The five interferers covered are FM, TV, shortwave HF broadcast, and Ham/Utility and 2-way radio communications.

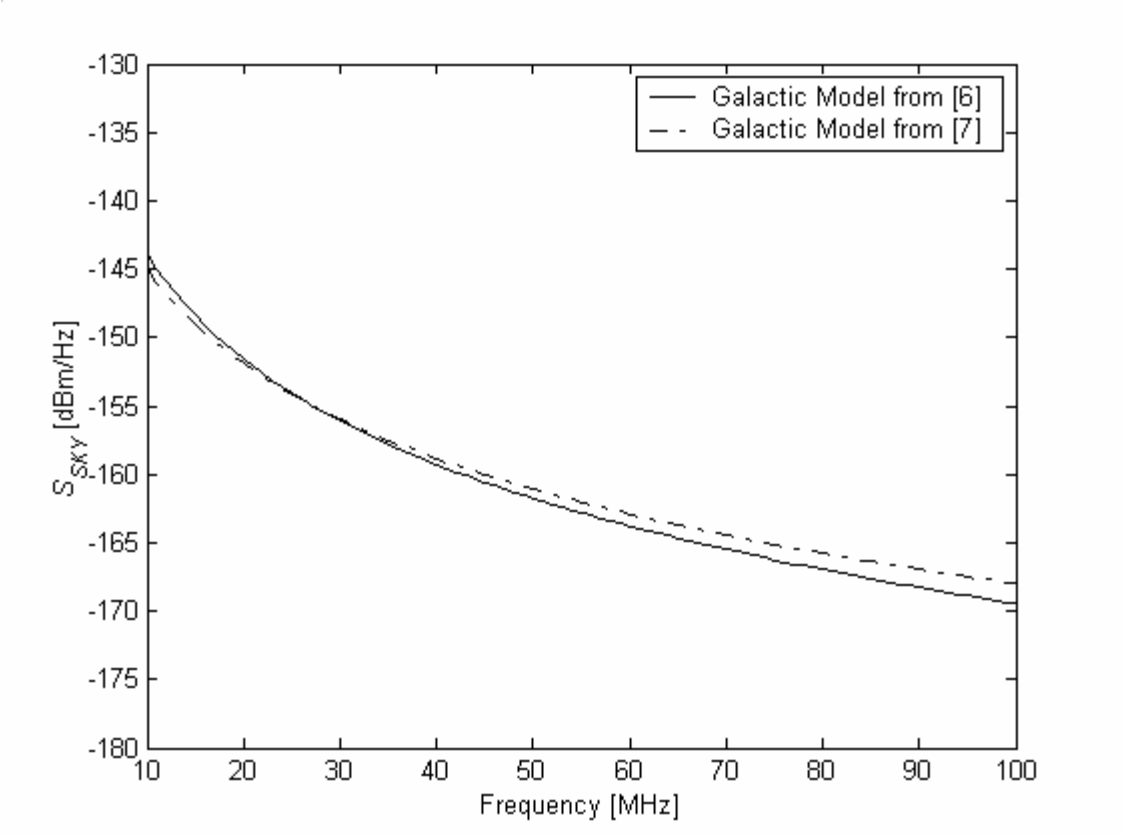

Figure 3.4. Comparison of S_{SKY} models presented in [6] and [7].

3.4.1 FM Broadcast

FM broadcast occupies the frequency range of 88-108 MHz. A block diagram for a model FM signal is shown in Figure 3.5. The components of Figure 3.5 are self explanatory, other than the DSB-SC block. This is a double-sideband suppressed carrier modulator [8]. *s(t)* is given by

$$s(t) = A_C \cos(\omega_C t + D_f \int_{-\infty}^{t} m_B(\lambda) d\lambda) \tag{29}$$

where A_C is the amplitude and D_f is the frequency deviation constant (15 kHz for FM broadcast). In simulation, the integral is implemented using a finite series summation, as shown in Equation (30).

$$\int_{-\infty}^{t} m_B(\lambda) d\lambda \approx \sum_{i=1}^{N-1} m_B\left(\frac{i}{f_S}\right)\frac{1}{f_S} \tag{30}$$

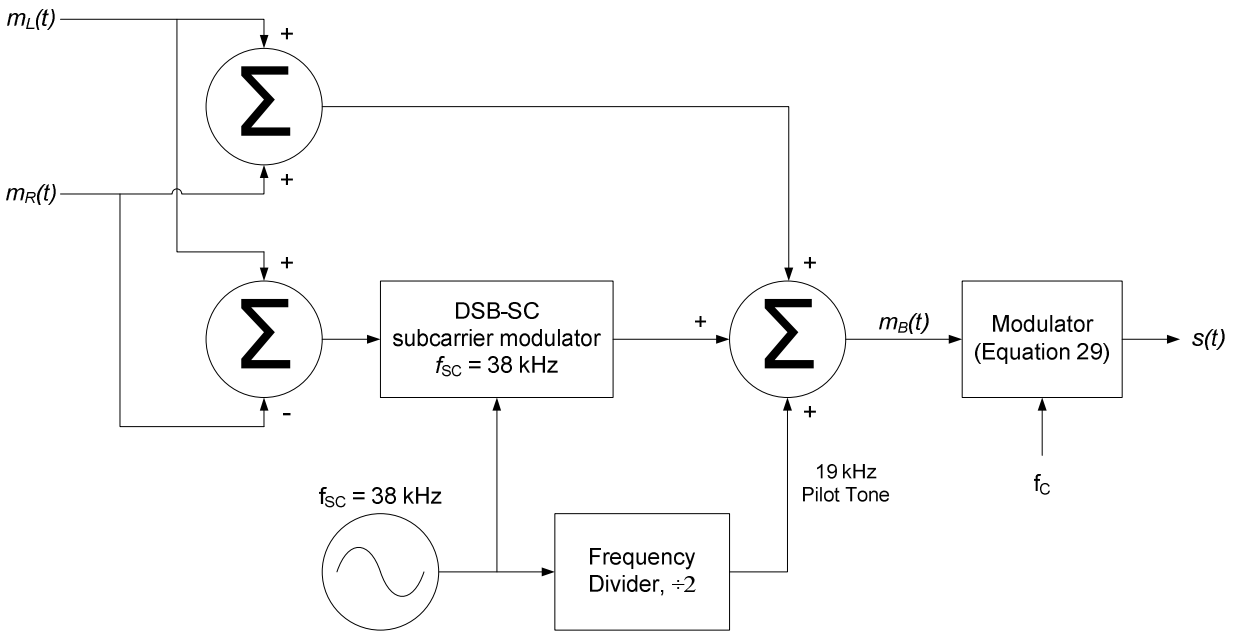

Figure 3.5. System diagram of an FM broadcast transmitter. [8]

Where $i = N$ corresponds to the current time (t), and f_S is the sample rate used in this discrete-time simulation. f_S = 200 MHz is used in this thesis. Using this model a representative FM signal can be synthesized. The example will be an FM station at 88.1 MHz. In this example, both m_L and m_R are uniform random signals with a bandwidth of 15 kHz, f_C is 88.1 MHz, and the amplitude is allowed to be full scale (0 dBm). The spectrum of this FM signal is shown in Figure 3.6.

3.4.2 TV Broadcast

Below 100 MHz, broadcast TV occupies the frequency ranges of 54-72 and 76-88 MHz (see Appendix C). The broadcast TV signal is the composite of video, aural, and color signals. Here, the color signal is not considered, so the model presented is for a black and white TV broadcast. This is justified because the color signal usually has very low power spectral density when compared to the corresponding video and aural signals. The aural signal can be modeled using the FM model from Section 3.4.1, and the video signal is a vestigial sideband (VSB) signal. The block diagram of a model TV broadcast is shown in Figure 3.7, where $-m_C(t)$ is the inverted video signal and $m_A(t)$ is the aural signal. It is easier, however, to implement the model of this signal in simulation using the block diagram shown in Figure 3.8, where the VSB filter is replaced with a low pass filter. The AM transmitter is shown in Figure 3.10, and the FM transmitter is shown in Figure 3.5. $s_{TV}(t)$ is given by [8]

$$s_{TV}(t) = A_C[1 + \mu m_C(t)]\cos\omega_C t + s(t) \tag{31}$$

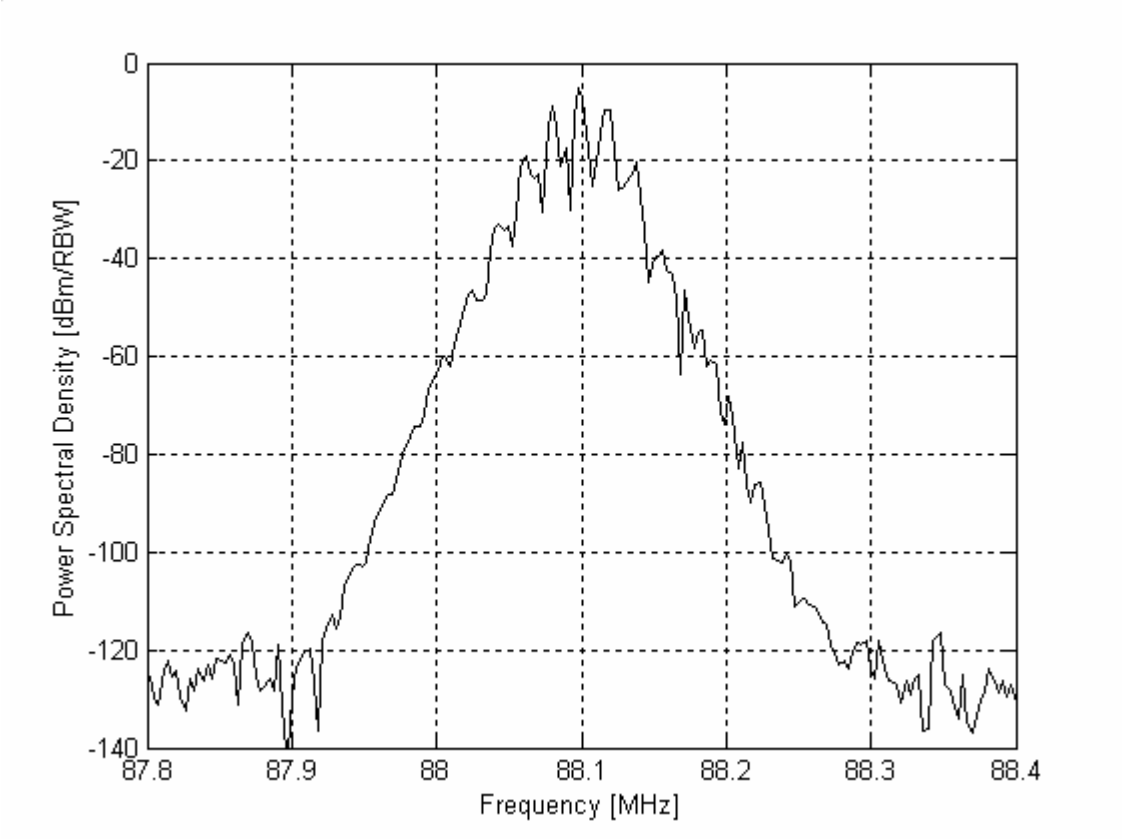

Figure 3.6. Simulated FM broadcast signal in the frequency domain, RBW = 3.05 kHz.

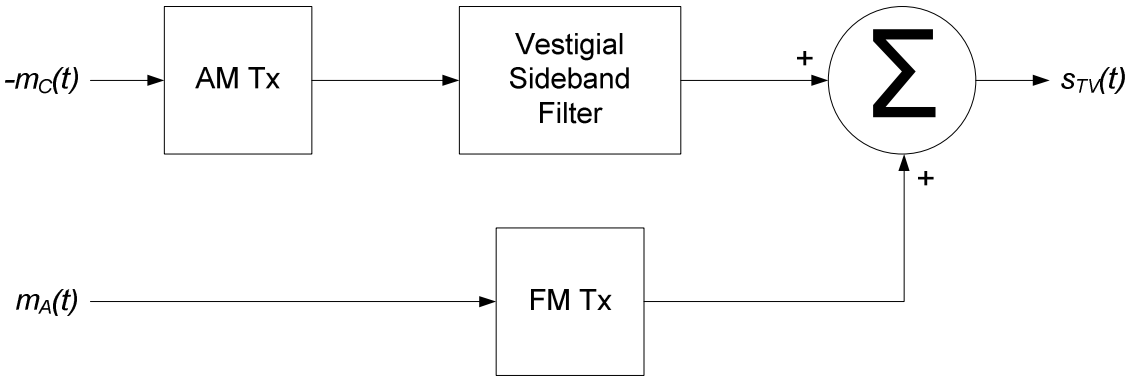

Figure 3.7. System diagram of a broadcast TV transmitter. [8]

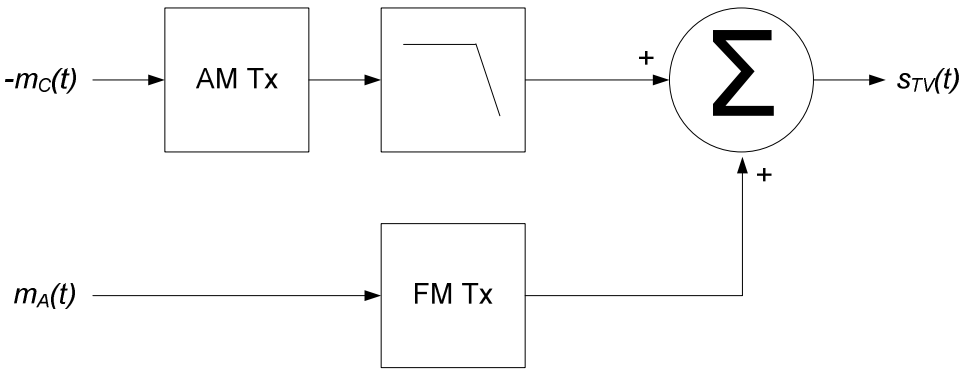

Figure 3.8. System diagram of a simplified broadcast TV transmitter.

where μ is the modulation index for the visual signal (-0.875 for TV), and *s(t)* is the same as Equation (29), except with D_f = 114 kHz. The bandwidth of the video signal for broadcast TV is 4.2 MHz, and the parameters for the audio transmission are similar to the FM broadcast case. A representative TV signal, created using Equation (31), is shown in Figure 3.9. The example will be Channel 2. In the example, both $m_C(t)$ and $m_A(t)$ are uniform random signals, with bandwidths of 4.2 MHz and 15 kHz, respectively. The amplitude of both signals is allowed to full scale.

3.4.3 Shortwave HF Broadcast

Shortwave HF broadcast is the first of two varieties of HF band transmission to be considered. HF band signals should be considered, even though they are outside the VHF low band, because they may be very strong and hard to filter out. They may also create harmonics and intermodulation products in the VHF low band. The block diagram of a shortwave HF broadcast system is shown in Figure 3.10. $s_{HF}(t)$ is given by [8]

$$s_{HF}(t) = A_C[1 + \mu m(t)]\cos \omega_C t \tag{32}$$

The modulation index, μ, is 1 for shortwave HF. Using this equation an example shortwave HF broadcast can be synthesized. For the example *m(t)* is assumed to be a uniform random signal with a bandwidth of 3 kHz, f_C is 20 MHz, and the amplitude is full scale. Figure 3.11 shows the spectrum of a representative shortwave HF broadcast signal.

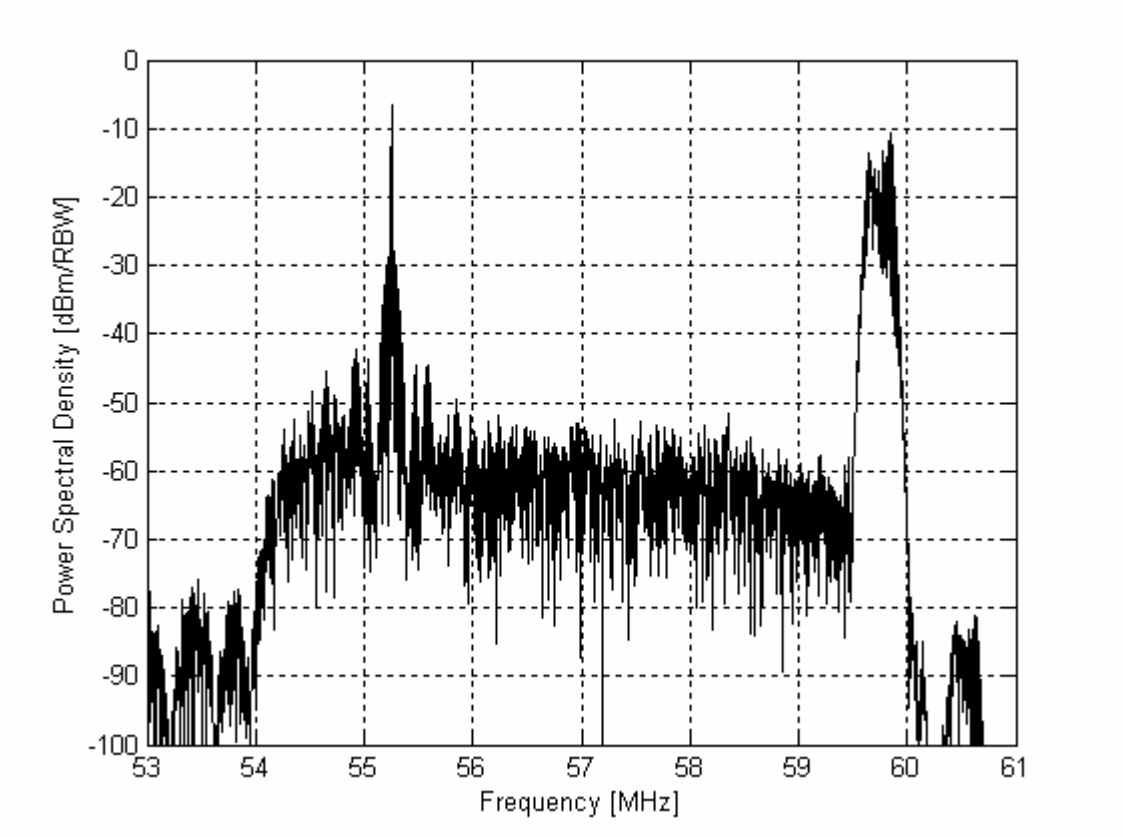

Figure 3.9. Simulated Channel 2 TV broadcast signal in the frequency domain, RBW = 3.05 kHz.

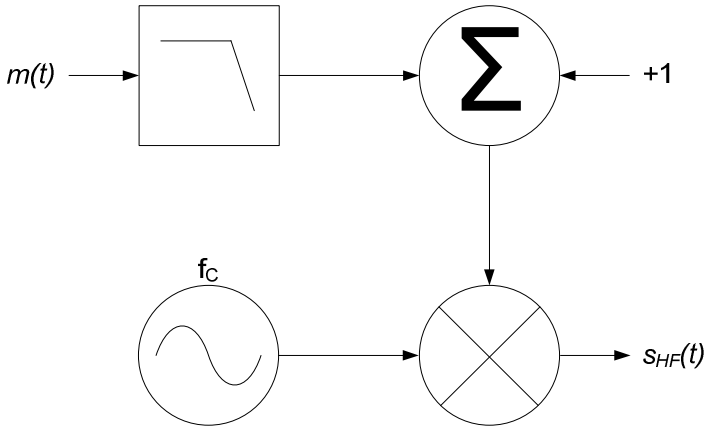

Figure 3.10. System diagram of Shortwave HF broadcast.

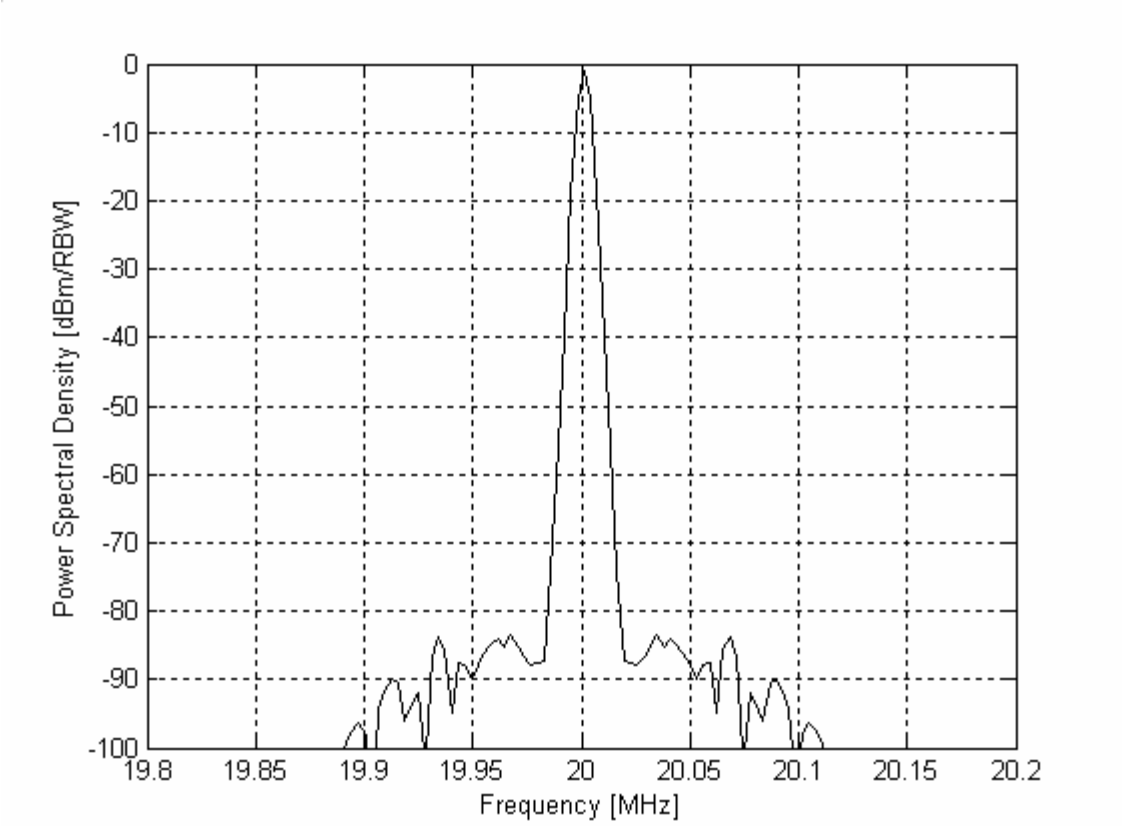

Figure 3.11. Simulated shortwave HF broadcast in the frequency domain, RBW = 3.05 kHz.

3.4.4 Ham/Utility Transmission

The second type of HF transmission interest is ham/utility communication. This communication uses single sideband (SSB) modulation. The block diagram of a SSB system using the upper sideband is shown in Figure 3.12. $s_{SSB}(t)$ is given by [8]

$$s_{SSB}(t) = A_C[m(t)\cos\omega_C t - m(t-90^\circ)\sin\omega_C t] \tag{33}$$

However, it is easier to implement $s_{SSB}(t)$ using the following equation

$$s_{SSB}(t) = A_C \,\mathrm{Re}\left\{m(t)\mathrm{e}^{j2\pi f_C t}\right\} \tag{34}$$

Using Equation (34) a representative ham/utility signal can be synthesized. For this example, f_C is 30 MHz, $m(t)$ is a uniform random signal with a bandwidth of 3 kHz, and the amplitude is full scale. The spectrum of this signal is shown in Figure 3.13.

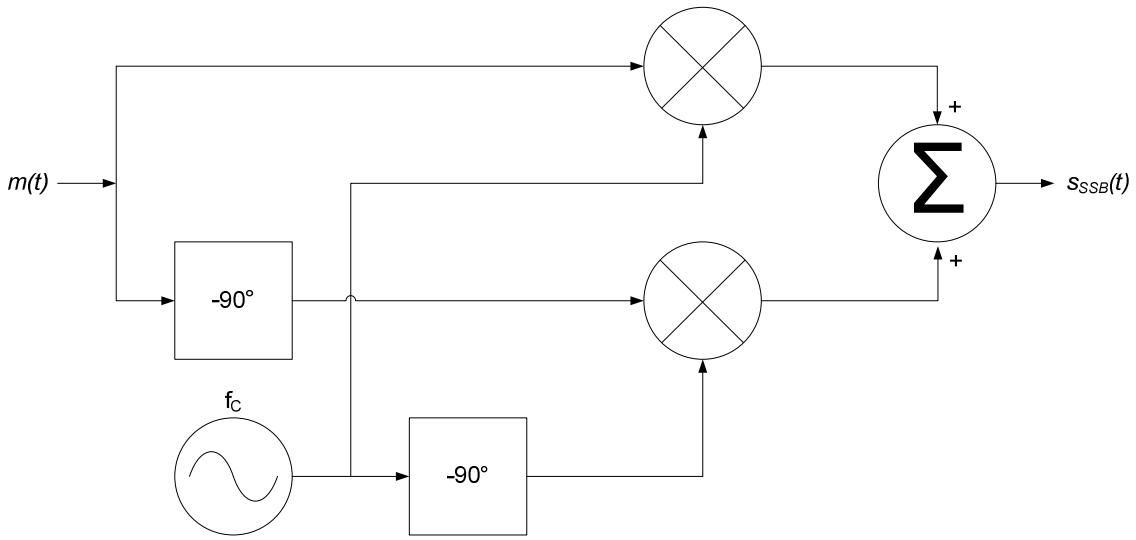

Figure 3.12. System diagram of Ham/Utility Transmission. [8]

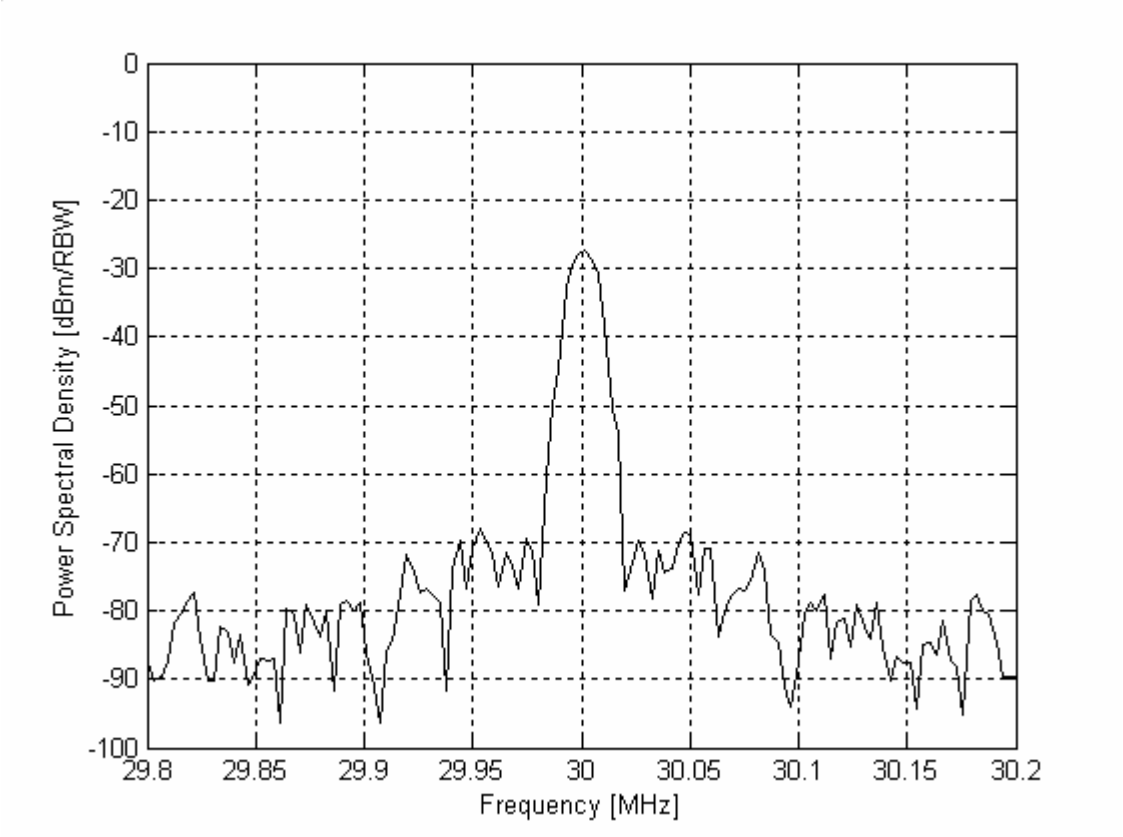

Figure 3.13. Ham/Utility transmission in the frequency domain, RBW = 3.05 kHz.

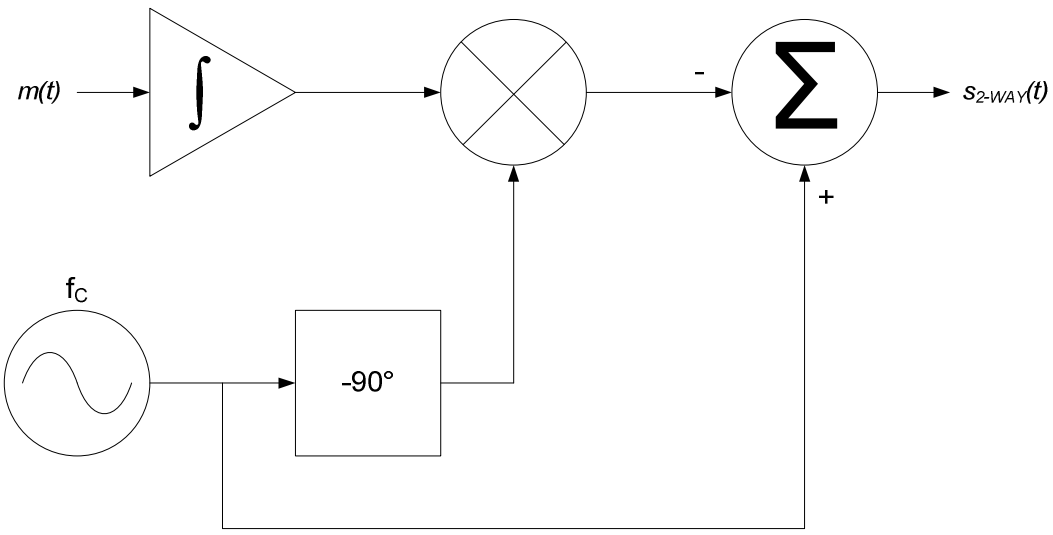

Figure 3.14. System diagram of a 2-way radio broadcast. [8]

3.4.5 2-Way Radio

The last signal to be modeled is 2-way radio communication in the VHF low band, which is typically narrowband FM modulation with a bandwidth of about 5 kHz. The block diagram for this system is shown in Figure 3.14. $s_{2\text{-}WAY}(t)$ is given by [8]

$$s_{2-WAY}(t) = A_C[\cos(\omega_C t) - D_f\left[\int_{-\infty}^{t} m(\sigma)d\sigma\right]\sin(\omega_C t)] \tag{35}$$

In simulation the integral is implemented using a finite series summation, as shown in Equation (30). To create the representative 2-way radio broadcast shown in Figure 3.15, f_C is 40 MHz, $m(t)$ is a uniform random signal with a bandwidth of 3 kHz, D_f is 3 kHz, and the amplitude is full scale.

3.5 Measurement Example

In this section, a field measurement of the radio spectrum below 100 MHz is presented. Then, this spectrum is simulated using the method described in the previous sections, using the measured spectrum as a guide to selecting frequencies, magnitudes, and so on. Comparison of the result will validate the technique.

Figure 3.16 shows a measurement from an urban location [9]. The strong signals between 65 and 90 MHz are broadcast TV channels 4, 5, and 6, as well as a few FM stations. The signals below 30 MHz are a combination of shortwave HF and ham/utility broadcast. A tabulation of these signals is provided in Table 3.2. Using this data and assuming the ITU "business" noise model, it is possible to generate a time-domain model of the signal due to sources at the antenna terminals.

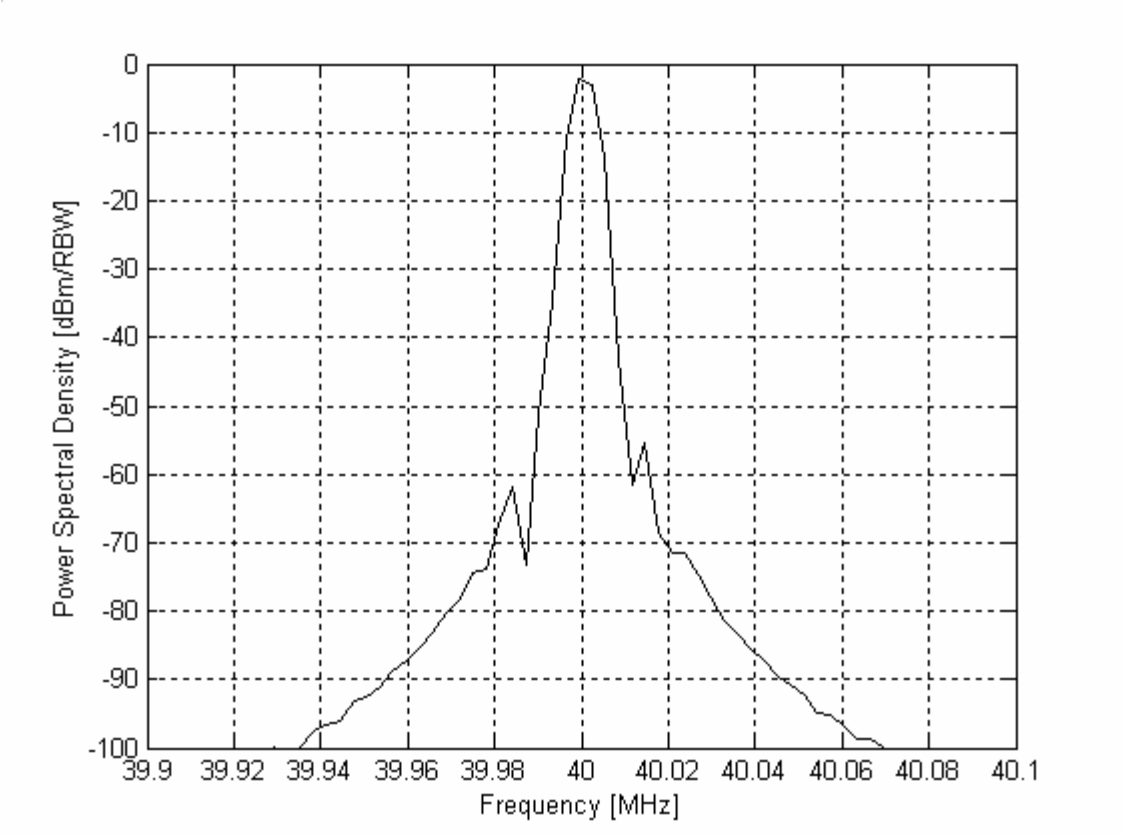

Figure 3.15. Simulated 2-way radio broadcast in the frequency domain, RBW = 3.05 kHz.

Taking the spectrum of this signal and adding the modeled noise, the result shown in Figure 3.17 is obtained. Note that the spectrum of the synthesized signals is quite similar to that in the measurement. However, the noise spectrum is dissimilar. This is for two reasons. First, the spectrum analyzer used to make the measurement has a limited sensitivity of about -90 dBm/30kHz. Second, the antenna used in the measurement exhibits a high pass frequency response with the cutoff frequency around 20 MHz, thus the noise below 20 MHz is suppressed. Another difference is the behavior of the power spectral density between the video and audio signal carriers of the TV signals. The simulated power spectral density is about 10 dB lower in this region. This is because the video sync pulse and color carrier of the TV signals are not included in the simulation. However, these components produce very small power spectral density relative to the video and audio carriers (as seen in Figure 3.16), and thus it is reasonable to neglect them for this analysis. In subsequent analysis, however, it cannot be assumed that this spectrum is available to the level indicated by the simulation. Because the differences between the measured and synthesized noise data can be explained, Figure 3.17 appears to be a usable model for the spectrum incident on the antenna.

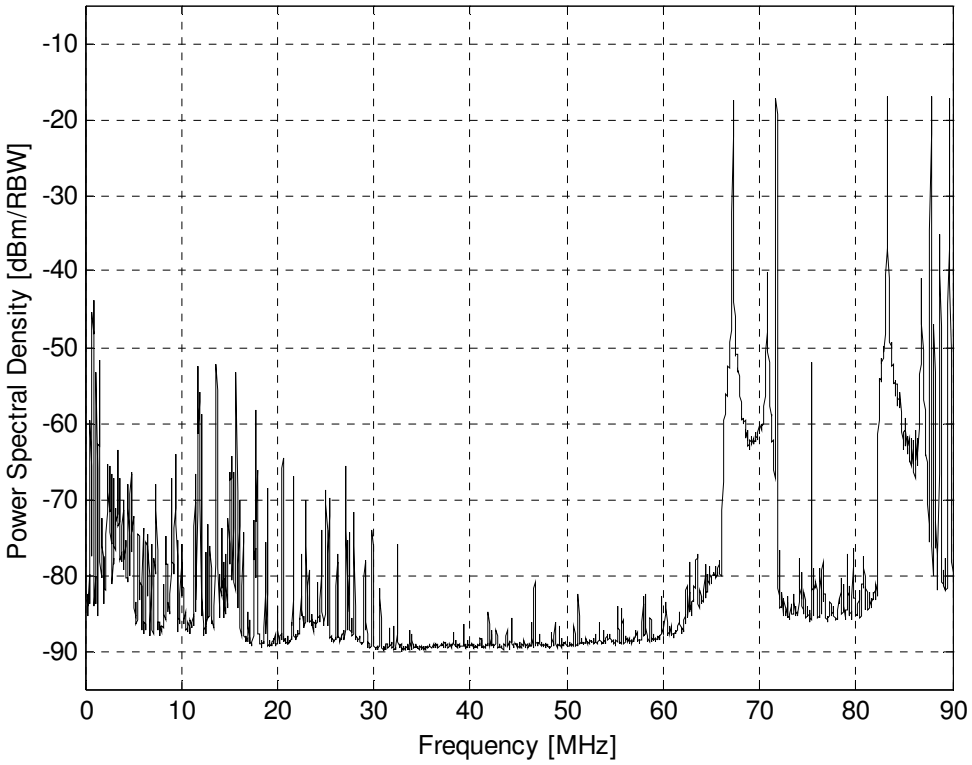

Figure 3.16. Measurement in the VHF band, corresponding to a "business" environment. RBW = 30 kHz. [9]

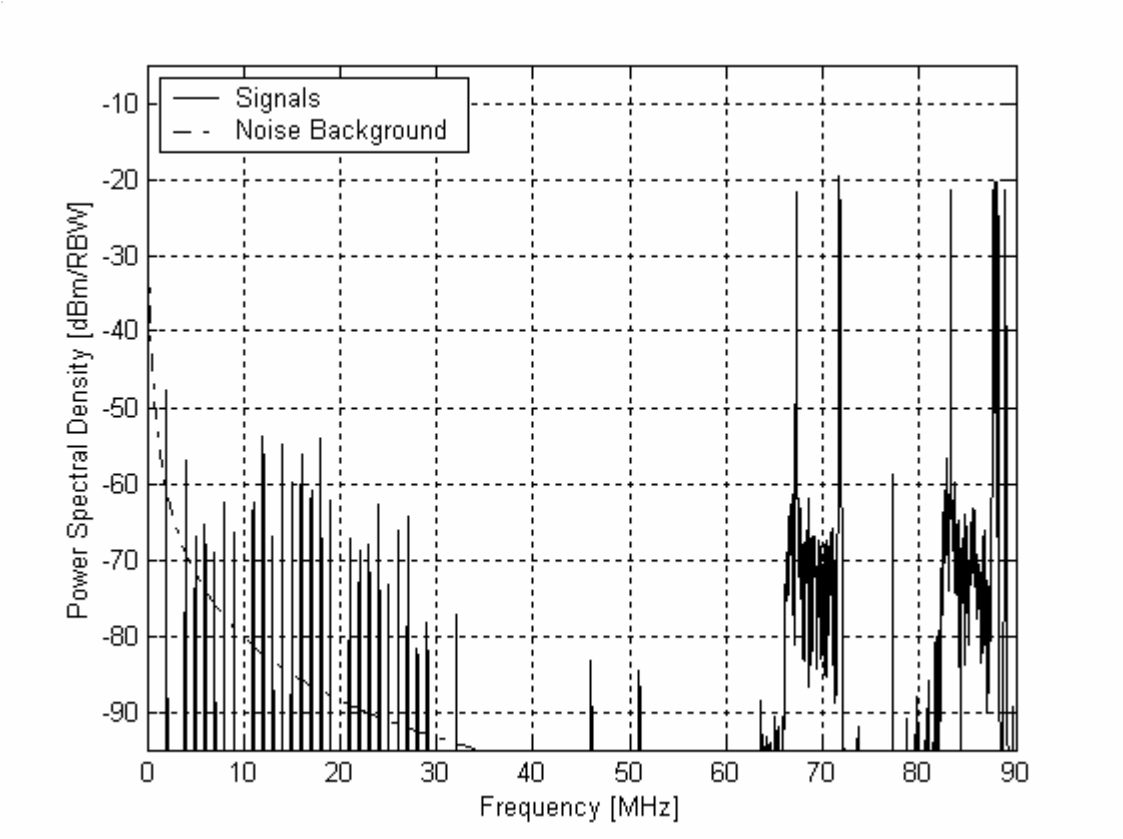

Figure 3.17. Synthesized business spectrum, RBW = 30 kHz.

Table 3.2. Frequency-Power data for “business” spectrum.

Frequency [MHz]	Power [dBm]	Source
2	-45	Shortwave HF
4	-55	Shortwave HF
5	-65	Shortwave HF
6	-63	Shortwave HF
7	-67	Shortwave HF
8	-60	Shortwave HF
9	-64	Shortwave HF
11	-60	Shortwave HF
12	-52	Shortwave HF
13	-65	Shortwave HF
14	-53	Shortwave HF
15	-59	Shortwave HF
16	-54	Shortwave HF
17	-58	Shortwave HF
18	-52	Shortwave HF
19	-60	Shortwave HF
21	-65	Shortwave HF
22	-66	Shortwave HF
23	-66	Shortwave HF
24	-61	Shortwave HF
25	-71	Shortwave HF
26	-64	Shortwave HF
27	-61	Shortwave HF
28	-79	Shortwave HF
29	-77	Shortwave HF
32	-75	2-Way Radio
46	-81	2-Way Radio
51	-83	2-Way Radio
67.25	-15	TV Channel 4
71.75	-15	TV Channel 4
77.25	-52	TV Channel 5
81.75	-75	TV Channel 5
83.25	-15	TV Channel 6
87.75	-15	TV Channel 6
88.1	-18	FM Station
88.9	-19	FM Station

3.6 Summary

The three primary components of the VHF spectrum are the Galactic background, anthropogenic noise, and manmade interferers. This chapter presented models for these sources that are suitable for spectrum simulation. The ability to simulate the spectrum due to signal sources using these models was verified, albeit with some limitations, by comparison with an actual VHF measurement. The ITU model for Galactic noise was verified by comparison to theoretical and measured results. Thus, the combined signals and noise model provides a tool for better-informed design of wideband direct sampling receivers. The transfer of the power spectral density captured by the antenna to the preamplifier is considered in the next chapter.

Chapter 4 Antenna Matching

4.1 Introduction

One of the design challenges identified in Chapter 2 was that the antennas used for wideband receivers are often narrowband themselves. This may result in the need for compensation for the wide range of impedances presented by the antenna. This compensation can be implemented by placing a matching network at the input of the preamplifier, as shown in Figure 4.1. The matching network has two functions: 1) to cancel the reactance difference between the source and the load; 2) to then equalize the resistance difference between source and load, allowing for efficient power transfer. Wideband matching network design is a difficult task, which will be further covered in this chapter. Section 4.2 will examine the fundamental limitations on matching networks. Section 4.3 will explore matching network techniques, and it will be shown that a suitable wideband matching technique is not readily available. Recognizing this, Section 4.4 will evaluate the receiver's performance if no matching network is used. Finally, Section 4.5 presents an example that demonstrates that "no match" performance can be acceptable under conditions which are easily achieved in the VHF low band.

4.2 Theoretical Limits

There are two constraints that will provide insight into the theoretical limitations on matching network performance: the Bode-Fano Bound and Foster's Reactance Theorem. The Bode-Fano Bound defines the trade-off between the gain and bandwidth of a matching network, whereas Foster's Reactance Theorem reveals the fundamental reason that wideband matching to antennas is so difficult.

4.2.1 Bode-Fano Bound

Initially, it would seem that a perfect match could be obtained for an unlimited amount of bandwidth. There exists, however, a trade-off between the bandwidth of a matching circuit and the gain through that matching circuit, and this trade-off has been described by Bode and Fano [10]. If a parallel RC circuit is to be matched to a resistive load, then the Bode-Fano bound is given by

$$\int_{\omega=0}^{\infty} \ln\left(\frac{1}{|\Gamma|}\right) d\omega \le \frac{\pi}{RC} \tag{36}$$

where Γ, the reflection coefficient, is given by

$$\Gamma = \frac{Z_M - Z_A}{Z_M + Z_A} \tag{37}$$

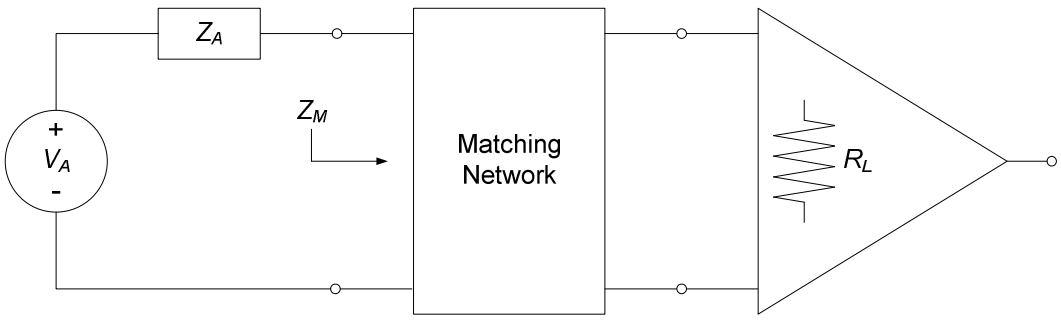

Figure 4.1. Circuit model for matching network analysis. When no matching network is used, $Z_M=R_L$.

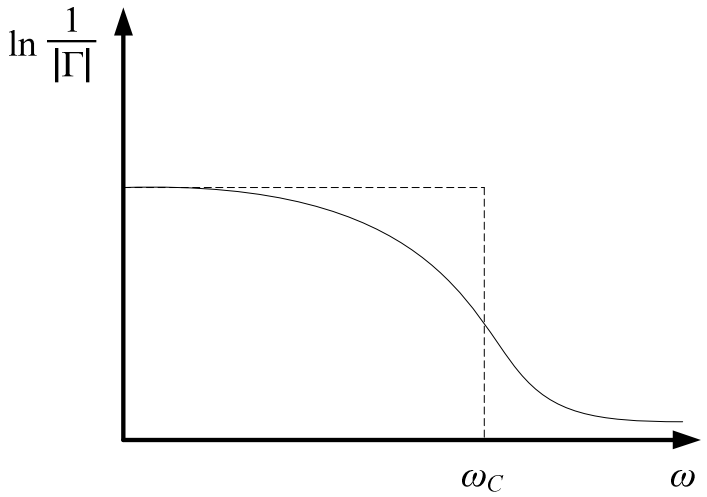

Figure 4.2. Visualization of the Bode-Fano limitation for a parallel RC circuit.

and Z_M is the input impedance of the matching network. Insight into the significance of the Bode-Fano equation can be gained by examining Figure 4.2. The Bode-Fano bound indicates that the area under the curve is bounded by

$$\text{Area Under Curve} \leq \frac{\pi}{\text{RC}} \tag{38}$$

There are two insights that can be gained from Equation (38). First, to obtain the best possible match over the widest bandwidth, the reflection coefficient should be equal to one outside of the passband. This allows for $|\Gamma|$ to be minimized inside the passband. Second, if the bandwidth needs to be increased, this can be done only by decreasing the gain (i.e. increasing $|\Gamma|$) through the matching circuit in the passband. When Equation (36) is analyzed using the assumptions that the reflection coefficient is *constant* in the passband and zero out of the passband, the resulting solution for the best attainable $|\Gamma|$ is

$$|\Gamma| = e^{\frac{-\pi}{\omega_C RC}} \tag{39}$$

Thus, it is seen that the effectiveness of a matching circuit which is constrained to have constant gain over its bandwidth decreases as that bandwidth increases. A second issue is that a network that obtains this constant |Γ| requires an infinite number of components, because the transition from passband to stopband is a step function.

This result generalizes to passive circuits containing arbitrary combinations of resistors, inductors, and capacitors. Thus, the consequences when matching to a more complex model (such as the TTG dipole model) are the same. In each case, equations similar to Equations (38) and (39) can be derived, which explicitly define the limits on the matching network's performance for a given bandwidth.

4.2.2 Foster's Reactance Theorem

Foster's Reactance Theorem [11] states that the first derivative of the reactance of a passive lossless circuit with respect to frequency is always positive. This is obvious for single inductors and capacitors, as shown in Equations (40) and (41).

$$Z_L = j\omega L; \qquad \frac{d}{d\omega} Z_L = jL \tag{40}$$

$$Z_C = \frac{-j}{\omega C}; \qquad \frac{d}{d\omega} Z_C = \frac{j}{\omega^2 C} \tag{41}$$

The effect of the introduction of loss (e.g., radiation, in the case of an antenna) is to smooth the discontinuity between frequencies at which the reactance transitions from asymptotically large (+∞) to asymptotically small (-∞); in those regions the slope of the reactance can be negative. This has implications for the design of antenna matching circuits, as will now be explained.

Assuming the preamplifier's input impedance is purely resistive (typical for commercially-available wideband amplifiers), the matching circuit should cancel the reactance presented by the antenna over the desired bandwidth. Consider the reactance of the dipole was shown in Figure 2.7. The antenna reactance and the corresponding input reactance desired for an ideal matching circuit are shown in Figure 4.3. Note that the dipole's reactance exhibits a positive slope below about 75 MHz. Thus, the corresponding ideal matching circuit's input reactance has a negative slope for the same frequency range. The consequence of Foster's Theorem is that the ideal matching circuit is impossible to attain using only passive lossless reactive components, such as capacitors and inductors. While it is possible for the matching circuit to cancel the reactance exactly at one frequency, it is not possible to cancel the reactance exactly over a range of frequencies. Thus the matching circuit fails to accomplish one of its two stated goals.

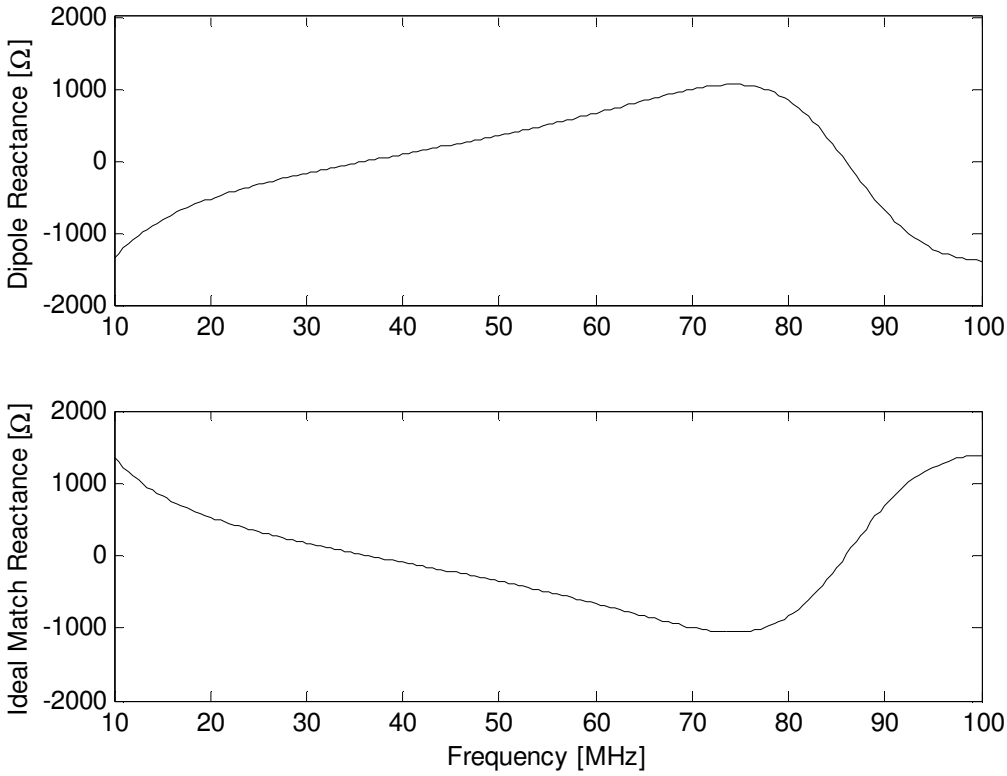

Figure 4.3. Dipole reactance from Figure 2.7 and the corresponding ideal matching circuit input reactance.

There are two ways to avoid this problem: to use active elements in the matching circuit, or, to include a resistor(s) is the matching circuit. However, these are both usually undesirable solutions. Including active elements greatly complicates the design and may introduce the stability, linearity, and noise problems that are associated with active device design. This is left as a problem for future research. Including resistors in a passive matching circuit is going to increase loss, which both raises noise temperature (affecting sensitivity) and decreases the realizable gain.

The best alternative for a match to a simple antenna may be to settle for a good match at one frequency and a degraded match (reduced efficiency) over a range of frequencies. When better performance is required, the antenna must be modified to have a flatter reactance over the desired bandwidth. Overcoming the limitations produced by the Foster Reactance Theorem is an issue that makes wideband matching to simple antennas very difficult.

4.3 Wideband Matching Techniques

The Bode-Fano Bound and Foster Theorem work together to limit the performance of passive wideband matching between simple antennas and preamplifiers. However, it is not yet

clear if a passive match can be used to optimize a tradeoff between bandwidth and gain efficiency. This possibility is considered next.

The Chen procedure is a popular method that results in a low pass match between a resistive source and a load with complex impedance [12]. Since the resulting circuit is passive, it is reciprocal, and therefore the procedure also applies to a source with complex impedance and a resistive load. The procedure is summarized in Appendix D. While the methodology often works well, it is limited by the fact that it is only valid when the complex impedance can be modeled by certain canonical circuit topologies; namely: parallel RC, parallel RC with series L, and certain others. As discussed in Appendix D, the procedure fails for various other circuit topologies, including series RC, and, unfortunately, the TTG circuit model. The inability of the Chen procedure to match the circuit shown in Figure 2.5 to a resistive load has been confirmed [13]. Since the Chen procedure fails to produce a matching circuit applicable to the dipole model, we conclude that is unlikely that any passive matching circuit can significantly improve the bandwidth-gain efficiency tradeoff in the wideband case.

4.4 No Match Performance

Assuming that redesigning the antenna or implementing an active match are not options, the best approach may be simply canceling the reactance at one frequency, e.g. the center frequency. Recall that the reactance of an antenna at resonance is zero, and the resistance of a dipole at resonance is about 70 Ω, which is close to the standard input impedances of commercially-available wideband amplifiers. Therefore, if the resonant frequency of the antenna and the desired "matched" frequency of the receiver are the same, the best matching may be simply to have no matching circuit. In this case the hope is that the mismatch away from resonance is not so great as to unacceptably degrade sensitivity. This section demonstrates that this is typically the case in the VHF low band.

The impedance mismatch efficiency, η, is defined as the fraction of the power provided by the antenna that is delivered to the preamplifier.

$$\eta = 1 - \left|\Gamma\right|^2 \tag{42}$$

The voltage standing wave ratio, ρ, is given in terms of Γ by

$$\rho = \frac{1+\left|\Gamma\right|}{1-\left|\Gamma\right|} \tag{43}$$

Resulting in

$$\eta = \frac{4\rho}{(1+\rho)^2} \tag{44}$$

The power spectral density provided to the load, S_L, is given by

$$S_L = \eta S_{SKY} \tag{45}$$

where S_{SKY} is given in Equation (26).

S_O, the power spectral density at the output of the preamplifier, is then given by

$$S_O \approx e_r \eta (1+m) k T_{SKY} G_{AMP} \tag{46}$$

where e_r is the efficiency of the antenna, and m is a parameter that accounts for additional manmade noise. This is justified in Figure 3.3, which showed that the Galactic background has approximately the same frequency dependence as anthropogenic noise. Assuming a lossless antenna, the efficiency is equal to one. m depends on the strength of the manmade noise, which, as shown in Figure 3.3 varies from 0.3 to 100 (an m of 0 indicates that only the Galactic background is present).

The preamplifier-generated noise at the output of the preamplifier is given by

$$N_O = k T_{AMP} G_{AMP} \tag{47}$$

where T_{AMP} is the noise temperature of the preamplifier. The ratio α of total external noise to amplifier noise is then given by

$$\alpha = \frac{S_O}{N_O} = e_r \eta (1+m) \frac{T_{SKY}}{T_{AMP}} \tag{48}$$

This result places a constraint on T_{AMP} if a known α is desired. This constraint is given by

$$T_{AMP} \le e_r \eta (1+m) \frac{T_{SKY}\Big|_{f_{MAX}}}{\alpha} \tag{49}$$

where T_{SKY} is evaluated at the maximum frequency of interest because T_{SKY} decreases with increasing frequency. Consider a receiver with a desired α of 5, using a lossless antenna (e_r=1), operating at a maximum frequency of 100 MHz in an environment where m=1. At 100 MHz, T_{SKY} is approximately 825 K. If the match is perfect (η=1, ρ=1) then T_{AMP} must be below 330 K to meet the specification on α. If a more realistic match is considered (η=0.5, ρ=5.83), then T_{AMP} must be below 165 K. As the requirements on α increase, it is easily seen that T_{AMP} will need to become quite small to satisfy the specifications. This finding implies that the ultimate limitation on system bandwidth in practice may be T_{AMP}. This is shown in Figure 4.4 which shows S_O and N_O for various η and demonstrates that α decreases with increasing frequency.

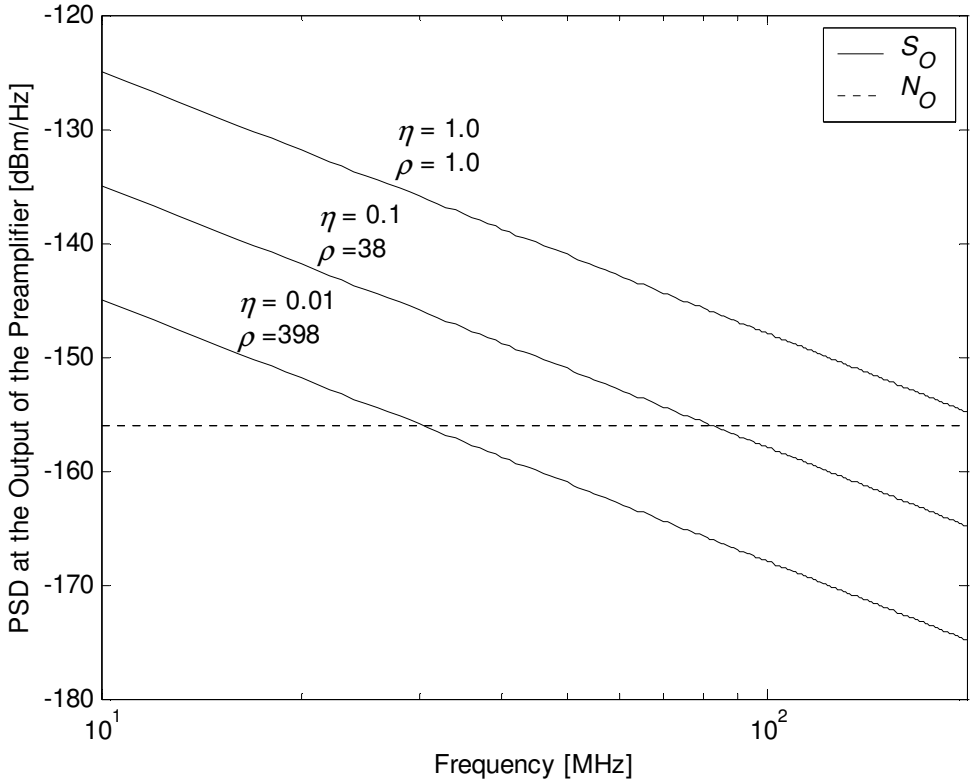

Figure 4.4. Power spectral density at the output of the preamplifier over a range of η. Here, $e_r = 1$, G_{AMP} = 17 dB, $T_{AMP} = 360$ K, and $m = 1$.

4.5 Example Receiver

The implications of this analysis can be seen by considering a simple example receiver. The receiver consists of the dipole antenna modeled in Figure 2.6 connected directly to an amplifier with a Z_L of 50 Ω, T_{AMP} of 360 K, and G_{AMP} of 17 dB. The η of this receiver is shown in Figure 4.5. For comparison, the result for other values of Z_L is also shown. Note that for Z_L of 50 Ω, $\eta \sim 1$ at 38 MHz, which is the expected result when the antenna's resonant frequency is the same as the receiver's center frequency. However, as Z_L is increased, the frequency of peak efficiency increases, peak η decreases, but the bandwidth also increases. This is a potentially simple way to broaden the usable bandwidth if the degradation in η (with respect to its value at resonance) is acceptable. Z_L can easily be increased using a transformer, albeit at the risk of introducing additional loss.

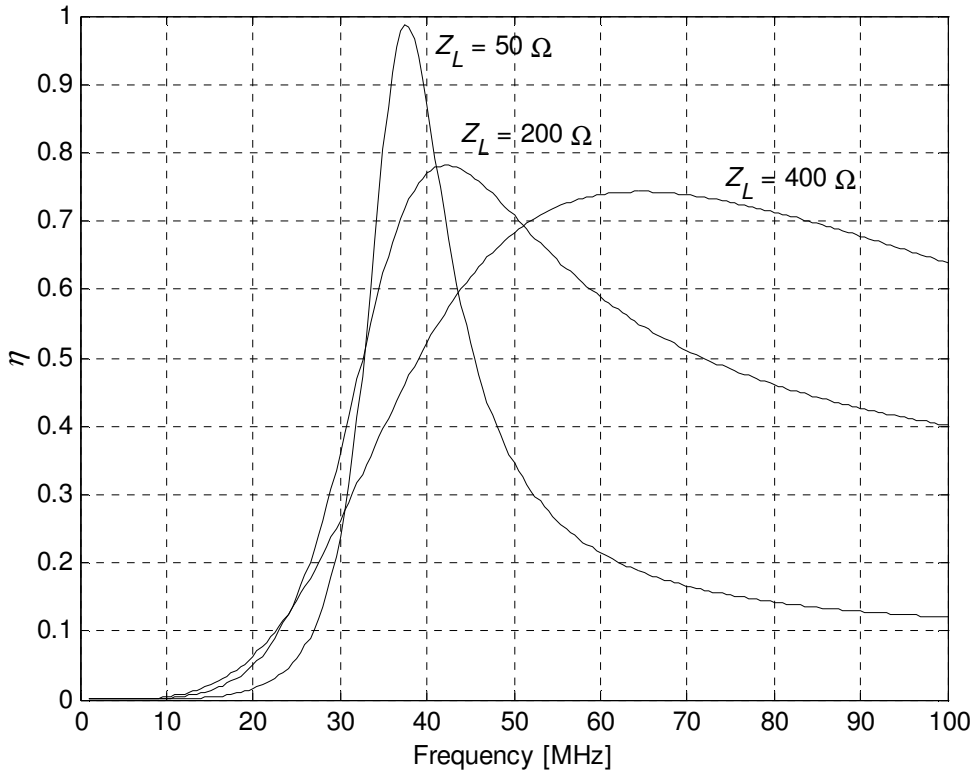

Figure 4.5. η of the example receiver chain, as well as for other values of Z_L.

The α of the receiver under the same circumstances is shown in Figure 4.6. Again, it is noted that as R_L is increased, peak α decreases, but the bandwidth increases. Also, the center frequency of α does not change. Since α is greater than 10 dB for a wide passband, using Z_L equal to 200 or 400 Ω may be a possible way to widen the bandwidth of this receiver. The analysis shows that the receiver exhibits potentially useful performance despite the lack of a matching network.

4.6 Summary

The constraints presented by the Bode-Fano Bound and Foster Theorem make wideband matching between narrowband antennas and wideband amplifiers ineffective. However, it has been shown that in the case where no matching circuit is used, the antenna and amplifier system can nevertheless be strongly limited be external noise, which makes improved matching irrelevant. It has been demonstrated that the "no match" case can in fact yield acceptable sensitivity (i.e. α > 10 dB or so) under conditions that are commonly achieved in the VHF low band.

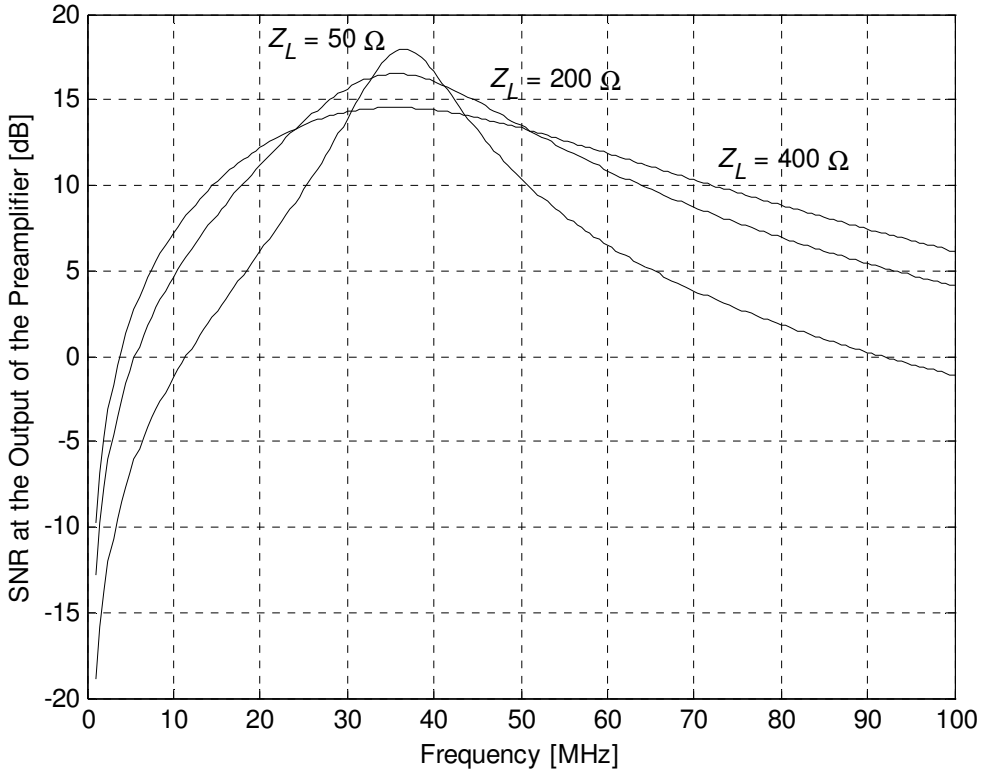

Figure 4.6. α of the example receiver: 38 MHz dipole antenna; preamplifier with T_{AMP} = 250 K. e_r = 1 and m = 0.3.

Chapter 5 Linearity Analysis

5.1 Introduction

As noted in Section 2.1, the nonlinearity of components in the receiver chain can be significant. In this chapter, a method is developed for characterizing the effect of nonlinearity in terms of blocked spectrum. Section 5.2 describes a method for modeling the transfer function of a nonlinear component or cascade of components. In Section 5.3 the effect of the nonlinear response on the received power spectral density is characterized. Finally, in Section 5.4 the effect of nonlinearity is evaluated using measured data.

5.2 Linearity Modeling

The linearity model shown in Equation (3) will be further investigated here. This model is a truncated Maclaurin series that often only needs three terms to be accurate. To model an amplifier, the output power as a function of input power must first be measured. An initial estimate for the values of *A*, *B*, and *C* is then made by curve fitting. Through trial and error these values will be modified until the model accurately represents the observed behavior.

One amplifier system that has been successfully modeled using this technique is an active balun [14] based on the Mini-Circuit's GALI-74 amplifier[1]. A block diagram of the active balun is shown in Figure 5.2. It has been found to have G = 24.5 dB, OIP_3 = 32 dBm, $P_{I,1dB}$ = -5 dBm, and F = 2.7 dB [14]. The Maclaurin series shown in Equation (50) has been found to reasonably model the active balun's nonlinear power transfer response up to about -10 dBm. [15]

$$y = 11.75x + 0.6x^2 - 9x^3 \qquad [\sqrt{\text{mW}}] \tag{50}$$

Figure 5.2 shows this amplifier's ideal linear response, additional measured data points above $P_{I,1dB}$, and the nonlinear model. From this plot it can be seen that the nonlinear model accurately represents the amplifier for input powers up to about -10 dBm, but does a poor job above that level. However, this is acceptable because it is not anticipated that the amplifier will be operated at or above that power, since it would then be in compression. Another limitation of this model is that it is difficult to find coefficients for which the resulting IP_2 and IP_3 are independent of input power. For example, Equation (50) yields OIP_3 = 46.1 dBm when extrapolated from the results for input power equal to -29 dBm, but also yields OIP_3 = 31.7 dBm (i.e., very close to the measured value of 32 dBm) when extrapolated from the results for input power equal to -17.9 dBm. In practice, however, this amount of variation does not significantly affect the results presented below.

[1] Information available at http://www.minicircuits.com/dg03-166.pdf.

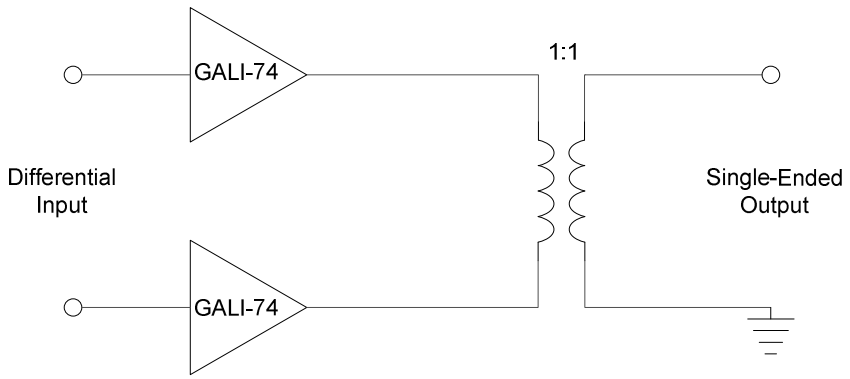

Figure 5.1. Active balun based on the GALI-74 amplifier.

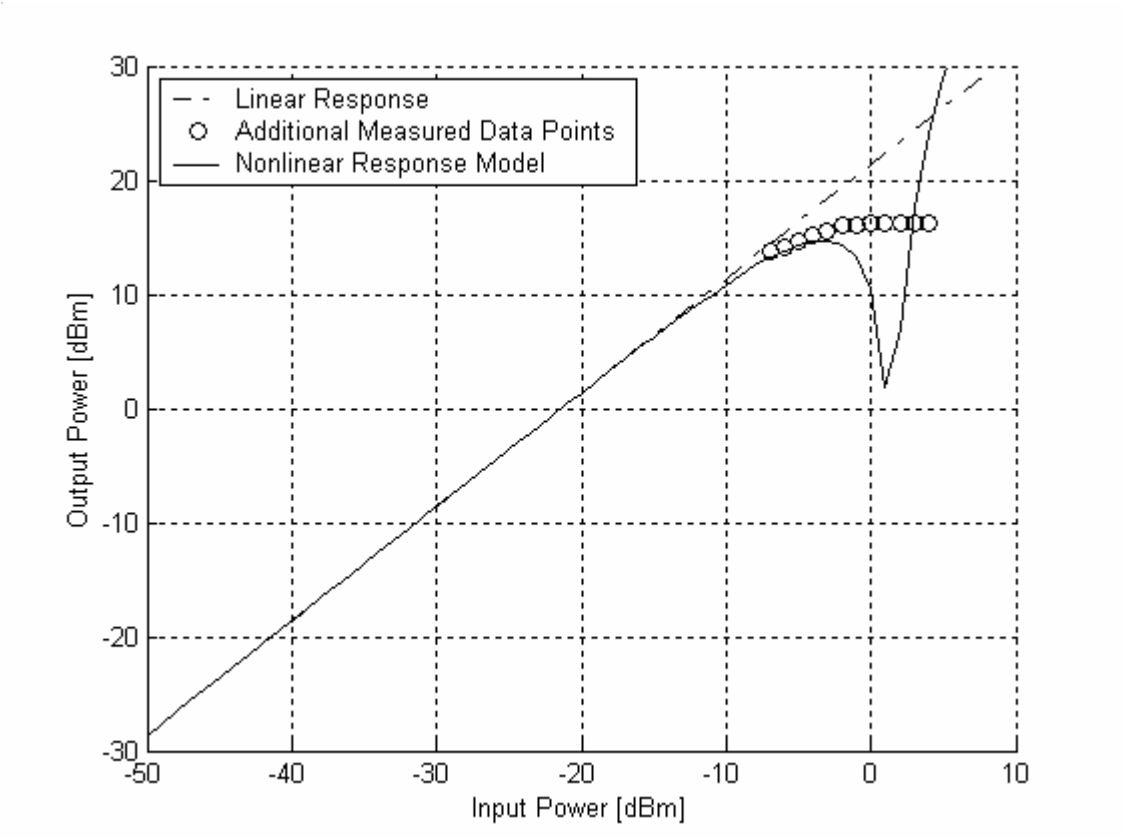

Figure 5.2. Ideal linear response, measured response, and nonlinear model of the active balun in Figure 5.1, measured data points above -10 dBm shown as "o".

Furthermore, it seems appropriate that the model should accurately predict the measured IP_3 for input power close to worst case (i.e., high) levels, which is the case for this example. The model produces G = 21.4 dB, $P_{I,1dB}$ = -8 dBm, and OIP_3 = 26 dBm, which are reasonably close to the measured values reported in [14].

5.3 Analysis of Intermodulation Blocking by Simulation

As described in Section 2.1, nonlinear behavior in a receiver is generally characterized by P_{1dB}, IP_2, and IP_3. While this is still useful for the wideband case, it does not always accurately depict the full ramifications of the nonlinear response. A more complete model of the nonlinear response can be obtained by observing how much of the spectrum has been blocked by intermodulation. In this analysis, a frequency bin is declared blocked if the spectral content due to intermodulation or existing signals in that bin has a power spectral density than the noise present in the same bin. It is convenient to represent this measure as a fraction that relates the number of bins blocked in the desired passband to the total number of bins in the desired passband, and this metric will be referred to as $B_{Blocked}$.

5.4 Examples of the Analysis

A simple example to illustrate this analysis proceeds as follows. Given the spectrum described in Table 5.1, and assuming the noise background is "rural" (m=6), a spectral representation can be synthesized, as shown in Figure 5.3. The desired passband in this case is the entire VHF low band, 30 to 100 MHz.

Calculating the number of blocked bins in the spectrum of interest at the input to the active balun results in a $B_{Blocked}$ of 18.9%, with respect to the spectral resolution (RBW) of 12.207 kHz. By applying the nonlinearity model in Equation (50), a model for the signal present at the output of the active balun is obtained. This spectrum, normalized for the gain of the active balun, is shown in Figure 5.4.

Calculating the number of blocked bins in the spectrum at the output of the active balun results in a $B_{Blocked}$ of 20.8%, with respect to the spectral resolution (RBW) of 12.207 kHz. Recall the spectrum at the input of the active balun had a $B_{Blocked}$ of 18.9%, meaning that the intermodulation generated by the active balun has resulted in an additional 1.9% of the spectrum being blocked.

It should be recognized that the RBW affects this metric. Consider the most extreme case where there is only one frequency bin, the result would be 100% blocking. Conversely, increasing the number of frequency bins (i.e. decreasing RBW) will most likely result in a decreased $B_{Blocked}$. In this thesis the RBW is on the order of tens of kHz, which is reasonably well matched to the bandwidths of the signals present in this frequency range.

Table 5.1. Spectrum for example nonlinear analysis.

Frequency [MHz]	Power [dBm]	Source
7.00	-50	Shortwave HF Broadcast
11.00	-70	Shortwave HF Broadcast
12.00	-60	Shortwave HF Broadcast
15.00	-45	Shortwave HF Broadcast
21.00	-50	Shortwave HF Broadcast
22.00	-40	Shortwave HF Broadcast
25.00	-60	Shortwave HF Broadcast
29.00	-55	Shortwave HF Broadcast
42.00	-75	2-Way Radio
55.25	-55	TV Channel 2 Video
59.75	-65	TV Channel 2 Audio
67.25	-30	TV Channel 4 Video
71.25	-40	TV Channel 4 Audio
89.10	-35	FM Station
92.30	-45	FM Station

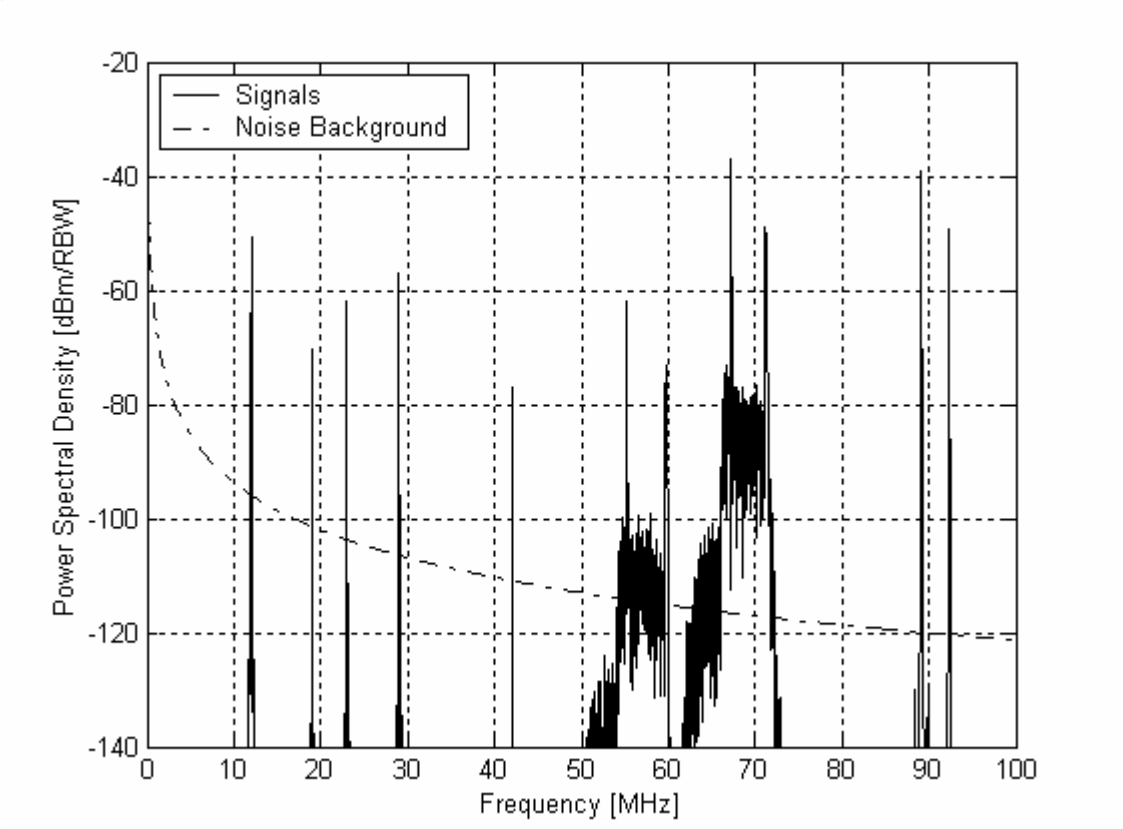

Figure 5.3. Representation of spectrum described in Table 5.1. RBW = 12.207 kHz.

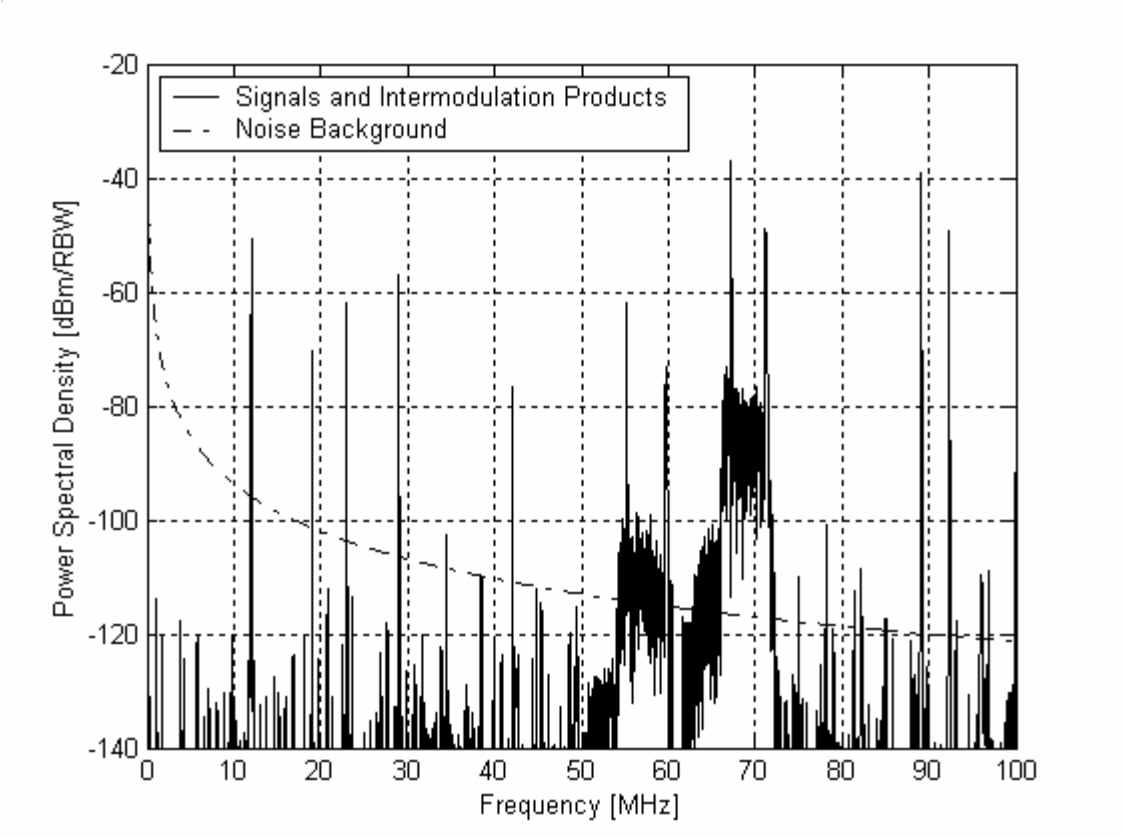

Figure 5.4. Representation of the example spectrum after the nonlinear behavior is applied, with power referenced to the antenna terminals. RBW = 12.207 kHz.

5.5 Summary

The nonlinear behavior of the receiver's components (and thus the receiver) can be reasonably well modeled with a truncated Maclaurin series. This model can then be applied to a spectral environment, which allows for insight into how the nonlinear behavior affects the received spectrum. Specifically, the $B_{Blocked}$ for an environment can be calculated, which shows the percentage of the spectrum that has been blocked.

Chapter 6 Receiver Design and Examples

6.1 Introduction

The issues associated with the design of wideband direct sampling receivers have been explored in the previous chapters. Taking these issues into consideration, a methodology for the analysis and design of such receivers will now be presented. Three receivers are designed and analyzed using this methodology.

6.2 Design Methodology

Inputs to the methodology are the following: 1) the antenna impedance vs. frequency (per Section 2.2.1), 2) the desired passband of the receiver, 3) the anticipated noise and signal environment the receiver will operate in (per Chapter 3), and 4) requirements for headroom (δ_r), signal to quantization noise ratio (γ_q), and so on (per Section 2.2.5). The methodology then proceeds as follows:

Step 1: The antenna to preamplifier interface should be analyzed to verify that the bandwidth requirement can be met using a simple matching network; i.e., one which is matched only in a narrowband sense. This is done by calculating the signal to noise ratio at the preamplifier output (α) as described in Section 4.4. If α is too low at this point, then a better antenna or active matching is needed.

Step 2: Determine the ADC specifications. The sampling rate should be at least twice the highest frequency for lowpass sampling or twice the bandwidth for bandpass (under-) sampling. In practice, however, the ADC should sample somewhat faster than this to allow for filter roll off. The minimum number of bits can be calculated using Equation (18). A candidate ADC is then selected. If the receiver chain is single-ended but the ADC has differential input, then one may want to insert a transformer at its input. This will both give the designer some additional control over the P_{clip} value and will present a differential signal to the ADC, which will typically improve its performance. It should be noted that unless the turns ratio is 1:1, transformer coupling will change the input impedance of the ADC, which complicates the gain calculation. Here, this will be accommodated by defining the ADC input to be the input to the transformer, and then to define P_{clip} and G_r at that point.

Step 3: Determine the nominal receiver gain using Equation (14).

Step 4: If the spectrum of interest is expected to be signal source (e.g. RFI) dominated then gain control through variable attenuation may be needed. The minimum useful gain is that which results in external noise greater than quantization noise by γ_q, i.e.

$$G_{MIN} = \frac{P_Q \gamma_q}{P_{ext}} \tag{51}$$

Variable attenuation is then designed such that the receiver gain can be varied from G_r to G_{MIN}.

Step 5: With the nominal gain and gain control requirements determined, an initial choice and arrangement of amplifiers, attenuators, and filters can be made.

Step 6: Determine the linearity (i.e., P_{1dB}, IP_2, IP_3) and sensitivity (F) using the GNI analysis in Appendix B, taking into account the possible filtering of signals and intermodulations products at each stage. Some substitution or reordering of components may be required to achieve acceptable performance at this point.

Step 7: Using the method presented in Chapter 5, determine the amount of blocking due to intermodulation in the anticipated spectral environment. Repeat steps 5 to 7 as needed until performance specifications are met.

Examples of the application of this methodology to various receiver designs are now considered.

6.3 Example: ETA

The Eight Meter Transient Array (ETA) is a radio telescope intended to operate over the 29 to 47 MHz band at a remote rural site in North Carolina [16]. The antenna is a 38 MHz resonant inverted-V shaped dipole antenna. In terms of the TTG model (not exactly appropriate since the antenna is not a straight dipole, but probably close enough for this analysis) h=1.88 m and a=0.019 m. It is known that the dominant source of external noise at the ETA site is the Galactic background. However, there are strong signal sources as described in Table 6.1. The desired α and γ_q are both 10 dB in the passband.

The methodology will now be applied to the ETA receiver.[1]

Step 1: The TTG model for this antenna is shown in Figure 6.1 and the frequency response is shown in Figure 6.2. The antenna to preamplifier interface can now be considered. The α for several values of preamplifier input impedance (Z_L) is shown in Figure 6.3. For now, T_{AMP} is assumed to be 250 K. Note that for all three values of Z_L the specification on α is met, so any of the three values are acceptable. For simplicity, the value of Z_L is chosen to be 100 Ω. Because the dipole presents a differential signal, a differential preamplifier will be used. If the two amplifiers in this circuit each have an input impedance of 50 Ω, such that the total (differential) input impedance is 100 Ω, no transformers will be needed at this stage, which is desirable.

[1] It should be noted that in the time since the work on this thesis was begun, the ETA receiver design has evolved such that the details are different from what is presented here. The design concepts and principles are the same, however.

Table 6.1. Spectrum for the ETA receiver, presented to the antenna.

Frequency [MHz]	Power [dBm]	Source
6.00	-55	Shortwave HF Broadcast
8.00	-75	Shortwave HF Broadcast
10.00	-80	Shortwave HF Broadcast
12.00	-70	Shortwave HF Broadcast
13.00	-85	Shortwave HF Broadcast
15.00	-97	Shortwave HF Broadcast
17.00	-93	Shortwave HF Broadcast
20.00	-95	Shortwave HF Broadcast
22.00	-90	Shortwave HF Broadcast
25.00	-90	Shortwave HF Broadcast
26.00	-85	Shortwave HF Broadcast
27.00	-87	Shortwave HF Broadcast
42.00	-85	2-Way Radio
55.25	-80	TV Channel 2 Video
59.75	-110	TV Channel 2 Audio
61.75	-70	TV Channel 3 Video
65.75	-95	TV Channel 3 Audio
67.25	-42	TV Channel 4 Video
71.25	-45	TV Channel 4 Audio
92.3	-45	FM Station
94.1	-40	FM Station

Step 2: The highest frequency the ETA receiver needs to receive is 47 MHz. For lowpass sampling, this requires an ADC with a minimum sampling frequency of 94 MSPS. The sample rate for ETA was selected to be 120 MSPS, which allows ample additional bandwidth for filter roll off. The minimum number of bits can now be calculated. P_{ext} for the Galactic background in the ETA bandwidth is about -85.5 dBm. P_S in the ETA bandwidth is about -80 dBm, resulting in a P_t of about -79 dBm. The minimum number of bits is given by

$$N_b \geq 1.67 \log_{10}\left(\frac{P_t}{P_{ext}}\frac{\gamma_q}{\delta_r}\right) = 1.67 \log_{10}\left(\frac{(-79\,\text{dBm})(10\,\text{dB})}{(-85.5\,\text{dBm})(-10\,\text{dB})}\right) = 4.43 \qquad (52)$$

Thus, an ADC with 5 or more effective bits should suffice. A commercially available ADC that meets these requirements and is used in the actual ETA design is the Analog Devices AD9433[1], which has 12 bits, yielding a conservative design. A 1:4 transformer is placed at the AD9433 input, with a 200 Ω resistor in parallel on the ADC side. Since

[1] Information available at http://www.analog.com/en/prod/0%2C%2CAD9433%2C00.html

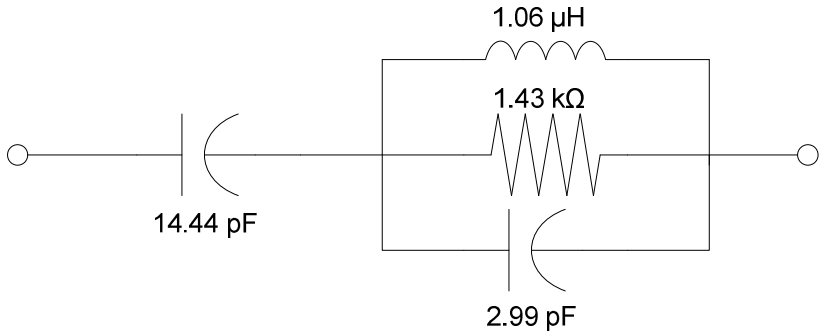

Figure 6.1. TTG model for the ETA 38 MHz dipole antenna.

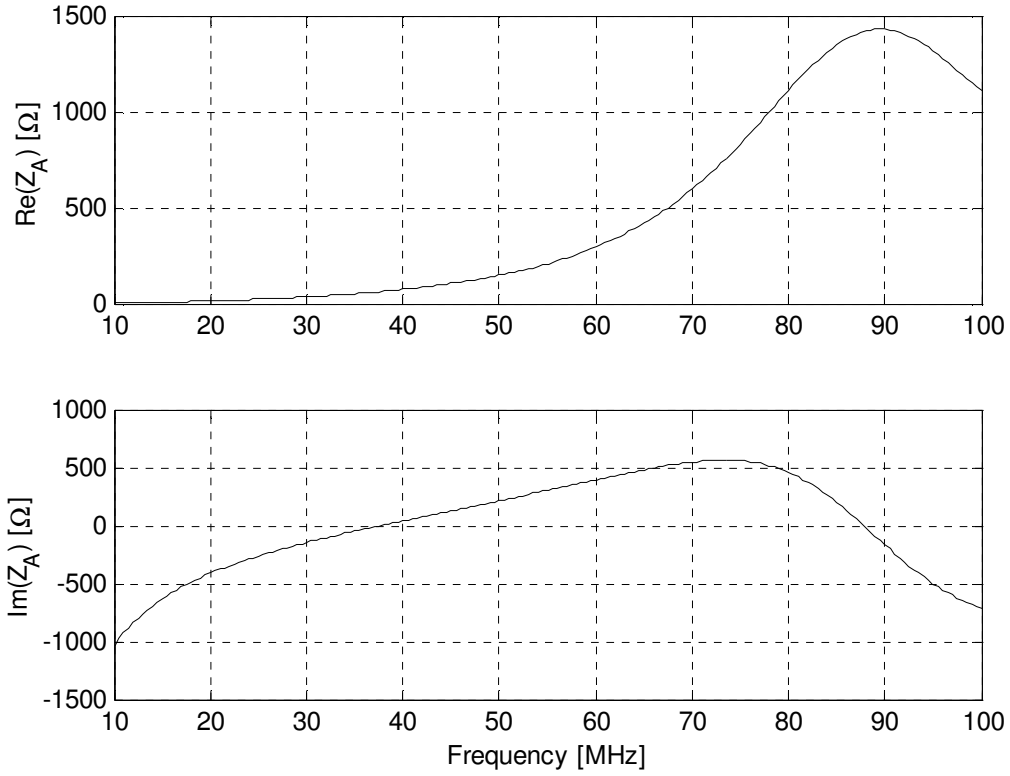

Figure 6.2. Frequency response of the TTG model for the ETA antenna.

the input impedance of the AD9433 is 3kΩ, the equivalent parallel impedance is still about 200 Ω. This results in a P_{clip} of about 4 dBm at the input of the transformer.

Step 3: The nominal gain can now be determined

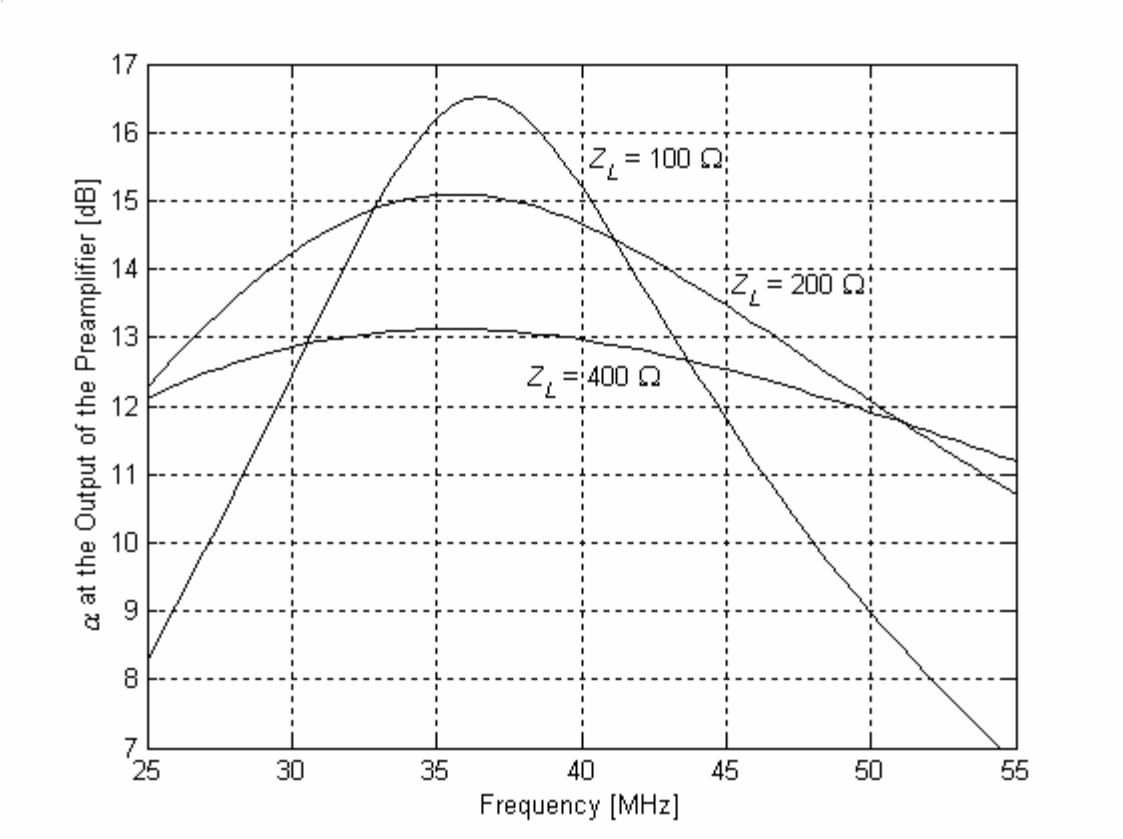

Figure 6.3. α for various values of Z_L using the ETA antenna, T_{AMP} = 250 K.

$$G_r = \frac{P_{clip}\delta_r}{P_t} = \frac{(4\,\text{dBm})(-10\,\text{dB})}{(-79\,\text{dBm})} = 73\,\text{dB} \tag{53}$$

Step 4: The low end of the attenuation needed for the ETA receiver can be calculated

$$G_{MIN} = \frac{P_Q\gamma_q}{P_{ext}} = \frac{(-68\,\text{dBm})(10\,\text{dB})}{(-85.5\,\text{dBm})} = 28\,\text{dB} \tag{54}$$

Step 5: The gain will be divided into three stages, each with about 25 dB of gain. The preamplifier shown in Figure 5.1 will be used, and the GALI-74 amplifier mentioned in Section 5.2 is a sufficiently wideband amplifier with a 50 Ω input impedance and 25.1 dB of gain that can be used for the other two stages. There is also a long coaxial cable between the preamplifier and the rest of the receiver chain, which contributes 4 dB of loss, and therefore should be considered.

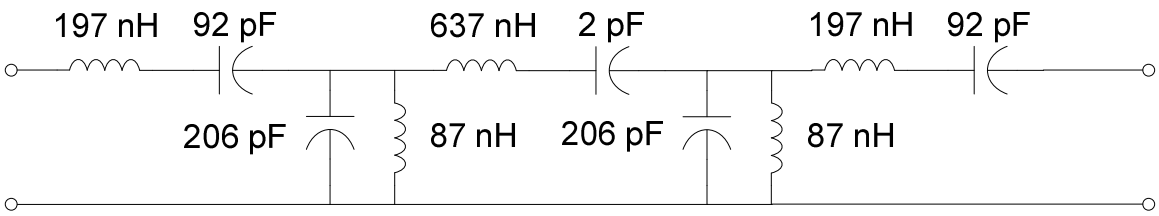

Figure 6.4. 5th order Butterworth filter network, 29 – 47 MHz passband.

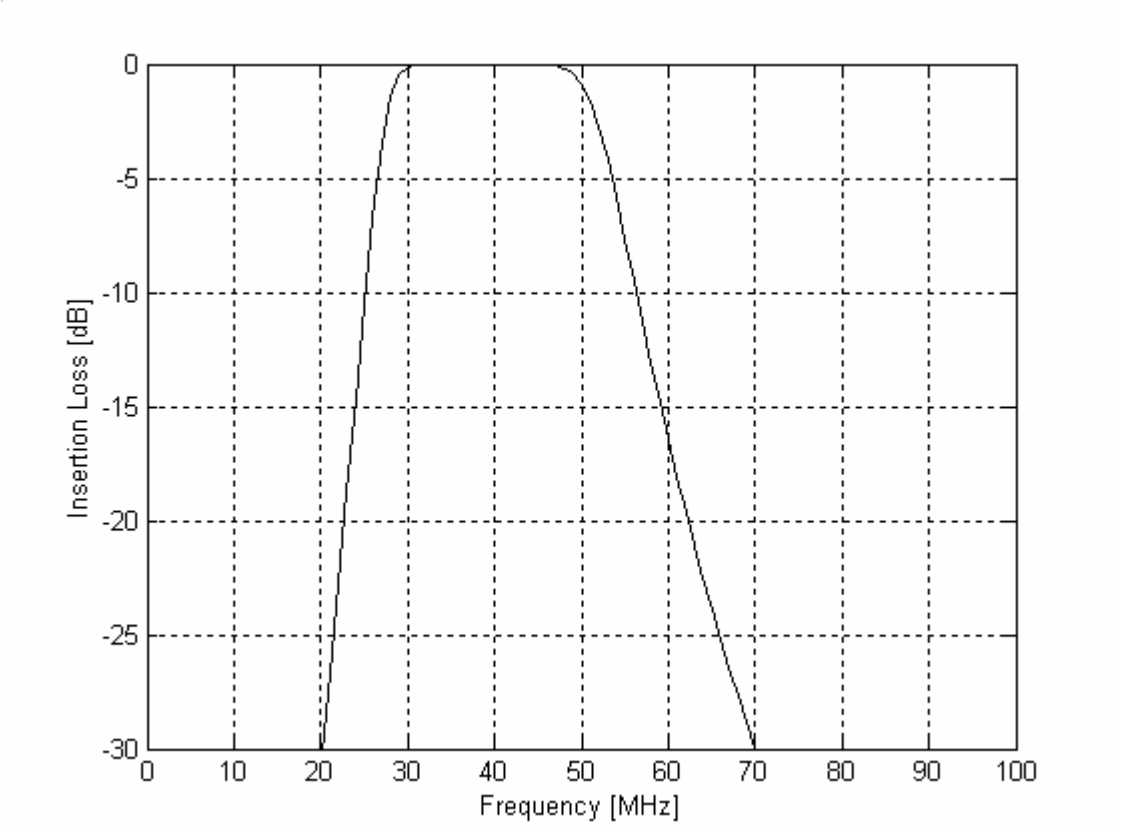

Figure 6.5. 5th order Butterworth filter frequency response.

For this receiver a 5th order Butterworth filter was designed, and the resulting network and frequency response are shown in Figure 6.4 and Figure 6.5. This filter exhibits a flat passband in the ETA bandwidth, and has a sharp cutoff into the stopband.

Step 6: The GNI analysis can now be completed for the receiver. The filter is assumed to have a maximum insertion loss of 1 dB and a very high IIP_3 (200 dBm). The long coax is assumed to have a very high IIP_3 as well. The variable attenuator is assumed to be at a

Table 6.2. ETA receiver parameters for GNI analysis at nominal gain.

Stage	Gain [dB]	IIP_3 [dBm]	F [dB]
Active Balun	24.4	7.6	2.7
Long Coax	-4	200	4
GALI-74	25.1	12.9	2.7
Variable Attenuator	-1	30	1
BPF	-1	200	1
GALI-74	25.1	12.9	2.7

Table 6.3. ETA receiver parameters for GNI analysis at minimal gain.

Stage	Gain [dB]	IIP_3 [dBm]	F [dB]
Active Balun	24.4	7.6	2.7
Long Coax	-4	200	4
GALI-74	25.1	12.9	2.7
Variable Attenuator	-42	30	42
BPF	-1	200	1
GALI-74	25.1	12.9	2.7

Table 6.4. ETA receiver parameters for GNI analysis at mid-range gain.

Stage	Gain [dB]	IIP_3 [dBm]	F [dB]
Active Balun	24.4	7.6	2.7
Long Coax	-4	200	4
GALI-74	25.1	12.9	2.7
Variable Attenuator	-21	30	21
BPF	-1	200	1
GALI-74	25.1	12.9	2.7

level that will achieve the nominal gain, and to have a constant IIP_3 of 30 dBm[1]. The receiver chain parameters are shown in Table 6.2. Completing the GNI analysis in Appendix B gives the receiver performance specifications of: G = 68.6 dB, IIP3 = -30.7 dBm, and F = 2.7 dB. The gain is a little more than 4 dB lower than the nominal gain. This is acceptable because the ADC has 12 bits instead of 5.

Recognizing that the results will vary according to the attenuator setting, it is important consider the performance for other settings. Table 6.3 shows the results for minimal gain. At this operating point G = 27.6 dB, IIP3 = -16.2 dBm, and F = 4.7 dB. The

[1] This assumption is not generally accurate. The IIP_3 of a variable attenuator is device specific, and usually will vary with attenuation. In actual practice this should be taken into account.

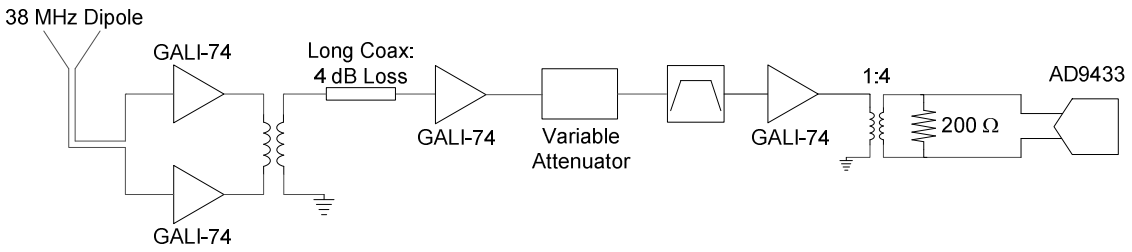

Figure 6.6. ETA receiver block diagram.

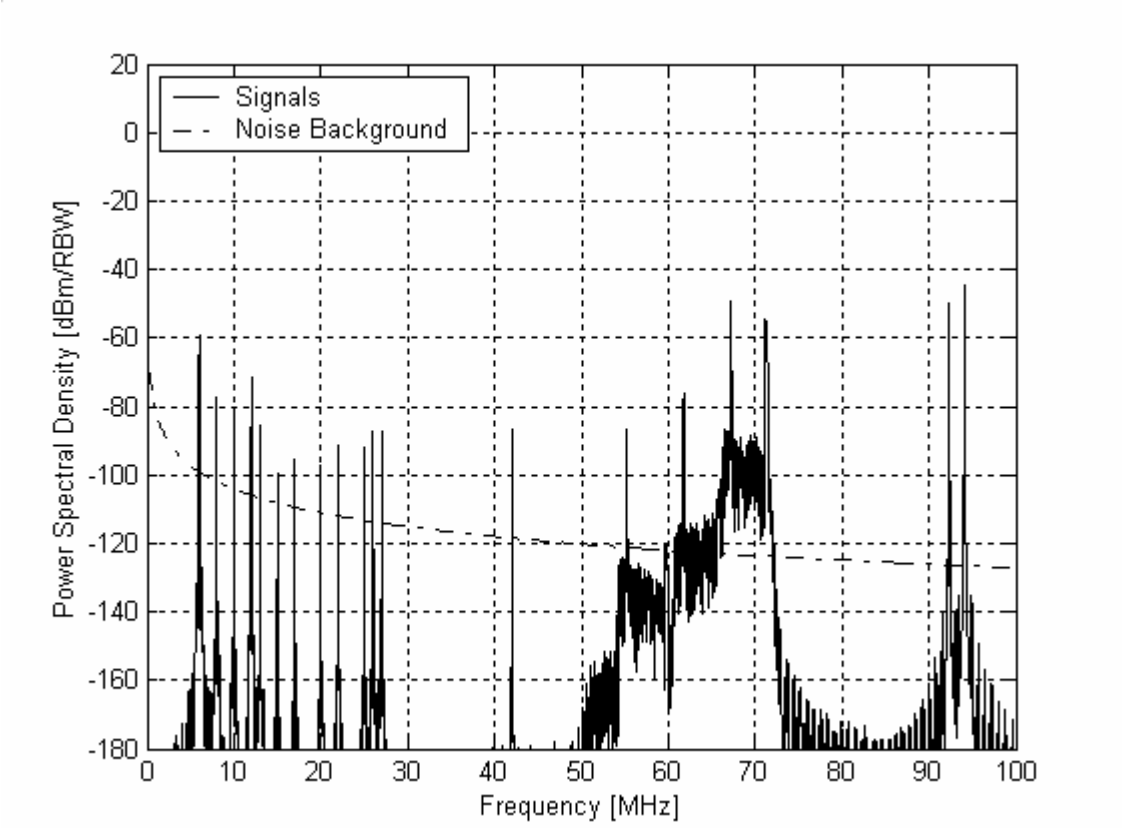

Figure 6.7. Simulated PSD at the ETA antenna terminals, RBW = 12.207 kHz.

linearity has been greatly improved, but at the cost of noise figure. Table 6.4 shows the results for midrange gain. At this operating point G = 48.6 dB, IIP3 = -17.2 dBm, and F = 2.8 dB. The linearity is still greatly improved and the noise figure has only been slightly increased.

Step 7: The ETA receiver has been designed, and the final receiver chain is shown in Figure 6.6. The simulated power spectral densities presented to the antenna and delivered to the AD9433 are shown in Figure 6.7 and Figure 6.8. These plots assume that the receiver is operating at the nominal gain. These plots show the signal sources and the noise

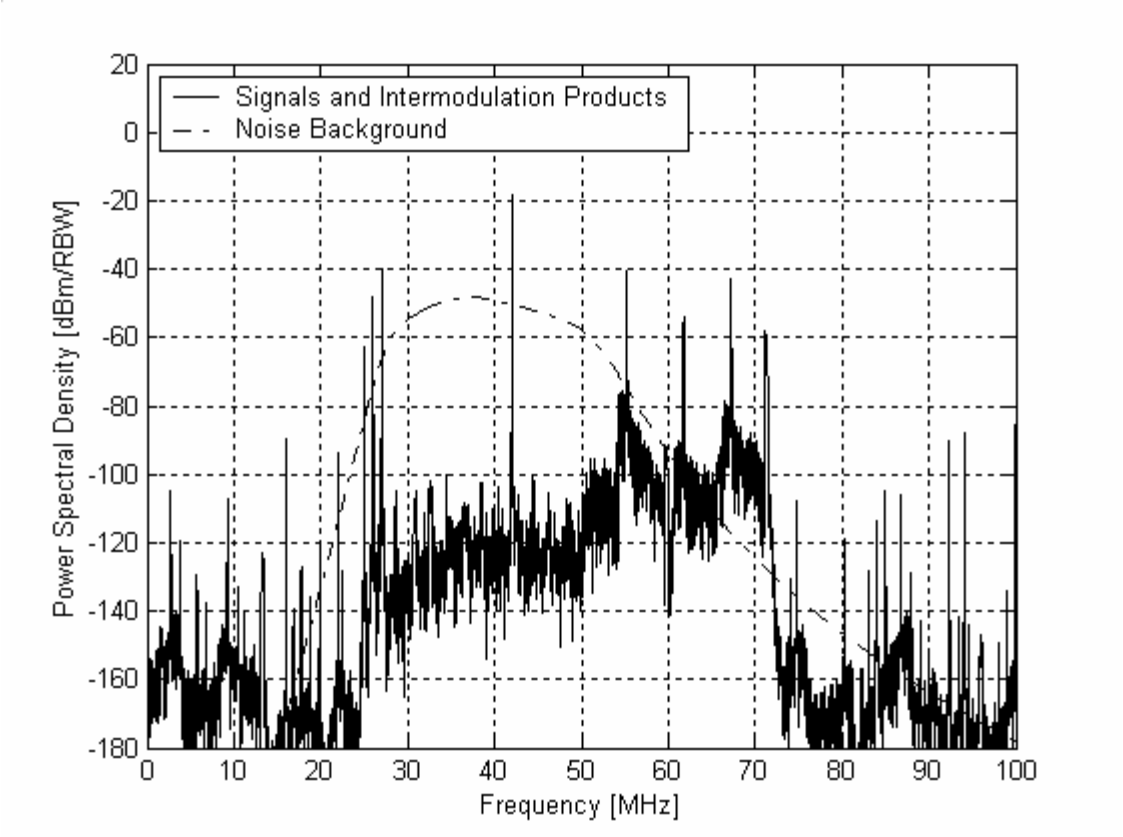

Figure 6.8. PSD provided to the AD9433 for the ETA receiver chain. RBW = 12.207 kHz.

background separately. This allows for easy visual confirmation as to whether or not the spectrum is dominated by the noise background or by signal sources and intermodulation products. The passband of the ETA receiver has been successfully defined, and the spectral environment in the stopband sufficiently attenuated. At the antenna $B_{Blocked}$ is 0.3%, while at the input to the AD9433 $B_{Blocked}$ is 0.3%, both with respect to the RBW of 12.207 kHz. This result implies the nonlinearity of the receiver did not significantly affect the received spectrum; i.e., any intermodulation products that were generated in the passband were of insignificant power when compared to the noise background.

6.4 Example: LWA

The Long Wavelength Array[1] (LWA) is a planned new radio telescope intended to operate in the 20 to 80 MHz band. Like ETA, it would consist of many dipoles, each with its own receiver.

[1] More information available at www.lwa.unm.edu

The antennas are 32 MHz resonant 'fat' dipole antennas[1], shown in Figure 6.9. This antenna provides broader bandwidth than a thin dipole. Unfortunately the fat dipole is "too fat" to be accurately modeled accurately by the TTG method. Therefore, the impedance of the LWA antenna was obtained using the moment method, with the result shown in Figure 6.10. The LWA will be located in a remote environment, so the noise model will be the Galactic background. The spectrum has been observed to have the form shown in Table 6.5 In the passband the desired α is 6 dB and the desired γ_q is 10 dB.

Step 1: Note that the impedance varies less for the fat dipole than for a thin dipole. This advantage of the fat dipole is needed to achieve the large desired bandwidth. Because this impedance range is not as broad, the mismatch between the fat dipole and the input impedance of the preamplifier will be less, and a wider bandwidth can be obtained. The antenna to preamplifier interface can now be considered. The α for several values of Z_L is shown in Figure 6.11. For now, T_{AMP} is assumed to be 250 K. Note that for all three values of Z_L the specification on α is met, so any of the three values are acceptable. For simplicity, a Z_L of 100 Ω will be chosen. Like the ETA receiver, this requires no transformers because amplifiers with 50 Ω input impedance are commonly available and can be implemented in a differential configuration to yield 100 Ω.

Step 2: The highest frequency the LWA receiver needs to receive is 80 MHz. Direct sampling of 20 to 80 MHz can only be done in lowpass, which requires an ADC with a minimum sampling frequency of 160 MSPS. In this thesis it is assumed the sample rate for LWA will be 200 MSPS, which allows ample additional bandwidth for filter roll off. The minimum number of bits can now be calculated. P_{ext} for the Galactic background in the LWA bandwidth is about -80.8 dBm. P_S in the LWA bandwidth is about -75.8 dBm, resulting in a P_t of about -74.6 dBm. The minimum number of bits is given by

$$N_b \geq 1.67 \log_{10}\left(\frac{P_t}{P_{ext}}\frac{\gamma_q}{\delta_r}\right) = 1.67 \log_{10}\left(\frac{(-74.6\,\text{dBm})(10\,\text{dB})}{(-80.8\,\text{dBm})(-10\,\text{dB})}\right) = 4.37 \tag{55}$$

Thus, an ADC with 5 or more effective bits should suffice. A commercially available ADC that meets these requirements is the Analog Devices AD9054A[2], which has 8 bits. This ADC encodes 1 $V_{p\text{-}p}$ into 62 Ω, resulting in a P_{clip} of about 3 dBm. In this example it is assumed that transformer coupling on the ADC input is not used.

[1] It should be noted that in the time since the work on this thesis was begun, the LWA antenna and receiver design has evolved such that the details are different from what is presented here. The design concepts and principles are the same, however.

[2] Information available at http://www.analog.com/en/prod/0%2C%2CAD9054A%2C00.html

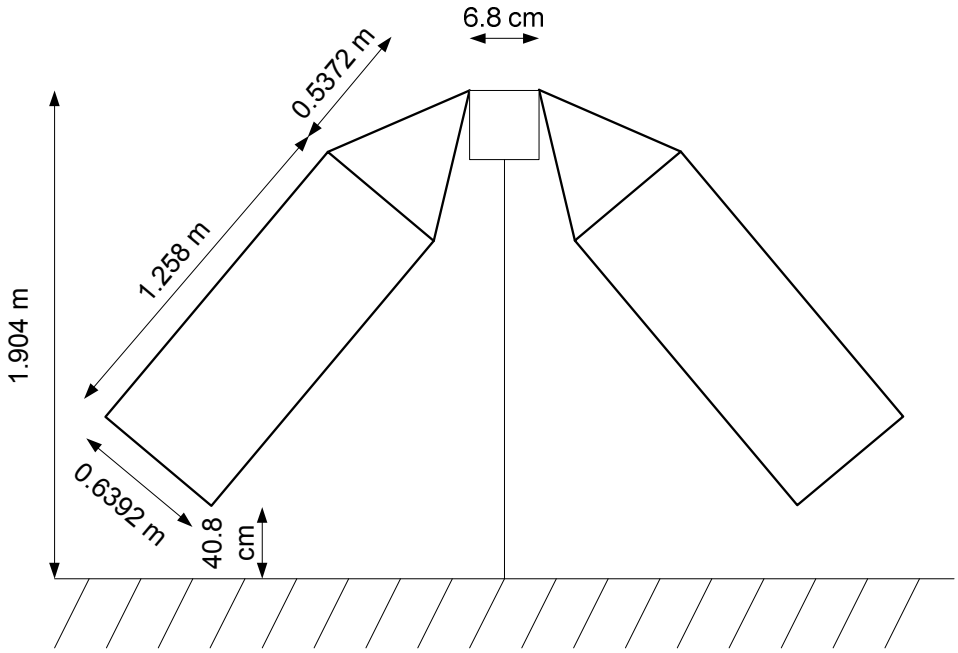

Figure 6.9. Dimensions for the LWA fat dipole antenna.

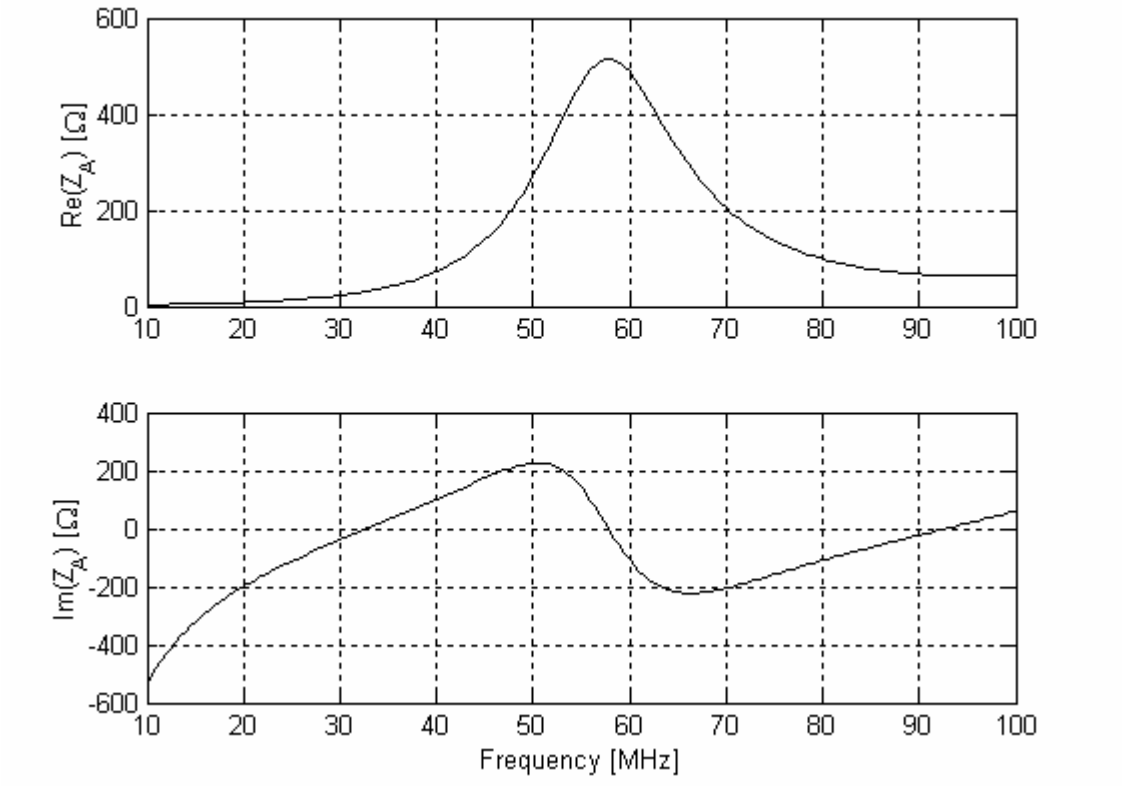

Figure 6.10. Frequency response of the LWA antenna.

Table 6.5. Spectrum for the LWA receiver, presented to the antenna.

Frequency [MHz]	Power [dBm]	Source
2.00	-70	Shortwave HF Broadcast
3.00	-70	Shortwave HF Broadcast
4.00	-70	Shortwave HF Broadcast
5.00	-70	Shortwave HF Broadcast
6.00	-70	Shortwave HF Broadcast
7.00	-70	Shortwave HF Broadcast
45.00	-80	2-Way Radio
55.25	-86	TV Channel 2 Video
61.75	-88	TV Channel 3 Video
67.25	-80	TV Channel 4 Video
71.25	-87	TV Channel 4 Audio
92.3	-70	FM Station
94.1	-70	FM Station

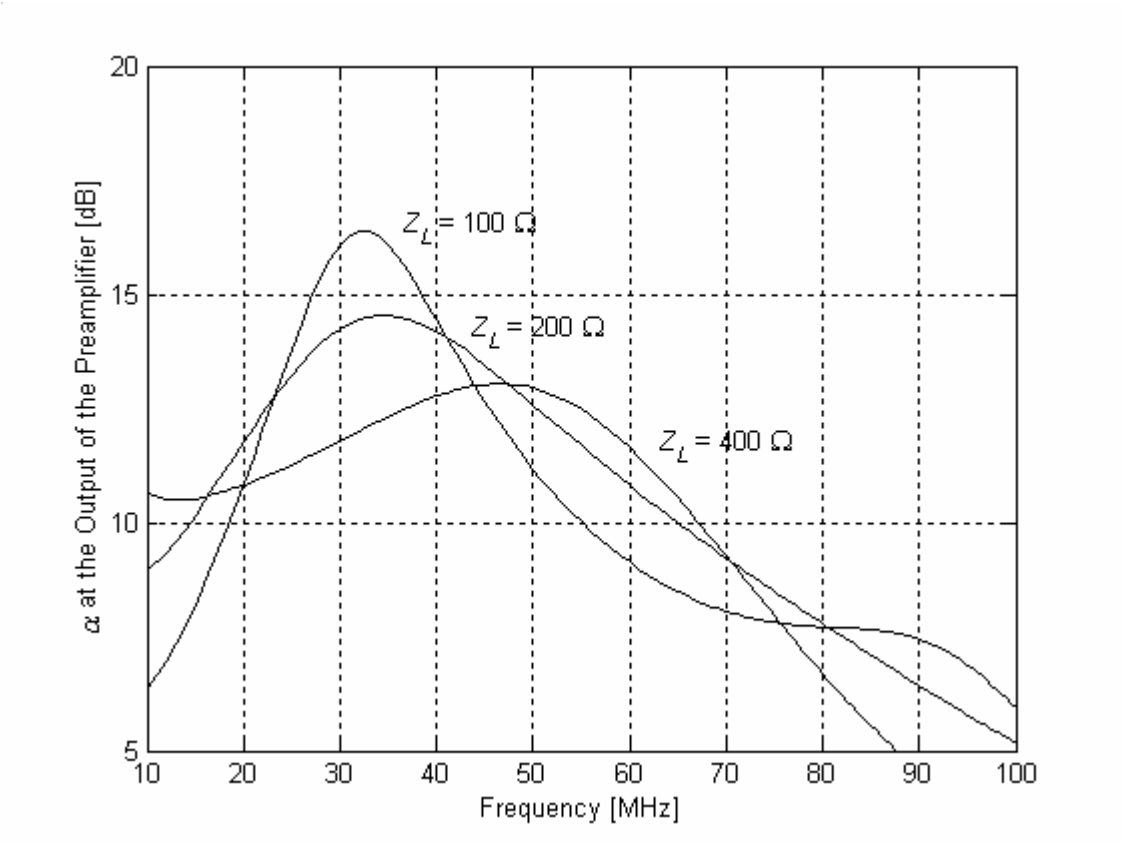

Figure 6.11. α for various values of Z_L using the LWA antenna, T_{AMP} = 250 K.

Step 3: The nominal gain can now be determined

$$G_r = \frac{P_{clip}\delta_r}{P_t} = \frac{(3\,\text{dBm})(-10\,\text{dB})}{(-74.6\,\text{dBm})} = 68\,\text{dB} \tag{56}$$

Step 4: The minimum gain needed for LWA can be calculated

$$G_{MIN} = \frac{P_Q\gamma_q}{P_{ext}} = \frac{(-45\,\text{dBm})(10\,\text{dB})}{(-80.8\,\text{dBm})} = 46\,\text{dB} \tag{57}$$

Step 5: The gain will be divided into four stages. The preamplifier shown in Figure 5.1 will be used, the GALI-74 amplifier is used for the middle two gain stages, and the Mini-Circuits ERA-6[1] (G = 12.6 dB, OIP_3 = 36 dBm, F = 4.5 dB) will be used for the final amplifier. There is also a long coaxial cable between the preamplifier and the rest of the receiver chain, which contributes 13 dB of loss, and should therefore be considered[2].
For this receiver a 5th order Butterworth filter is designed, and the resulting network and frequency response are shown in Figure 6.12 and 6.13. This filter exhibits a flat passband in the LWA bandwidth, and has a fairly sharp cutoff on the low end, but not at the high end. Because there are multiple amplifiers in the receiver chain, two bandpass filters will be used to improve the out-of-band rejection. The same circuit will be used for both bandpass filters in the receiver chain.

Step 6: The GNI analysis can now be completed for the receiver. The filters are assumed to each have an insertion loss of 1 dB and a very high IIP_3 (200 dBm). The long coax cable is assumed to have a very high IIP_3 as well. The variable attenuator is assumed to be at a level that will achieve the nominal gain, and to have an IIP_3 of 30 dBm. The receiver chain parameters are given in Table 6.6. Completing the GNI analysis in Appendix B gives the receiver performance specifications of: G = 68.2 dB, IIP_3 = -33.7 dBm, and F = 2.7 dB.
Recognizing that the results will vary with attenuator setting, it is important to consider the performance for other settings. Table 6.7 shows the results for minimal gain. At this operating point G = 46.2 dB, IIP_3 = -19.0 dBm, and F = 2.7 dB. Table 6.8 shows the results for midrange gain. At this operating point G = 58.2 dB, IIP_3 = -26.1 dBm, and F = 2.7 dB. As expected, the IIP_3 and F take on values in between those attained for the nominal and minimal cases.

[1] Information available at http://www.minicircuits.com/dg03-168.pdf
[2] In fact, the loss of this cable varies with frequency. The value at 80 MHz is used here. Properly, the frequency dependence of the cable should be taken into account.

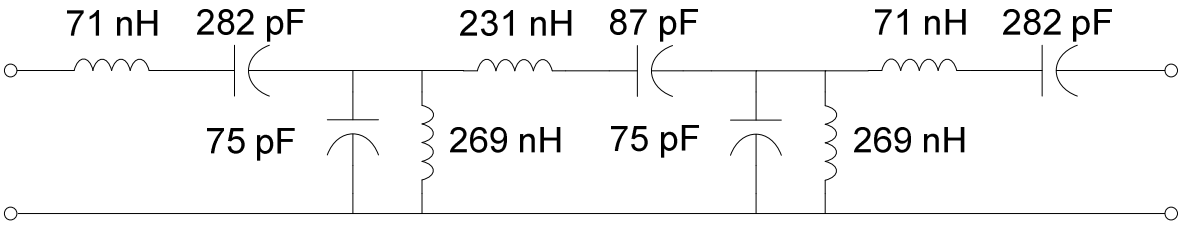

Figure 6.12. 5th order Butterworth filter network, 20 - 80 MHz passband.

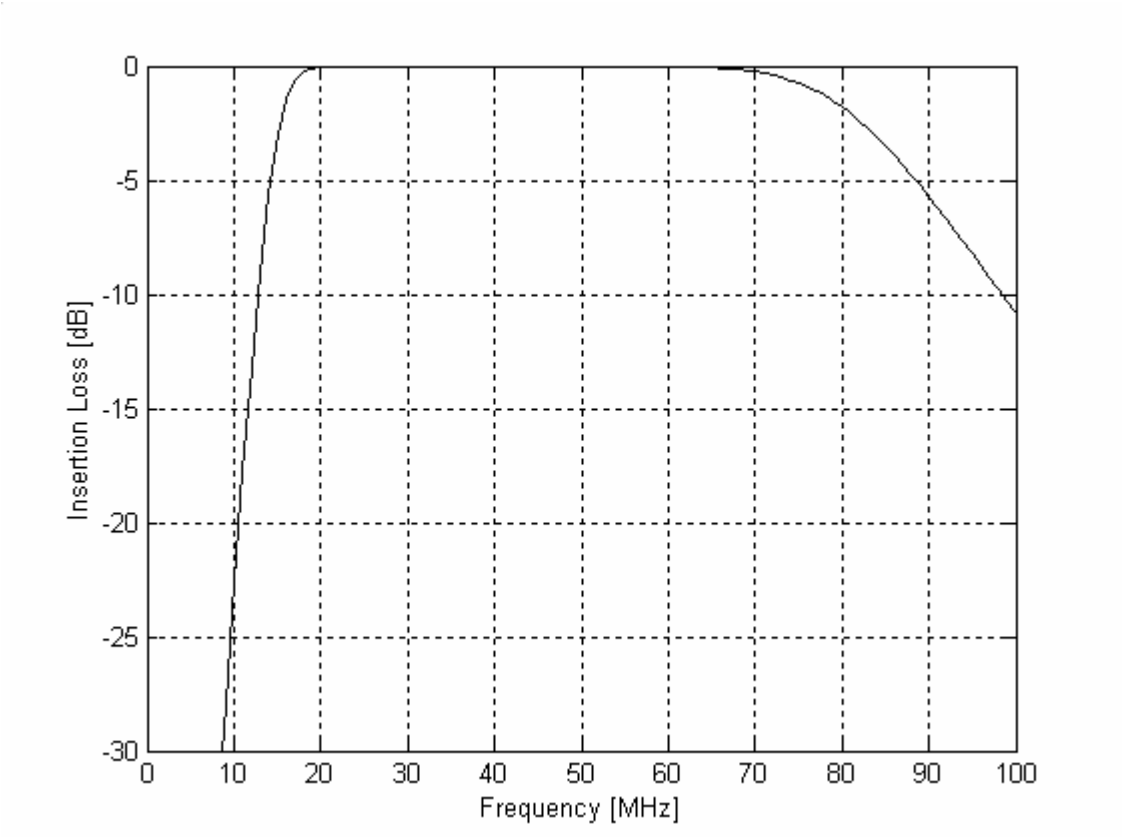

Figure 6.13. 5th order Butterworth filter frequency response.

Table 6.6. LWA receiver parameters for GNI analysis at nominal gain.

Stage	Gain [dB]	IIP_3 [dBm]	F [dB]
Active Balun	24.4	7.6	2.7
BPF	-1	200	1
GALI-74	25.1	12.9	2.7
Long Coax	-13	200	13
Variable Attenuator	-2	30	2
GALI-74	25.1	12.9	2.7
BPF	-1	200	1
Variable Attenuator	-2	30	2
ERA-6	12.6	23.4	4.5

Table 6.7. LWA receiver parameters for GNI analysis at minimal gain.

Stage	Gain [dB]	IIP_3 [dBm]	F [dB]
Active Balun	24.4	7.6	2.7
BPF	-1	200	1
GALI-74	25.1	12.9	2.7
Long Coax	-13	200	13
Variable Attenuator	-13	30	13
GALI-74	25.1	12.9	2.7
BPF	-1	200	1
Variable Attenuator	-13	30	13
ERA-6	12.6	23.4	4.5

Table 6.8. LWA receiver parameters for GNI analysis at mid-range gain.

Stage	Gain [dB]	IIP_3 [dBm]	F [dB]
Active Balun	24.4	7.6	2.7
BPF	-1	200	1
GALI-74	25.1	12.9	2.7
Long Coax	-13	200	13
Variable Attenuator	-7	30	7
GALI-74	25.1	12.9	2.7
BPF	-1	200	1
Variable Attenuator	-7	30	7
ERA-6	12.6	23.4	4.5

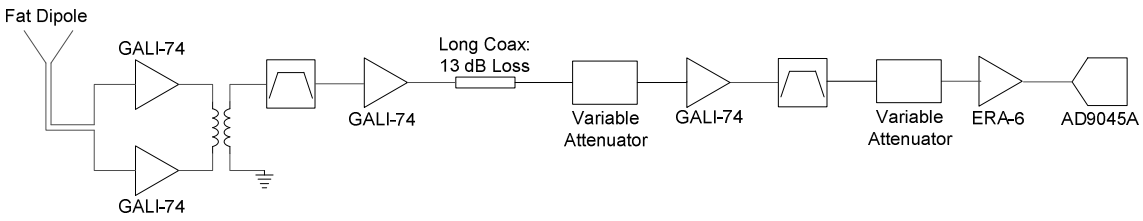

Figure 6.14. LWA receiver block diagram.

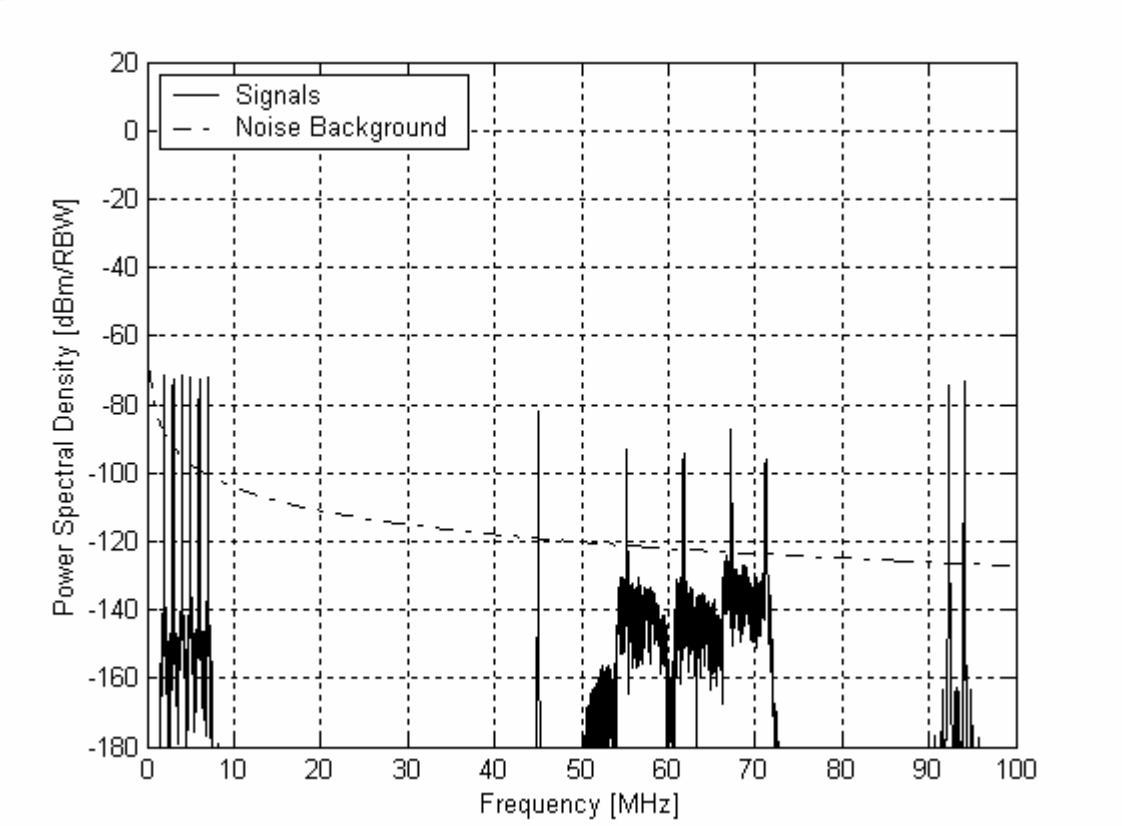

Figure 6.15. Simulated PSD at the LWA antenna terminals, RBW=12.207 kHz.

Step 7: The LWA receiver has been fully designed, and the final receiver chain is shown in Figure 6.14. The simulated power spectral densities presented to the antenna and delivered to the AD9045A are shown in Figure 6.15 and Figure 6.16. These plots assume that the receiver is operating at the nominal gain. The passband of the LWA receiver has been successfully defined, and the spectral environment in the stopband sufficiently attenuated. At the antenna $B_{Blocked}$ is 1.1%, while at the input to the AD9045A $B_{Blocked}$ is 1.2%, both with respect to the RBW of 12.207 kHz. The nonlinear response of the receiver has only slightly affected the received spectrum.

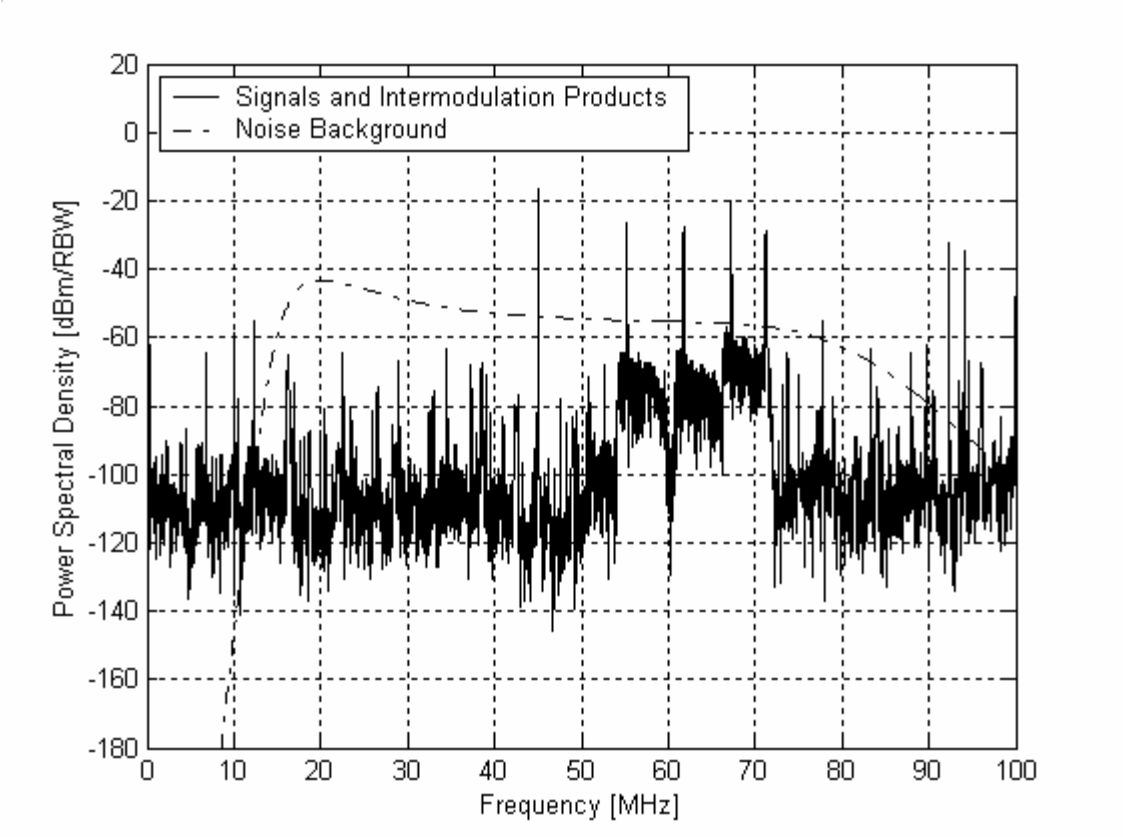

Figure 6.16. PSD provided to the AD9045A for the LWA receiver chain, RBW=12.207 kHz.

6.5 Example: Frequency-Adaptive Cognitive Radio for Operation in a "Business" Spectral Environment

A cognitive radio is one which monitors its environment and dynamically changes its operating parameters in response. A cognitive radio which is frequency adaptive can detect interference and retune to a "clear" channel as needed. This requires the ability to monitor a bandwidth that is much wider than the signal bandwidth. One such radio could conceivably be used in the 30 to 50 MHz portion of the VHF band. This band is currently allocated mostly to a variety of "push-to-talk" radios, which typically transmit only a tiny fraction of the time. This creates the potential for a network of radios to operate in this bandwidth by opportunistically exploiting the free spectrum. In this example, the antenna is assumed to be a 40 MHz resonant monopole antenna. In terms of the TTG model, h = 1.875 m and a = 0.01 m. The radio operates in the ITU "business" noise environment (m = 60) and the spectrum is described in Table 6.9. In the passband the desired α is 15 dB and the desired γ_q is 5 dB.

Table 6.9. Spectrum for cognitive radio receiver.

Frequency [MHz]	Power [dBm]	Source
4	-55	Shortwave HF
6	-63	Shortwave HF
7	-67	Shortwave HF
8	-60	Shortwave HF
9	-64	Shortwave HF
11	-60	Shortwave HF
12	-52	Shortwave HF
13	-65	Shortwave HF
16	-54	Shortwave HF
17	-58	Shortwave HF
18	-52	Shortwave HF
19	-60	Shortwave HF
21	-65	Shortwave HF
24	-61	Shortwave HF
25	-71	Shortwave HF
26	-64	Shortwave HF
27	-61	Shortwave HF
28	-79	Shortwave HF
29	-77	Shortwave HF
32	-75	2-Way Radio
33	-65	2-Way Radio
38	-77	2-Way Radio
39	-55	2-Way Radio
46	-62	2-Way Radio
47	-71	2-Way Radio
48	-51	2-Way Radio
49	-58	2-Way Radio
50	-83	2-Way Radio
67.25	-25	TV Channel 4
71.75	-25	TV Channel 4
77.25	-52	TV Channel 5
81.75	-75	TV Channel 5
83.25	-15	TV Channel 6
87.75	-15	TV Channel 6
88.1	-18	FM Station
88.9	-19	FM Station

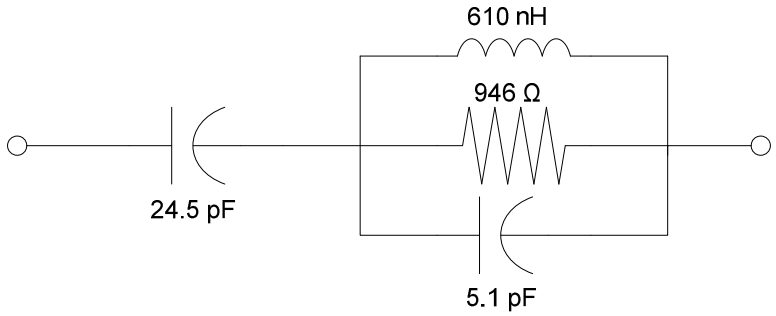

Figure 6.17. TTG model for a 40 MHz resonant monopole antenna.

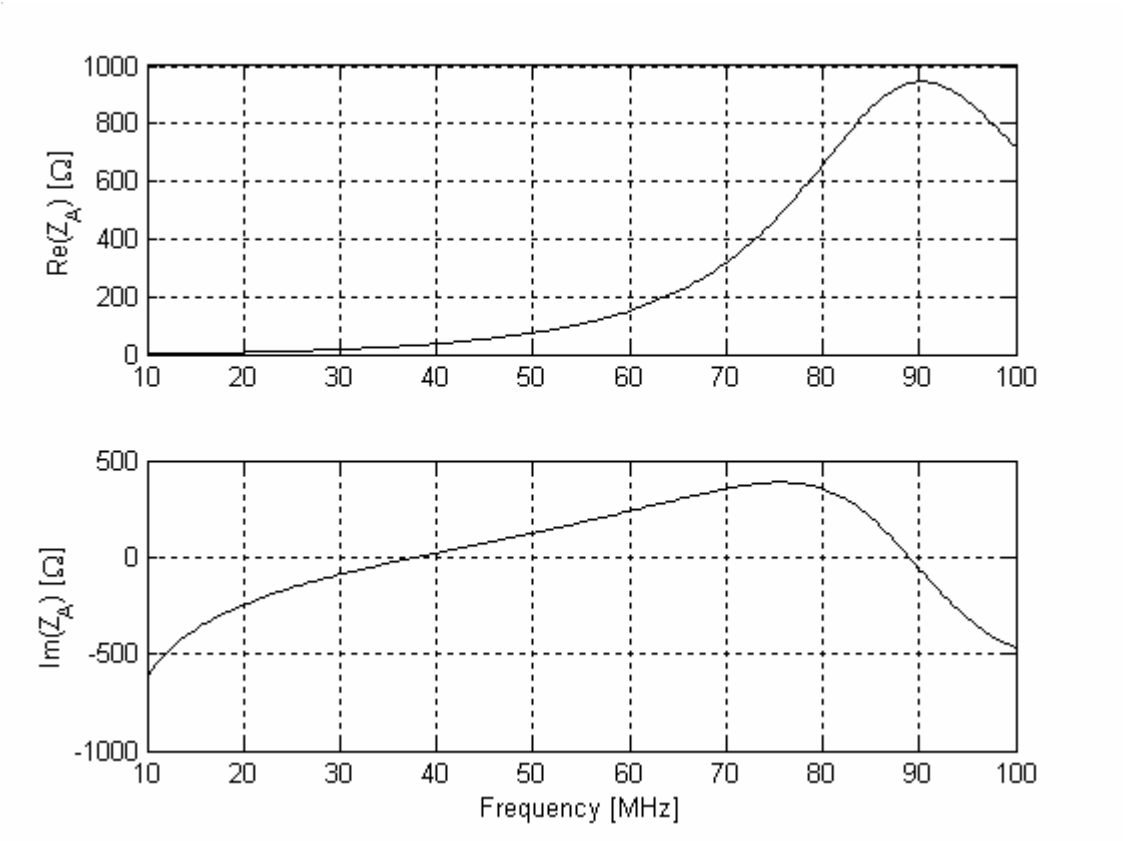

Figure 6.18. Frequency response of the antenna model shown in Figure 6.17.

Step 1: The monopole circuit model and its frequency response are shown in Figure 6.17 and Figure 6.18 The antenna to preamplifier interface can now be considered. The α for several values of preamplifier input impedance (Z_L) values is shown in Figure 6.19. For now, T_{AMP} is assumed to be 300 K. Note that for all three values of Z_L the specification on is α easily met. A Z_L of 50 Ω is chosen. Because the antenna is a monopole, its output

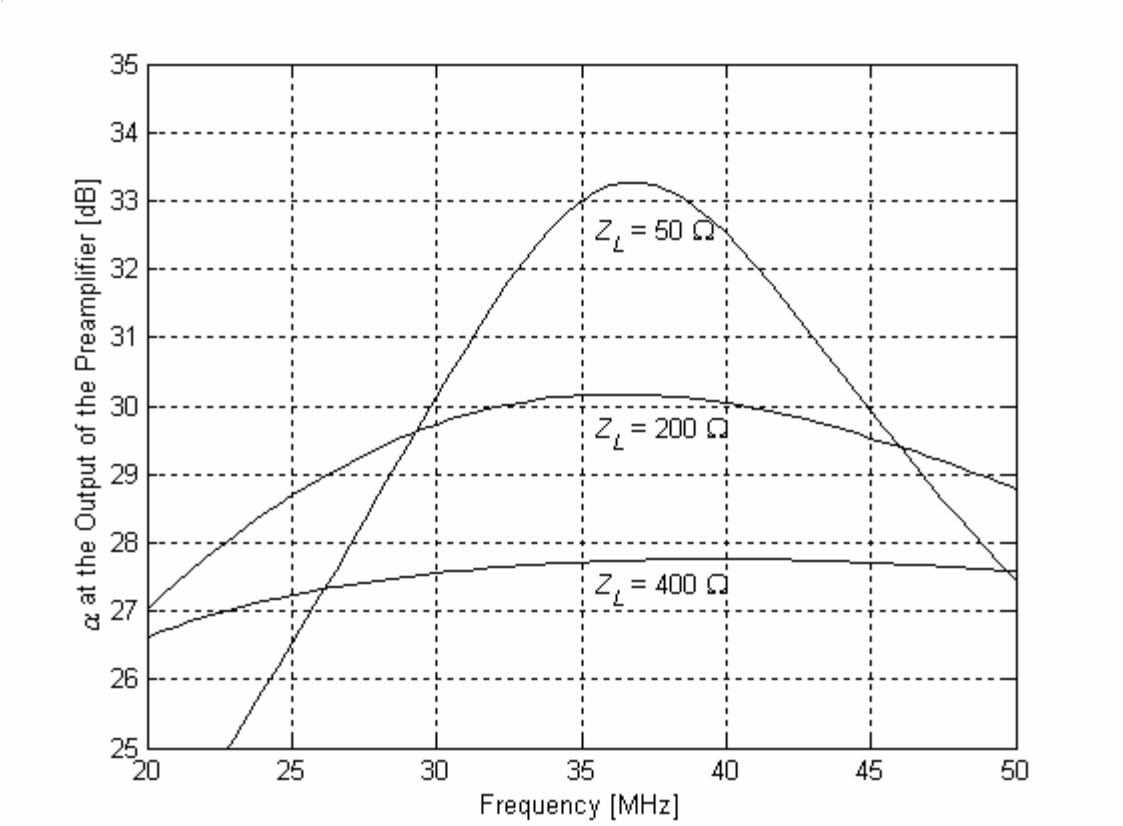

Figure 6.19. α for the cognitive radio receiver over a range of Z_L values, T_{AMP}=300 K.

will be single-ended. Thus, the preamplifier will be a single-ended amplifier with an input impedance of 50 Ω.

Step 2: The highest frequency the cognitive radio receiver needs to receive is 50 MHz. For lowpass sampling, this requires an ADC with a minimum sampling frequency of 100 MSPS. The sample rate for the cognitive radio is selected to be 125 MSPS, which allows ample additional bandwidth for filter roll off. The minimum number of bits can now be calculated. P_{ext} for the "business" noise background in the cognitive radio's passband is about -68 dBm. P_S in the passband is about -48.6 dBm, resulting in a P_t of about -48.5 dBm. The minimum number of bits is given by

$$N_b \geq 1.67 \log_{10}\left(\frac{P_t}{P_{ext}}\frac{\gamma_q}{\delta_r}\right) = 1.67 \log_{10}\left(\frac{(-48.5\,\text{dBm})(5\,\text{dB})}{(-68\,\text{dBm})(-10\,\text{dB})}\right) = 5.76 \tag{58}$$

Thus, an ADC with 6 or more effective bits should suffice. A commercially available ADC that meets these requirements is the Analog Devices AD9433[1], which has 12 bits. This ADC encodes 2 $V_{p\text{-}p}$ into 3 kΩ, resulting in a P_{clip} of about -7.8 dBm. A 1:1

[1] Information available at http://www.analog.com/en/prod/0%2C%2CAD9433%2C00.html

transformer is placed at the AD9433 input, with a 50 Ω resistor in parallel on the ADC side. Since the input impedance of the AD9433 is 3kΩ, the equivalent parallel impedance is still about 50 Ω. This results in a P_{clip} of about 16 dBm at the input of the transformer.

Step 3: The nominal gain can now be determined

$$G_r = \frac{P_{clip}\delta_r}{P_t} = \frac{(16\,\text{dBm})(-10\,\text{dB})}{(-48.5\,\text{dBm})} = 54.5\,\text{dB} \tag{59}$$

Step 4: The low end of the attenuation needed for the cognitive radio receiver can be calculated

$$G_{MIN} = \frac{P_Q\gamma_q}{P_{ext}} = \frac{(-56\,\text{dBm})(5\,\text{dB})}{(-68\,\text{dBm})} = 17\,\text{dB} \tag{60}$$

Step 5: The gain will be divided into two stages, both of which will use the GALI-74.
For this receiver a 5th order Chebyshev filter is designed with 0.1 dB of ripple in the passband, and the resulting network and frequency response are shown in Figure 6.20 and Figure 6.21

Step 6: The GNI analysis can now be completed on the receiver. The filter and is assumed to have an insertion loss of 1 dB and a very high IIP_3 (200 dBm). The variable attenuator is assumed to be at a level that will result in nominal gain, and to have an IIP_3 of 30 dBm. The receiver chain parameters are shown in Table 6.10. Completing the GNI analysis in Appendix B gives the receiver performance specifications of: G = 48.2 dB, IIP_3 = -10.4 dBm, and F = 2.7 dB. This is about 6 dB lower than the calculated nominal gain, but this is acceptable because the ADC has 12 bits instead of 6.
Recognizing that the results will vary according to the attenuator setting, it is important to consider the performance for other settings. Table 6.11shows the results for minimal gain. At this operating point G = 16.2 dB, IIP_3 = 4.2 dBm, and F = 12.1 dB. The linearity has been improved, while the noise figure has increased by about 10 dB. However, this is of no consequence since α is already so large (Figure 6.19). Table 6.12 shows the results for midrange gain. At this operating point G = 33.2 dB, IIP_3 = 1.5 dBm, and F = 3.3 dB. The linearity has again been improved, but the noise figure has only been slightly increased.

Step 7: The cognitive radio receiver has been fully designed, and the final receiver chain is shown in Figure 6.22. The simulated power spectral densities presented to the antenna and delivered to the AD9433 are shown in Figure 6.23 and Figure 6.24. The passband of the cognitive radio receiver has been successfully defined, and the spectral environment sufficiently attenuated. At the antenna $B_{Blocked}$ is 2.4%, while at the input to the AD9433 $B_{Blocked}$ is 2.5%, both with respect to the RBW of 12.207 kHz. The nonlinear response has only slightly increased the amount of blocked spectrum.

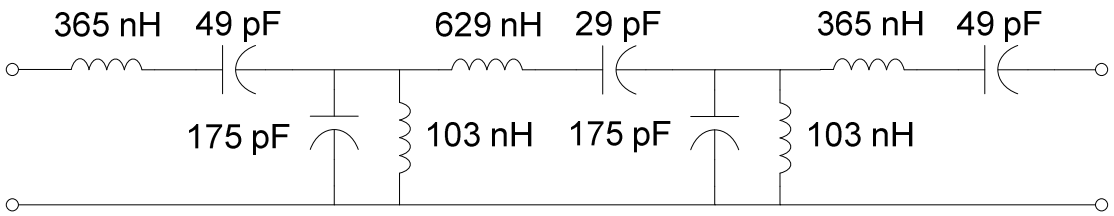

Figure 6.20. 5th order Chebyshev filter network, 0.1 dB ripple, 30 - 50 MHz passband.

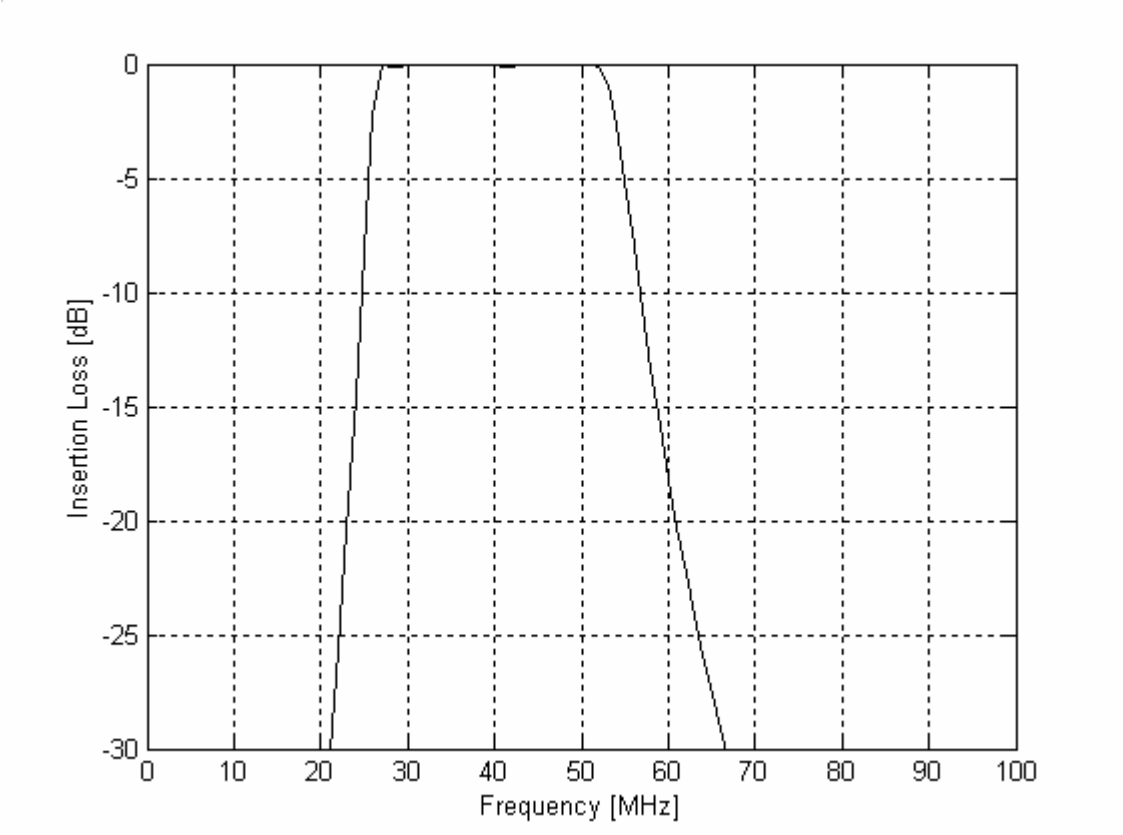

Figure 6.21. 5th order Chebyshev filter frequency response.

Table 6.10. GNI parameters for cognitive radio receiver at nominal gain.

Stage	Gain [dB]	IIP_3 [dBm]	F [dB]
GALI-74	25.1	12.9	2.7
Variable Attenuator	-1	30	1
BPF	-1	200	1
GALI-74	25.1	12.9	2.7

Table 6.11. GNI parameters for cognitive radio receiver at minimal gain.

Stage	Gain [dB]	IIP_3 [dBm]	F [dB]
GALI-74	25.1	12.9	2.7
Variable Attenuator	-33	30	33
BPF	-1	200	1
GALI-74	25.1	12.9	2.7

Table 6.12. GNI parameters for cognitive radio receiver at mid-range gain.

Stage	Gain [dB]	IIP_3 [dBm]	F [dB]
GALI-74	25.1	12.9	2.7
Variable Attenuator	-17	30	17
BPF	-1	200	1
GALI-74	25.1	12.9	2.7

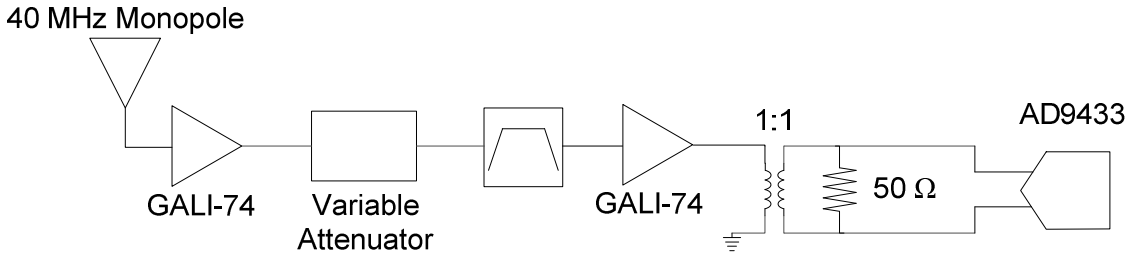

Figure 6.22. Cognitive radio receiver block diagram.

6.6 Summary

The design methodology presented in Section 6.1 has been applied to three different receivers. For each case a successful receiver chain was designed and simulated, with the results shown. The success of these three receiver designs verifies the design methodology presented in Section 6.1.

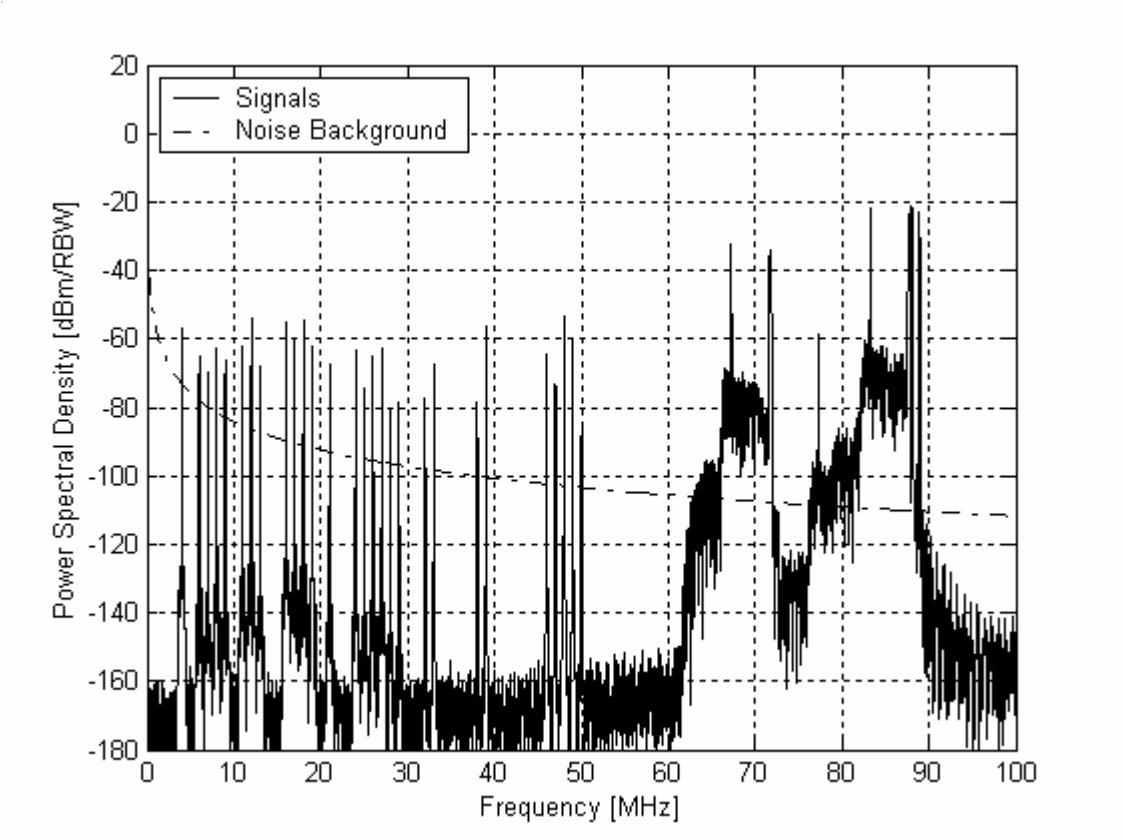

Figure 6.23. Simulated PSD at the cognitive radio antenna terminals, RBW=12.207 kHz.

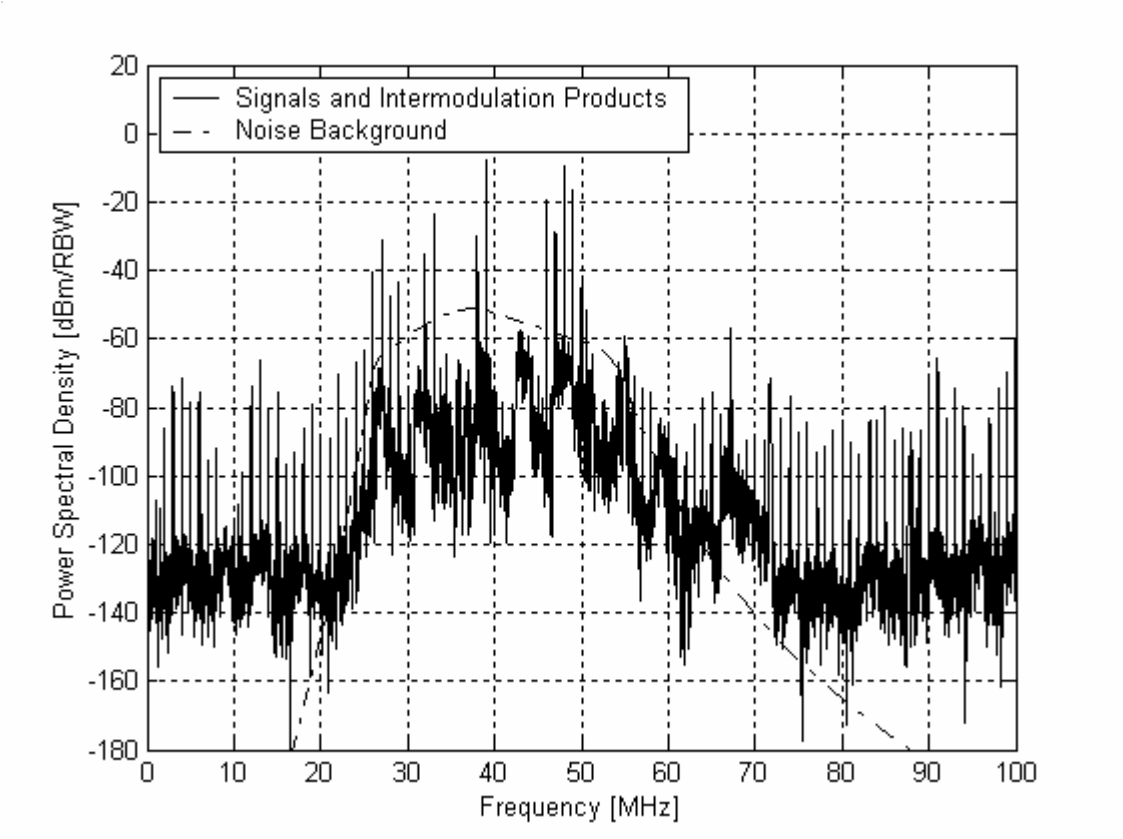

Figure 6.24. PSD provided to the AD9433 for the cognitive radio receiver chain. RBW = 12.207 kHz.

Chapter 7 Conclusions

7.1 Summary

The goal of this thesis was to describe and analyze the problem of wideband receiver design in the VHF low band (30 to 100 MHz), and to develop a methodology for designing such a receiver. In Chapter 2, the value of approaching this problem using a wideband direct sampling architecture was discussed. A procedure for designing such a receiver was developed and presented in Chapter 6. The procedure accounts for the unique noise and spectral characteristics of the VHF low band (per Chapter 3), limitations of wideband antenna matching circuits (per Chapter 4), and the impact of intermodulation products blocking the spectrum (per Chapter 5). The methodology was demonstrated by example for three types of receivers.

7.2 Proposed Future Work

There is, however, future work that could improve the results presented here. The TV broadcast model should be extended to include the color signal and the video sync pulse. Also, broadcast digital TV, which is gradually replacing analog TV in this band, should be modeled as well. Active ("non-Foster") matching circuits should be further considered to allow for the design of very wideband matching between antennas and receivers. More detailed analysis of gain control algorithms should be considered. Expanding the simulation to include a more detailed model of the ADC behavior would provide insight into the spectrum that the post-digitization stages receive. The analysis would benefit from a more accurate linearity model than the one presented in Chapter 5, perhaps including higher-order terms or memory effects, which would allow for more accurate simulations. Finally, the construction and testing of the receivers shown here would provide validation of the design methodology.

Appendix A Dipole to Monopole Transform

The methodology described in [3] allows for a dipole to be modeled by a four element circuit. However, it is often useful to instead model a monopole, which has half of the impedance of a dipole. One way to do this would be to calculate the impedance of the analogous dipole and divide the impedance by two. This, however, only gives a list of impedance values, not a circuit. To obtain a four element circuit for a monopole from the dipole circuit obtained by using the equations in [3], the following method can be used.

Consider two impedances in series. Their combination would be

$$Z_{SERIES,1} = Z_1 + Z_2 \tag{61}$$

If both of these impedances are divided by two, then their combination would be

$$Z_{SERIES,2} = \frac{1}{2}Z_1 + \frac{1}{2}Z_2 = \frac{1}{2}(Z_1 + Z_2) = \frac{1}{2}Z_{SERIES,1} \tag{62}$$

It can be seen that for elements in series, the end result of dividing each element's impedance by two is that the total impedance of the elements is divided by two as well.

Now, consider two impedances in parallel. Their combination would be

$$Z_{PARALLEL,1} = \frac{Z_1 Z_2}{Z_1 + Z_2} \tag{63}$$

If both of these impedances are divided by two, then their combination would be

$$Z_{PARALLEL,2} = \frac{\frac{1}{2}Z_1 \frac{1}{2}Z_2}{\frac{1}{2}Z_1 + \frac{1}{2}Z_2} = \frac{1}{2}\frac{Z_1 Z_2}{Z_1 + Z_2} = \frac{1}{2}Z_{PARALLEL,1} \tag{64}$$

It can be seen that for elements in parallel, the end result of dividing each element's impedance by two is that the total impedance of the elements is divided by two as well.

Recall that the impedance of any passive circuit can be calculated as a sequence of series and parallel calculations. Thus, to transform the dipole model into a monopole all that needs to be done is to divide each element's impedance by two, giving.

For resistors: $$\frac{1}{2}Z_R = \frac{1}{2}R = \frac{R}{2} \tag{65}$$

For inductors: $$\frac{1}{2}Z_L = \frac{1}{2}sL = s\frac{L}{2} \tag{66}$$

For capacitors: $$\frac{1}{2}Z_C = \frac{1}{2}\frac{1}{sC} = \frac{1}{s(2C)} \tag{67}$$

Therefore the impedance of a monopole can be obtained from the analogous dipole model by dividing the resistor and inductor values by two, and multiplying each capacitor value by two.

Appendix B GNI Analysis

It is often necessary to determine the overall gain, noise figure, and intermodulation intercept points for a receiver chain. If these metrics are known for each element in the receiver chain shown in Figure B.1, then the analysis presented in [1] can be applied as follows.

Analyzing the gain is a simple task

$$G_{total} = G_1 G_2 ... G_n \tag{68}$$

The combined noise figure of the elements in the receiver chain is

$$F_{total} = 1 + (F_1 - 1) + \frac{F_2 - 1}{G_1} + ... \frac{F_n - 1}{G_{n-1}} \tag{69}$$

Finally, the receiver chain's intermodulation intercept points (2^{nd} or 3^{rd}) are given by

$$\frac{1}{IIP_{total}} = \frac{1}{IIP_1} + \frac{G_1}{IIP_2} + ... \frac{G_1 G_2 ... G_{n-1}}{IIP_n} \tag{70}$$

$$OIP_{total} = \frac{1}{OIP_1 G_2 ... G_{n-1} G_n} + \frac{1}{OIP_2 ... G_{n-1} G_n} + ... \frac{1}{OIP_n} \tag{71}$$

Where the relationship between input and output intercept points is

$$OIP_{total} = G_{total} IIP_{total} \tag{72}$$

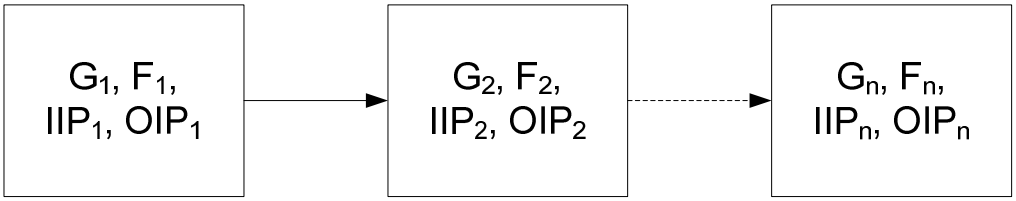

Figure B.1. Generic receiver chain for GNI analysis, all values are linear (non-dB).

Appendix C TV Station Frequency Allocation

Table C.1. Frequency allocation for broadcast TV stations below 100 MHz in the United States.

TV Channel	Video Carrier [MHz]	Color Carrier [MHz]	Audio Carrier [MHz]
2	55.25	58.83	59.75
3	61.75	64.83	65.75
4	67.25	70.83	71.75
5	77.25	80.83	81.75
6	83.25	86.83	87.75

Appendix D Chen Matching Technique

In [12], Chen defines an eight step procedure that creates a low pass matching circuit for a resistive element and a complex impedance element. The eight steps are:

Step 1: Choose a Butterworth, Chebyshev, or Elliptical power transducer gain characteristic, $G(\omega^2)$, and verify that it is an even rational real function and that

$$0 \le G(\omega^2) \le 1 \tag{73}$$

Step 2: Once the load impedance z(s) is known and has been normalized, find the following expressions.

$$r(s) = \frac{1}{2}[z(s) + z(-s)] \tag{74}$$

$$A(s) = \prod_{i=1}^{v} \frac{s - s_i}{s + s_i} \tag{75}$$

$$F(s) = 2r(s)A(s) \tag{76}$$

Where s_i (i = 1, 2,…v) are the open right-hand-side poles of z(-s).

Step 3: Determine the location and order of the zeroes of transmission of z(s), which are the closed RHS zeroes of

$$w(s) = \frac{r(s)}{z(s)} \tag{77}$$

Where $s_0 = \sigma_0 + j\omega_0$ is the form of a zero of order k. Once the zeroes of transmission are known, the class of the zero must be determined.

Class I: $\sigma_0 > 0$ (78)

Class II: $\sigma_0 = 0$ and $z(j\omega_0) = 0$ (79)

Class III: $\sigma_0 = 0$ and $0 < |z(j\omega_0)| < \infty$ (80)

Class IV: $\sigma_0 = 0$; and $|z(j\omega_0)| = \infty$ (81)

Step 4: Perform the unique factorization of the function

$$\rho(s)\rho(-s) = 1 - G(-s^2) \tag{82}$$

Step 5: Obtain the Laurent series expansions of $A(s)$, $F(s)$, and $\rho(s)$ around the zeroes of transmission of z(s).

$$A(s) = \sum_{m=0}^{\infty} A_0 + \frac{A_1}{s} + \frac{A_2}{s^2} + \frac{A_3}{s^3} \ldots \tag{83}$$

$$F(s) = \sum_{m=0}^{\infty} F_0 + \frac{F_1}{s} + \frac{F_2}{s^2} + \frac{F_3}{s^3} \ldots \tag{84}$$

$$\rho(s) = \sum_{m=0}^{\infty} \rho_0 + \frac{\rho_1}{s^1} + \frac{\rho_2}{s^2} + \frac{\rho_3}{s^3} \ldots \tag{85}$$

Step 6: Check that the expansions satisfy the following conditions.

Class I: $A_X = \rho_X$ for $x = 0, 1, \ldots, k\text{-}1$ (86)

Class II: $A_X = \rho_X$ for $x = 0, 1, \ldots, k\text{-}1$ and $(A_K - \rho_K) / F_{K+1} \geq 0$ (87)

Class III: $A_X = \rho_X$ for $x = 0, 1, \ldots, k\text{-}1$ and $(A_{K-1} - \rho_{K-1}) / F_K \geq 0$, where $k \geq 2$ (88)

Class IV: $A_X = \rho_X$ for $x = 0,1,\ldots,k\text{-}1$ and $F_{K-1} / (A_K - \rho_K) \geq a_{-1}$, where a_{-1} is the residue of $z(s)$ at the pole $j\omega_0$ (89)

Step 7: Determine the equalizer back end impedance from

$$Z(s) = \frac{F(s)}{A(s) - \rho(s)} - z(s) \tag{90}$$

Step 8: Expand $Z(s)$ using a continued fraction expansion, resulting in values for an LC ladder.

Applying this procedure to matching a simple antenna to a resistive load does not work, as will now be demonstrated. The general Z_A equation for the TTG antenna model is

$$Z_A(s) = \frac{L_{31}R_{31}(C_{31} + C_{32})s^2 + L_{31}s + R_{31}}{L_{31}R_{31}C_{31}C_{32}s^3 + L_{31}C_{31}s^2 + R_{31}C_{31}s} \tag{91}$$

The steps in the procedure are as follows

Step 1: Allow the transducer gain to have a 4^{th} order Butterworth characteristic.

$$G(\omega^2) = \frac{K_4}{1 + \omega^8} \qquad 0 \leq K_4 \leq 1 \tag{92}$$

Step 2: The $r(s)$, $A(s)$ and $F(s)$ are

$$r(s) = \frac{-R_{31}L_{31}{}^2 s^2}{(L_{31}R_{31}C_{32}s^2 + L_{31}s + R_{31})(L_{31}R_{31}C_{32}s^2 - L_{31}s + R_{31})} \tag{93}$$

$$A(s) = \frac{L_{31}R_{31}C_{32}s^2 - L_{31}s + R_{31}}{L_{31}R_{31}C_{32}s^2 + L_{31}s + R_{31}} \tag{94}$$

$$F(s) = \frac{-R_{31}L_{31}{}^2 s^2}{(L_{31}R_{31}C_{32}s^2 + L_{31}s + R_{31})^2} \tag{95}$$

Step 3: Finding the RHS zeroes of

$$w(s) = \frac{-R_{31}C_{31}L_{31}{}^2 s^3}{(L_{31}R_{31}C_{32}s^2 + L_{31}s + R_{31})(L_{31}R_{31}C_{32}s^2 - L_{31}s + R_{31})} \tag{96}$$

results in a Class IV zero of transmission of order 3 at $s = 0$, and a Class II zero of transmission of order 1 at $s = \infty$.

Step 4: The unique factorization of the function $\rho(s)\rho(-s)$ is

$$\hat{\rho}(s) = (1-K_4)^{1/2}\frac{x^4 + 2.6131x^3 + 3.4142x^2 + 2.6131x + 1}{s^4 + 2.6131s^3 + 3.4142s^2 + 2.6131s + 1} \tag{97}$$

where K_4 will be determined in the next step, and x is given by

$$x = \frac{s}{(1-K_4)^{1/8}} \tag{98}$$

Step 5: Expanding $A(s)$, $F(s)$, and $\rho(s)$ first at $s = \infty$ gives

$$A(s)|_{s=\infty} = 1 - \frac{2}{R_{31}C_{32}s} + \frac{2}{R_{31}{}^2C_{32}{}^2s^2}\ldots \tag{99}$$

$$F(s)|_{s=\infty} = 0 + 0 + \frac{2}{R_{31}C_{32}{}^2s^2}\ldots \tag{100}$$

$$\hat{\rho}(s)|_{s=\infty} = 1 + \frac{2.6131(\zeta - 1)}{s} + \frac{3.4142(\zeta^2 - 2\zeta + 1)}{s^2}\ldots \tag{101}$$

Where ζ is given by

$$\zeta = (1-K_4)^{1/8} \qquad 0 \le \zeta \le 1 \tag{102}$$

Step 6: Because the expansion was done around $s = \infty$, ensure that the conditions of a Class II zero are met

$$A_O = \rho_O = 1 = 1 \tag{103}$$

$$\frac{A_1 - \rho_1}{F_2} \ge 0 \qquad \frac{-2/R_{31}C_{32} - 2.6131(\zeta - 1)}{2/R_{31}C_{32}{}^2} \ge 0 \;\; \zeta \le 1 - \frac{0.765}{R_{31}C_{32}} \tag{104}$$

Both conditions are met as long as the constraint on ζ is satisfied. Now the zero of transmission $s = 0$ in considered.

Step 5: Expanding $A(s)$, $F(s)$, and $\rho(s)$ first at $s = 0$ gives

$$A(s)|_{s=0} = 1 - \frac{2L_{31}}{R_{31}} s + \frac{2L_{31}^{\ 2}}{R_{31}^{\ 2}} s^2 \ldots \tag{105}$$

$$F(s)|_{s=0} = 0 + 0 - \frac{2L_{31}^{\ 2}}{R_{31}} s^2 \ldots \tag{106}$$

$$\hat{\rho}(s)|_{s=0} = \zeta^4 + 2.6131\zeta^3(1-\zeta)s + 3.4142\zeta^2(\zeta-1)^2 s^2 \ldots \tag{107}$$

Step 6: Because the expansion was done around $s = 0$, ensure that the conditions of a Class IV zero are met

$$A_O = \rho_O = 1 = \zeta^4 \qquad \zeta = 1 \tag{108}$$

Without continuing the analysis, it can be seen that the necessary ζ to satisfy Equation (108) violates Equation (104) because it would require either R_{31} or C_{32} to be negative or infinite, and thus no match can be obtained.

The only option to try to acquire a match is to insert an allpass function into the A(s) equation. This has been attempted, and also produces an invalid result. Thus, the Chen method cannot be used to match a simple antenna to a resistive load.

Appendix E MATLAB Code for Spectrum Simulation

```
%*******************************************************************************
%   ReceiverSim.m
%   Written By: Wyatt Taylor
%   Called Functions: RFIgenerate, Noise, BlockingAnalysis, Simulate
%*******************************************************************************

close all; clear all;

Receiver=1;         %1=ETA, 2=LWA, 3=Cognitive Radio, 4=Test Case

N=2^14;            %# of samples
fs=200e6;             %sampling frequency
F=fs*([0:N]/N-.5);    %frequency scale for axis
t=[0:N]/(fs);      %time scale

RBW=fs/N;                                              %calculate the resolution bandwidth in
kHz
disp('Resolution Bandwidth [kHz]:'); disp(RBW/1000);    %display RBW for user

[RFI_t]=RFIgenerate(Receiver,N,fs,t);                  %returns the time domain RFI environment
for the receiver

w=0.42-.5*cos(2*pi*(0:N)/(N))+0.08*cos(4*pi*(0:N)/(N)); %Blackman window for FFT
RFI_F=fftshift(fft(w.*RFI_t)/N);                                %FFT the waveform

[Noise_Model_F]=Noise(Receiver,F,RBW);                 %returns the frequency domain of the
noise environment

[B_Blocked_i]=BlockingAnalysis(RFI_F,Noise_Model_F,N,F,Receiver);  %calculates B_blocked for at
the input of the antenna
disp('Percentage of Spectrum Blocked At the Antenna Input:'); disp(B_Blocked_i);

[S_F,N_F]=Simulate(Receiver,RFI_F,Noise_Model_F,N,F,w,t); %simulate the receiver chain
performance

[B_Blocked_o]=BlockingAnalysis(S_F,20*log10(abs(fftshift(N_F,1))),N,F,Receiver);     %calculates
B_blocked at the input of the ADC
disp('Percentage of Spectrum Blocked At the ADC Input:'); disp(B_Blocked_o);

figure(1); plot(F/1e6,20*log10(abs(RFI_F))+12,'k',F/1e6,Noise_Model_F,'k-.');  %plot results
axis([0 100 -180 20]); xlabel('Frequency [MHz]'); ylabel('Power Spectral Density [dBm/RBW]');
grid on; legend('Signals','Noise Background',2)

figure(2); plot(F/1e6,20*log10(abs(S_F))+12,'k',F/1e6,20*log10(N_F),'k-.');  %plot results
axis([0 100 -180 20]); xlabel('Frequency [MHz]'); ylabel('Power Spectral Density [dBm/RBW]');
grid on; legend('Signals and Intermodulation Products','Noise Background',2)

return

%*******************************************************************************
%   RFIgenerate.m
%   Written By: Wyatt Taylor
%   Called Functions: COMPUTEfunc
%*******************************************************************************

function [RFI]=RFIgenerate(Receiver,N,fs,t)

switch Receiver

case 1

    [Category,Frequency,Power]=textread('ETA.dat','%s %f %f');     %read in RFI data for ETA

case 2

    [Category,Frequency,Power]=textread('LWA.dat','%s %f %f');     %read in RFI data for LWA
```

```
case 3

    [Category,Frequency,Power]=textread('CR.dat','%s %f %f');      %read in RFI data for
cognitive radio

case 4

    [Category,Frequency,Power]=textread('RFI.dat','%s %f %f');     %read in RFI data for test
case

end

[RFI]=COMPUTEfunc(Category,Frequency,Power,N,fs,t);             %compute the corresponding time
domain signal

%*******************************************************************************
%   COMPUTEfunc.m
%   Written By: Wyatt Taylor
%   Called Functions: TVfunc, FMfunc, RADIOfunc, HFfunc, HAMfunc, SINEfunc
%*******************************************************************************

function [RFI]=COMPUTEfunc(Category,Frequency,Power,N,fs,t)

Inputi=0;          %initialize
TVvideoi=0;        %initialize
TVaudioi=0;        %initialize
FMi=0;          %initialize
RADIOi=0;          %initialize
HFi=0;          %initialize
HAMi=0;         %initialize
Cosi=0;         %initialize

for Inputi=1:length(Category)        %this loop parses the data into arrays

       if strcmp(Category(Inputi),'TVvideo')==1

      TVvideoi=TVvideoi+1;
      TVvideo_f_MHz(TVvideoi)=Frequency(Inputi);
      TVvideo_Ac_dB(TVvideoi)=Power(Inputi);

   elseif strcmp(Category(Inputi),'TVaudio')==1

      TVaudioi=TVaudioi+1;
      TVaudio_f_MHz(TVaudioi)=Frequency(Inputi);
      TVaudio_Ac_dB(TVaudioi)=Power(Inputi);

   elseif strcmp(Category(Inputi),'FM')==1

      FMi=FMi+1;
      FM_f_MHz(FMi)=Frequency(Inputi);
      FM_Ac_dB(FMi)=Power(Inputi);

   elseif strcmp(Category(Inputi),'RADIO')==1

      RADIOi=RADIOi+1;
      RADIO_f_MHz(RADIOi)=Frequency(Inputi);
      RADIO_Ac_dB(RADIOi)=Power(Inputi);

   elseif strcmp(Category(Inputi),'HF')==1

      HFi=HFi+1;
      HF_f_MHz(HFi)=Frequency(Inputi);
      HF_Ac_dB(HFi)=Power(Inputi);

   elseif strcmp(Category(Inputi),'HAM')==1

      HAMi=HAMi+1;
      HAM_f_MHz(HAMi)=Frequency(Inputi);
      HAM_Ac_dB(HAMi)=Power(Inputi);

   elseif strcmp(Category(Inputi),'Sine')==1
```

```
      Cosi=Cosi+1;
      Cos_f_MHz(Cosi)=Frequency(Inputi);
      Cos_Ac_dB(Cosi)=Power(Inputi);

   else

      disp('Improper formatting of data file')      %error if input file is incorrect

      return

   end

end

Df_TV=1.1404e5;            %frequency deviation constant for TV
Df_FM=3.4212e5/16;     %frequency deviation constant for FM
Df_2WAY=3e3;         %frequency deviation constant for 2way radio
filt_FMTV=15e3;      %15kHz filter for FM and TV
filt_2WAY=3e3;       %3kHz filter for 2way radio
filt_HF=3e3;         %3kHz filter for HF
filt_HAM=3e3;        %3kHz filter for HAM

RFI=0;  %initialize

if TVvideoi~=0      %this series of IF statements calls the comm signal functions

       TVvideoi=0;    %initialize

       for TVvideoi=1:length(TVvideo_f_MHz)

              fc_video=1e6*TVvideo_f_MHz(TVvideoi); %get center frequency for TV channel video
              Ac_video=sqrt(2)*(10^(((TVvideo_Ac_dB(TVvideoi))-10)/20));  %get amplitude for TV
channel video
              [TVwave_video]=TVfunc(fc_video,Ac_video,N,fs,t);            %calculate TV channel
video waveform

       RFI=RFI+TVwave_video;  %save TV channel video waveform

   end

end

if TVaudioi~=0

       TVaudioi=0;

       for TVaudioi=1:length(TVaudio_f_MHz)

        Df=Df_TV;      %set Df for TV
        filt=filt_FMTV;       %set bandwidth for TV
           fc_audio=1e6*TVaudio_f_MHz(TVaudioi);    %get cneter frequency for TV channel audio
           Ac_audio=sqrt(2)*(10^(((TVaudio_Ac_dB(TVaudioi))-10)/20));      %get amplitude for TV
channel audio
           [TVwave_audio]=FMfunc(Df,fc_audio,Ac_audio,N,fs,t,filt);       %calculate TV channel
audio waveform
           RFI=RFI+TVwave_audio;     %save TV channel audio waveform

   end

end

if FMi~=0

       FMi=0;  %initialize

       for FMi=1:length(FM_f_MHz)

        Df=Df_FM;      %set Df for FM
        filt=filt_FMTV;       %set bandwidth for FM
           fc_audio=1e6*FM_f_MHz(FMi);       %get center frequency for FM channel
```

```
            Ac_audio=sqrt(2)*(10^(((FM_Ac_dB(FMi))-10)/20)); %get amplitude for FM channel
            [FMwave]=FMfunc(Df,fc_audio,Ac_audio,N,fs,t,filt);              %calculate FM channel
waveform
            RFI=RFI+FMwave;    %save FM channel

        end

end

if RADIOi~=0

   RADIOi=0;

   for RADIOi=1:length(RADIO_f_MHz)

         Df=Df_2WAY;
         filt=filt_2WAY;
         fc_audio=1e6*RADIO_f_MHz(RADIOi);
         Ac_audio=sqrt(2)*(10^(((RADIO_Ac_dB(RADIOi))-10)/20));
         [RADIOwave]=RADIOfunc(Df,fc_audio,Ac_audio,N,fs,t,filt);
         RFI=RFI+RADIOwave;

   end

end

if HFi~=0
   HFi=0;

   for HFi=1:length(HF_f_MHz)

         filt=filt_HF;
         fc_audio=1e6*HF_f_MHz(HFi);
         Ac_audio=sqrt(2)*(10^(((HF_Ac_dB(HFi))-10)/20));
         [HFwave]=HFfunc(fc_audio,Ac_audio,N,fs,t,filt);
         RFI=RFI+HFwave;

   end

end

if HAMi~=0

   HAMi=0;

   for HAMi=1:length(HAM_f_MHz)

         filt=filt_HAM;
         fc_audio=1e6*HAM_f_MHz(HAMi);
         Ac_audio=sqrt(2)*(10^(((HAM_Ac_dB(HAMi))-10)/20));
         [HAMwave]=HAMfunc(fc_audio,Ac_audio,N,fs,t,filt);
         RFI=RFI+HAMwave;

   end

end

if Cosi~=0

   Cosi=0;

   for Cosi=1:length(Cos_f_MHz)

         fc_cos=1e6*Cos_f_MHz(Cosi);
         Ac_cos=sqrt(2)*(10^(((Cos_Ac_dB(Cosi))-10)/20));
         [Coswave]=SINEfunc(fc_cos,Ac_cos,t);
         RFI=RFI+Coswave;

   end

end
```

```
%*******************************************************************************
%   TVfunc.m
%   Written By: Wyatt Taylor
%   Called Functions: none
%*******************************************************************************

function [vsb]=TVfunc(fc_video,Ac_video,N,fs,t)

x=ceil(t(end)/63.5e-6);
for I=1:x
       d(I)=63.5e-6*(I-1);
end

bla=pulstran(t',d','rectpuls',10.5e-6);      %blanking pulse

bs_lvl=-.25*pulstran(t',d','rectpuls',4.25e-6);      %blanking and sync levels
bs_lvl=bs_lvl+.25;

raw_v=rand(1,length(t));      %video signal is random and uniformly distributed

comp_v=raw_v;  %Blanling operation
temp=find(bla>max(bla)/2);
comp_v(temp)=bs_lvl(temp);

temp=fft(comp_v);
fidx=(fs)*([0:length(temp)-1]/(length(temp)-1)-.5);
wn=4.2e6/fidx(end);
M=2e2;
bn=fir1(M,wn,'DC-1');  %FIR filter for 4.2MHz bandwidth
flt_comp_v=filter(bn,1,comp_v);

u=-.875;              %modulation index for video

dsb_carrier=cos(2*pi*fc_video*t+rand*2*pi);  %carrier signal
mod_dsb=dsb_carrier.*(1+u*flt_comp_v);       %carrier signal with modulated signal

Filt=[fc_video-1.25e6 fc_video-.625 fc_video+4.3e6 fc_video+4.925e6];      %FSB filter and
specifications
A=[0 1 0];     %FSB filter and specifications
dev=[.1 .01 .1];      %FSB filter and specifications
[N0,F0,A0,W]=remezord(Filt,A,dev,fs); %FSB filter and specifications
bn = remez(N0,F0,A0,W);              %FSB filter and specifications
vsb=filter(bn,1,mod_dsb);     %full scale TV signal
vsb=Ac_video*vsb;             %TV signal at desired amplitude

%*******************************************************************************
%   FMfunc.m
%   Written By: Wyatt Taylor
%   Called Functions: none
%*******************************************************************************

function [FM]=FMfunc(Df,fc_audio,Ac_audio,N,fs,t,filt)

scale=2^8; %scale for lower sampling rate
rN=round(length(t)/scale);
rfs=fs/scale;   %lower sampling rate

mR=2*rand(1,rN)-1;     %right channel assuming audio is random and uniformly distributed
mL=2*rand(1,rN)-1;     %left channel assuming audio is random and uniformly distributed

temp=fft(mR);
rfidx=rfs*([0:length(temp)-1]/(length(temp)-1)-.5);
wn=filt/rfidx(end);
M=50;
bn=fir1(M,wn); %lowpass filter with 15kHz cutoff
mR15=filter(bn,1,mR);  %filtered right channel
mL15=filter(bn,1,mL);  %filtered left channel

rt=t(end)*[0:length(temp)-1]/(length(temp)-1);
```

```
rsm=mL15+mR15;         %sum of channels
rdm=mL15-mR15;         %difference of channels

fsc=38e3;      %subcarrier modulator frequency
rdm1=rdm.*cos(2*pi*fsc*rt);          %subcarrier signal

fp=fsc/2;      %pilot tone frequency
rsp=cos(2*pi*fp*rt);  %pilot tone signal

rmb=rsm+rdm1+rsp;      %sum of signals before transmit

rint_mb(1)=0;
for I=1:length(rmb)-1
   rint_mb(I+1)=rint_mb(I)+rmb(I)*(1/rfs);   %integration of audio signal
end

int_mb=[0 interp(rint_mb,scale)];

FM=Ac_audio*cos(2*pi*fc_audio*t+2*pi*Df*int_mb);     %carrier signal with modulated signal

%*******************************************************************************
%   RADIOfunc.m
%   Written By: Wyatt Taylor
%   Called Functions: none
%*******************************************************************************

function [RADIO]=RADIOfunc(Df,fc_audio,Ac_audio,N,fs,t,filt)

scale=2^8; %scale for lower sampling rate
rN=round(length(t)/scale);
rfs=fs/scale;   %lower sampling rate

m=2*rand(1,rN)-1;      %channel assuming audio is random and uniformly distributed

temp=fft(m);
rfidx=rfs*([0:length(temp)-1]/(length(temp)-1)-.5);
wn=filt/rfidx(end);
M=50;
bn=fir1(M,wn); %lowpass filter with 15kHz cutoff
m_final=filter(bn,1,m);       %filtered signal

rint_mb(1)=0;
for I=1:length(m)-1
   rint_mb(I+1)=rint_mb(I)+m_final(I)*(1/rfs);       %integration of audio signal
end

int_mb=[0 interp(rint_mb,scale)];

RADIO=Ac_audio*(cos(2*pi*fc_audio*t)-Df*int_mb.*sin(2*pi*fc_audio*t));     %carrier signal with
modulated signal

%*******************************************************************************
%   HFfunc.m
%   Written By: Wyatt Taylor
%   Called Functions: none
%*******************************************************************************


function [HF]=HFfunc(fc_audio,Ac_audio,N,fs,t,filt)

scale=2^8; %scale for lower sampling rate
rN=round(length(t)/scale);
rfs=fs/scale;   %lower sampling rate

m=2*rand(1,rN)-1;      %signal assuming audio is random and uniformly distributed

temp=fft(m);
rfidx=rfs*([0:length(temp)-1]/(length(temp)-1)-.5);
wn=filt/rfidx(end);
M=50;
bn=fir1(M,wn);  %lowpass filter
```

```
m_filt=filter(bn,1,m); %filtered signal

m_final=[1 interp(m_filt,scale)];   %return to original sampling rate

HF=Ac_audio*(1+m_final).*cos(2*pi*fc_audio*t);  %generate AM signal

%*******************************************************************************************
%   HAMfunc.m
%   Written By: Wyatt Taylor
%   Called Functions: none
%*******************************************************************************************

function [HAM]=HAMfunc(fc_audio,Ac_audio,N,fs,t,filt)

scale=2^8; %scale for lower sampling rate
rN=round(length(t)/scale);
rfs=fs/scale;   %lower sampling rate

m=2*rand(1,rN)-1;      %signal assuming audio is random and uniformly distributed

temp=fft(m);
rfidx=rfs*([0:length(temp)-1]/(length(temp)-1)-.5);
wn=filt/rfidx(end);
M=50;
bn=fir1(M,wn);  %lowpass filter
m_filt=filter(bn,1,m); %filtered signal

m_final=[1 interp(m_filt,scale)];   %return to original sampling rate

HAM=Ac_audio*real(m_final.*exp(j*2*pi*fc_audio*t));

%*******************************************************************************************
%   SINEfunc.m
%   Written By: Wyatt Taylor
%   Called Functions: none
%*******************************************************************************************

function [Coswave]=SINEfunc(fc_cos,Ac_cos,t)

Coswave=Ac_cos*cos(2*pi*fc_cos*t+rand*2*pi);

%*******************************************************************************************
%   Noise.m
%   Written By: Wyatt Taylor
%   Called Functions: none
%*******************************************************************************************

function [dSa]=Noise(Receiver,F,RBW)

warning off

To=290;
k=1.38e-23;

switch Receiver

case 1

    C=52.0; D=23.0;

case 2

    C=52.0; D=23.0;

case 3

    C=76.8; D=27.7;

case 4

    C=67.2; D=27.7;     %rurul
```

```
    %C=52.0; D=23.0;    %galactic
    %C=76.8; D=27.7;     %business

end

Counter=0;

for Counter=1:length(F)

    dSa(Counter)=10*log10(k*To*RBW/0.001)+C-D*log10(F(Counter)/1e6);   %noise model in dBm/RBW

end

for i=1:max(size(F)), if (dSa(i)==inf), dSa(i)=(0); end; end

%*********************************************************************************
%   BlockingAnalysis.m
%   Written By: Wyatt Taylor
%   Called Functions: none
%*********************************************************************************

function [PercentageBlocked]=BlockingAnalysis(RFI_F,Noise_Model_F,N,F,Receiver)

switch Receiver

case 1

    F1=29e6;
    F1=floor((N/2)*(F1/F(N+1)))+(N/2)+1;
    F2=47e6;
    F2=ceil((N/2)*(F2/F(N+1)))+(N/2)+1;

case 2

    F1=20e6;
    F1=floor((N/2)*(F1/F(N+1)))+(N/2)+1;
    F2=80e6;
    F2=ceil((N/2)*(F2/F(N+1)))+(N/2)+1;

case 3

    F1=30e6;
    F1=floor((N/2)*(F1/F(N+1)))+(N/2)+1;
    F2=50e6;
    F2=ceil((N/2)*(F2/F(N+1)))+(N/2)+1;

case 4

    F1=30e6;
    F1=floor((N/2)*(F1/F(N+1)))+(N/2)+1;
    F2=100e6;
    F2=ceil((N/2)*(F2/F(N+1)))+(N/2)+1;

end

Counter=0;          %initialize
NumberBlocked=0;

for Counter=F1:F2

    if 20*log10(abs((RFI_F(Counter))))+12 > Noise_Model_F(Counter) == 1  %if the PSD of the RFI
is stronger than the noise...

        NumberBlocked=NumberBlocked+1;         %...then that bin is blocked

    end

end

PercentageBlocked=100*NumberBlocked/(F2-F1);      %calculate the percentage blocked
```

```
%*******************************************************************************
%   Simulate.m
%   Written By: Wyatt Taylor
%   Called Functions: AntennaIME, Nonlinear, BPF
%*******************************************************************************

function [Si_F,N_F]=Simulate(Receiver,S_SKY_F,Noise_Model_F,N,F,w,t)

Noise_Model_F=10.^(ifftshift(Noise_Model_F,1)./20);

switch Receiver

case 1

    [Antenna_IME]=AntennaIME(Receiver,F);      %returns the IME between the antenna and the
preamp
    Si_F=Antenna_IME.*S_SKY_F;      %frequency domain signal at the input of the active
balun/long coax
    N_F=Antenna_IME.*Noise_Model_F;

    Si_t=ifft(Si_F*N)./w;          %time domain signal at the input of the active balun/long coax
    for i=1:max(size(F)), if (abs(Si_t(i))>1), Si_t(i)=(0); end; end

    A=-180; B=0.6; C=188.4;           %active balun/long coax parameters/GALI74
    [So_t]=Nonlinear(Si_t,A,B,C);   %time domain signal at the output of the active balun/long
coax
    So_F=fft(w.*So_t)/N;            %frequency domain signal at the output of the active
balun/long coax
    N_F=N_F*C;

    [Filter_IME]=BPF(Receiver,F);    %filter response of BPF
    Si_F=Filter_IME.*So_F;          %frequency domain signal at the input of the GALI-
74/attenuator/GALI-74
    N_F=Filter_IME.*N_F;

    Si_t=ifft(Si_F*N)./w;          %time domain signal at the input of the GALI-
74/attenuator/GALI-74
    for i=1:max(size(F)), if (abs(Si_t(i))>1), Si_t(i)=(0); end; end

    A=-2; B=1; C=16;               %GALI-74/transformer
    [So_t]=Nonlinear(Si_t,A,B,C);      %time domain signal at the output of the GALI-
74/attenuator/GALI-74
    So_F=fft(w.*So_t)/N;               %frequency domain signal at the output of the GALI-
74/attenuator/GALI-74
    N_F=N_F*C;

    Si_F=So_F;

case 2

    [Antenna_IME]=AntennaIME(Receiver,F);      %returns the IME between the antenna and the
preamp

    Si_F=Antenna_IME.*S_SKY_F;      %frequency domain signal at the input of the active
balun/long coax
    N_F=Antenna_IME.*Noise_Model_F;

    Si_t=ifft(Si_F*N)./w;          %time domain signal at the input of the active balun/long coax
    for i=1:max(size(F)), if (abs(Si_t(i))>1), Si_t(i)=(0); end; end

    A=-9; B=0.6; C=16.6;           %active balun/long coax parameters
    [So_t]=Nonlinear(Si_t,A,B,C);   %time domain signal at the output of the active balun/long
coax
    So_F=fft(w.*So_t)/N;            %frequency domain signal at the output of the active
balun/long coax
    N_F=N_F*C;

    [Filter_IME]=BPF(Receiver,F);   %filter response of BPF
    Si_F=Filter_IME.*So_F;          %frequency domain signal at the input of the GALI-74
    N_F=Filter_IME.*N_F;
```

```
    Si_t=ifft(Si_F*N)./w;          %time domain signal at the input of the active balun/long coax
    for i=1:max(size(F)), if (abs(Si_t(i))>1), Si_t(i)=(0); end; end

    A=-40; B=2; C=57.5;           %GALI-74 parameters
    [So_t]=Nonlinear(Si_t,A,B,C);   %time domain signal at the output of the GALI-74
    So_F=fft(w.*So_t)/N;            %frequency domain signal at the output of the GALI-74
    N_F=N_F*C;

    Si_F=Filter_IME.*So_F;          %frequency domain signal at the input of the GALI-
74/attenuator/GALI-74
    N_F=Filter_IME.*N_F;

    Si_t=ifft(Si_F*N)./w;          %time domain signal at the input of the active balun/long coax
    for i=1:max(size(F)), if (abs(Si_t(i))>1), Si_t(i)=(0); end; end

    A=-2; B=1; C=3.4;           %GALI-74/attenuator/GALI-74 parameters
    [So_t]=Nonlinear(Si_t,A,B,C);   %time domain signal at the output of the GALI-
74/attenuator/GALI-74
    So_F=fft(w.*So_t)/N;            %frequency domain signal at the output of the GALI-
74/attenuator/GALI-74
    N_F=N_F*C;

    Si_F=So_F;          %frequency domain signal at the input of the AD9045A

case 3

    [Antenna_IME]=AntennaIME(Receiver,F);      %returns the IME between the antenna and the
preamp
    Si_F=Antenna_IME.*S_SKY_F;      %frequency domain signal at the input of the
transformer/preamplifier/attenuator
    N_F=Antenna_IME.*Noise_Model_F;

    Si_t=ifft(Si_F*N)./w;          %time domain signal at the input of the active balun/long coax
    for i=1:max(size(F)), if (abs(Si_t(i))>1), Si_t(i)=(0); end; end

    A=-10; B=1; C=16;           %transformer/preamplifier/attenuator coax parameters
    [So_t]=Nonlinear(Si_t,A,B,C);   %time domain signal at the output of the
transformer/preamplifier/attenuator
    So_F=fft(w.*So_t)/N;            %frequency domain signal at the output of the
transformer/preamplifier/attenuator
    N_F=N_F*C;

    [Filter_IME]=BPF(Receiver,F);   %filter response of BPF
    Si_F=Filter_IME.*So_F;          %frequency domain signal at the input of the GALI-
74/attenuator/GALI-74
    N_F=Filter_IME.*N_F;

    Si_t=ifft(Si_F*N)./w;          %time domain signal at the input of the active balun/long coax
    for i=1:max(size(F)), if (abs(Si_t(i))>1), Si_t(i)=(0); end; end

    A=-13; B=1; C=18;           %transformer/preamplifier/attenuator coax parameters
    [So_t]=Nonlinear(Si_t,A,B,C);   %time domain signal at the output of the
transformer/preamplifier/attenuator
    So_F=fft(w.*So_t)/N;            %frequency domain signal at the output of the
transformer/preamplifier/attenuator
    N_F=N_F*C;

    Si_F=So_F;

case 4

    Si_t=ifft(S_SKY_F*N)./w;          %time domain signal at the input of the active balun/long
coax
    for i=1:max(size(F)), if (abs(Si_t(i))>1), Si_t(i)=(0); end; end

    A=-9; B=0.6; C=11.75;           %GALI74
    [So_t]=Nonlinear(Si_t,A,B,C);   %time domain signal at the output of the
transformer/preamplifier/attenuator
    So_F=fft(w.*So_t)/N;            %frequency domain signal at the output of the
transformer/preamplifier/attenuator
    N_F=Noise_Model_F*C;
```

```
    Si_F=So_F/C;
    N_F=N_F/C;

    %Si_F=S_SKY_F;
    %N_F=Noise_Model_F;

end
```

References

[1] B. Razavi. *RF Microelectronics*. Prentice Hall. 1998.

[2] W. Stutzman, G. Thiele. *Antenna Theory and Design*. J. Wiley. 1998.

[3] T. Tang, Q. Tieng, M. Gunn. Equivalent Circuit of a Dipole Antenna Using Frequency-Independent Lumped Elements. *IEEE Transactions On Antennas And Propagation*. Volume 41, Number 1. January 1993.

[4] J. H. Reed. *Software Radio: A Modern Approach to Radio Engineering*. Prentice Hall. 2002.

[5] S. W. Ellingson. Receivers for Low-Frequency Radio Astronomy. *From Clark Lake to the Long Wavelength Array: Bill Erickson's Radio Science (N.E. Kassim et al., eds.)*. ASP Conference Series. Volume 345. ISBN 1-58381-213-X2005. Page 321.

[6] H. V. Cane. Spectra of the Nonthermal Radio Radiation from the Galactic Polar Regions. *Monthly Notice Royal Astronomical Society*. Volume 189. Page 465. November 1979.

[7] International Telecommunication Union (2003), "Radio Noise", ITU-R Rec. P.372-8.

[8] L.W. Couch II. *Digital and Analog Communication Systems*. Prentice Hall. 1997, 2001.

[9] S. W. Ellingson. Spectral occupancy at VHF: Implications for Frequency-Agile Cognitive Radios. *IEEE 62nd Vehicular Technology Conference – Fall*. Volume 2. September 2005. Pages 1379 - 1382.

[10] R. M. Fano. Theoretical Limitations on the Broadband Matching of Arbitrary Impedances. *Journal of Franklin Institute*. January – February 1950.

[11] S. Ramo, J. R. Whinnery, and T. Van Duzer, *Fields and Waves in Communication Electronics*, Wiley, 1984.

[12] W.K. Chen. *Theory and Design of Broadband Matching Networks*. Pergamon Press. 1976.

[13] Personal communication with Dr. W.K. Chen. University of Illinois at Chicago. August 2005.

[14] R.F. Bradley. Evaluation of the NRL LWA Active Balun Prototype. National Radio Astronomy Observatory NTC-DSL Laboratory Report. *Dynamic Spectroscopy Laboratory Report Series*. February 2005.

[15] S. W. Ellingson. Preliminary Analysis of the Effects of Front End Non-Linearity of LWA/LWDA Spectroscopy. Virginia Polytechnic Institute and State University Project Report. May 16, 2005.

[16] S.W. Ellingson, C.D. Patterson, J.H. Simonetti. Design and Demonstration of an Antenna for a New 29 - 47 MHz Radio Telescope Array. *IEEE Int'l Ant. & Prop. Symp.* July 2006.